

# **The development of a selective heterogeneous catalyst for the cross-dehydrogenative coupling of *o*-xylene**

De ontwikkeling van een selectieve heterogene katalysator voor de dehydrogenatieve "cross-coupling" van *o*-xylene

Promotor:  
Prof. Dirk De Vos  
Departement Microbiële en Moleculaire Systemen  
Centrum voor Oppervlaktechemie en Katalyse

Masterproef voorgedragen  
tot het behalen van het diploma van  
Master of Science in de bio-ingenieurswetenschappen:  
katalytische technologie

**Riet Van Deun**

juni 2019

*"Dit proefschrift is een examendocument dat na de verdediging niet meer werd gecorrigeerd voor eventueel vastgestelde fouten. In publicaties mag naar dit proefwerk verwezen worden mits schriftelijke toelating van de promotor, vermeld op de titelpagina."*

# Acknowledgment

This part, I will attribute to all the people who have supported me during my research process. I have learned a lot this year, both on a personal and scientific level and I hope my insights are useful for further research and development.

In the first place, I would like to thank Prof. Dirk De Vos to give me the possibility to work on this project in his group and to do a part of my research abroad at the Christian Albrechts Universität in Kiel. I enjoyed my short stay at Kiel and I also would like to thank every member of the research team of Prof. Stock, especially Steve Waitschat, who guided me fantastically in my research. Moreover, I want to thank the others for their advice on exploring the surroundings. I also would like to thank my supervisor, Niels Van Velthoven, for his guidance, his suggestions and his knowledge during my thesis, but also for the opportunity to work independent and to introduce and execute my own ideas.

Finally, I want to thank the people who are indirectly involved, such as my friends who from time to time took me out of my comfort zone and provided me some distraction. I want to thank the rest of the master students and PhD's for the good atmosphere in the lab. Furthermore, I want to thank my parents for their support during my whole career as Bioscience engineer.

# Abstract

The goal of this master thesis is the development of a selective heterogeneous catalyst for the cross-dehydrogenative coupling (CDC) of *o*-xylene. *O*-xylene is easy to study since only homocoupling takes place and 3 regio-isomers are formed. The challenge is to increase the isomer selectivity towards the 3,3',4,4'-tetramethylbiphenyl isomer, which has industrial relevance in a shorter production route towards the polymer Upilex®.

First, the CDC of *o*-xylene was studied homogeneously based on literature described by Stahl *et al.* and Fernández-Ibáñez *et al.* Ligands, acids, temperature and concentrations were screened to obtain appropriate conditions for the heterogeneous reaction. Since both Stahl and Fernández-Ibáñez made use of pyridine-type ligands, efforts were made to immobilize these pyridine ligands. Several metal-organic frameworks (MOFs), such as MOF-808, have great potential for incorporating ligands with a secondary functionality (e.g. carboxylate), since MOF-808 has a large pore size (18.4 Å) and contains open coordination sites (OCSs) at the Zr<sub>6</sub>-cluster, which are susceptible for ligand incorporation. Moreover, this system is tunable since the nitrogen atom of the pyridine-type ligand can be positioned in *ortho*, *meta* or *para* position in respect to the carboxylate group. The same was done for pyridine phosphonate functionalized TiO<sub>2</sub> nanoparticles (NPs) and the polymer poly(4-vinylpyridine).

The isomer selectivity of the reactions with heterogeneous materials (immobilized ligands), deviated strongly from the selectivity of reactions in presence of homogeneous ligands, but resembled the selectivity of homogeneous conditions in absence of ligands. A bimetallic mechanism (two C-H activations at two different Pd centers, followed by a transmetalation between two neighboring Pd centers) was observed for a homogeneous system with Pd(TFA)<sub>2</sub> and 1:1 pyridine. The low selectivity observed under heterogeneous conditions indicated that both palladium atoms require a pyridine-type ligand during the transmetalation, which is impossible when immobilized ligands are used, since one Pd center has to detach from its immobilized ligand (i.e. being ligandless) to perform the transmetalation. Therefore, reactions were performed with immobilized ligands and subequivalent amounts of homogeneous 'mobile' ligand. An increase in selectivity is expected, when both 'mobile' and immobilized ligands are used, compared to reactions with only immobilized ligands or only 'mobile' ligands.

This was the case for poly(4-vinylpyridine), while  $\text{TiO}_2$ -pyridine phosphonate functionalized NPs and MOF-808-ligand<sub>x</sub> rather showed a decrease in isomer selectivity. The hot filtration tests indicated that poly(4-vinylpyridine) acts merely as a reservoir of palladium to obtain 1:1 ratios ligand/Pd in solution. Moreover, MOF-808 and  $\text{TiO}_2$  NPs contain respectively OCSs and surface functional groups, which can interact with Pd, and have negative implications on the selectivity, (e.g. by changing the ligand/Pd ratio in solution or by stabilizing ligandless Pd on the surface).

As a side project, new MOFs were synthesized in Kiel (Germany) consisting of special biphenylhexacarboxylic acid (BPHeC) linkers and different metal salts. Two new Zr-MOFs were obtained, i.e. a UiO-67-BPHeC (UiO = University of Oslo) and a PCN-700-BPHeC. In addition, two other MOFs were obtained using a cerium(IV) ammoniumhexantrate solution and iron(III) chloride hexahydrate as metal precursors.

# Samenvatting

Het doel van deze masterproef is de ontwikkeling van een selectieve vaste drager voor de dehydrogenatieve “cross-coupling” van *o*-xylene. *O*-xylene is een makkelijk bestudeerbare molecule, omdat ze enkel met zichzelf kan koppeling ter vorming van drie verschillende isomeren. De uitdaging is de verhoging van de selectiviteit naar het 3,3',4,4'-tetramethylbiphenyl isomeer, omdat dit een belangrijk intermediair is in een kortere productieroute van het polymeer Upilex®.

Eerst werd de CDC van *o*-xylene homogeen bestudeerd, gebaseerd op literatuur beschreven door Stahl en Fernández-Ibáñez. Liganden, zuren, temperatuur en concentraties werden gescreend om geschikte reactie condities te bekomen waarin de vaste drager gebruikt kan worden. Aangezien Stahl en Fernández-Ibáñez allebei pyridine-achtige liganden gebruikten, werd een poging gedaan om deze pyridine liganden te immobilizeren op vaste dragers. Verschillende metaal-organische roosters, zoals MOF-808 hebben potentieel om liganden met een tweede functionele groep (vb. een carboxylaat) te incorporeren, omdat MOF-808 grote poriën bevat (18.4 Å diameter) en OCSs op de Zr<sub>6</sub>-cluster, die gevoelig zijn voor ligand incorporatie. Dit systeem is modificeerbaar omdat het N-atoom van de pyridine ligand gepositioneerd kan zijn in *ortho*, *meta* of *para* positie t.o.v. de carboxylaatgroep. Dit werd ook toegepast op pyridine phosphonaat gefunctionalizerende TiO<sub>2</sub> NPs en het polymeer poly(4-vinylpyridine).

De isomeer selectiviteiten van de reacties met geïmmobiliseerde liganden weken sterk af van de selectiviteiten verkregen in analoge homogene condities met liganden, maar leken sterk op selectiviteiten van homogene condities zonder liganden. Er werd een bimetallische stap vastgesteld in de katalytische cyclus van een homogeen systeem met Pd(TFA)<sub>2</sub> en 1:1 pyridine (d.w.z. twee C-H activaties op twee verschillende Pd centers, gevolgd door een transmetalatie tussen twee naburige Pd centers). De lage isomeer selectiviteiten, verkregen met geïmmobiliseerde liganden, gaven aan dat elk palladium center een pyridine-achtige ligand vereist tijdens de transmetalatie. Dit is onmogelijk wanneer geïmmobiliseerde liganden gebruikt worden, omdat minstens één van de Pd centers moet loskomen van het geïmmobiliseerde ligand (d.w.z. ligandloos is) om een transmetalatie uit te voeren. Daarom werden er reacties uitgevoerd met geïmmobiliseerde liganden en kleine hoeveelheden ‘mobiele’ homogene liganden. Er werd een toename in isomeer selectiviteit verwacht, wanneer zowel ‘mobiele’ als geïmmobiliseerde liganden toegevoegd werden, in vergelijking met de reacties die enkel geïmmobiliseerde liganden of enkel ‘mobiele’ liganden gebruikten.

Dit was inderdaad het geval wanneer poly(4-vinylpyridine) gebruikt werd, terwijl in de systemen met pyridine fosfonaat  $\text{TiO}_2$  NPs en MOF-808-ligand<sub>x</sub> geen verhoogde selectiviteit kon bekomen worden. Uit de “hot filtration test” bleek dat poly(4-vinylpyridine) voornamelijk als reservoir optrad optimale ligand/Pd ratios in oplossing te verkrijgen.

In een project in Kiel (Duitsland) werden nieuwe MOFs gesynthetiseerd d.m.v. een biphenylhexacarboxylzuur linker. Op deze manier werden twee nieuwe Zr-MOFs bekomen, nl. een UiO-67-BPHeC en een PCN-700-BPHeC. Bovendien werden er ook twee andere MOFs gevormd door gebruik te maken van een cerium(IV) ammoniumhexanitraat oplossing en ijzer(III) chloride hexahydraat.

# List of Abbreviations

abtc <sup>4-</sup>	3,3',5,5'-azobenzene-tetracarboxylate
bdc <sup>2-</sup>	1,4-benzeendicarboxylate
bpdc <sup>2-</sup>	biphenyl-4,4'-dicarboxylate
BPhEC	biphenylhexacarboxylic acid
bptc <sup>4-</sup>	3,3',5,5'-biphenyltetracarboxylate
btc <sup>3-</sup>	1,3,5-benzenetricarboxylate
CDC	cross-dehydrogenative coupling
CMD	concerted metalation deprotonation
CNRS	Le Centre National de la Recherche Scientifique
DCM	dichloromethane
DG	directing group
DMF	dimethylformamide
GC-FID	gas chromatography flame ionization detector
HT-PXRD	high throughput powder X-ray diffraction
KIE	kinetic isotope effect
Me <sub>2</sub> -bpdc <sup>2-</sup>	2,2'-dimethylbiphenyl-4,4'-dicarboxylate
MOF	metal-organic framework
NHC	N-heterocyclic carbene
NMR	nuclear magnetic resonance
NP	nanoparticle
OCS	open coordination site
<sup>-</sup> OTf	trifluoromethanesulfonate
<sup>2F</sup> pyr	2-fluoropyridine
<sup>2F3C</sup> pyr	2-fluoro-3-pyridinecarboxylic acid
<sup>2F4C</sup> pyr	2-fluoropyridine-4-carboxylic acid
PCN	porous coordination network
PivOH	pivalic acid
PSM	post-synthetic modification
RPM	rotations per minute
RR	regio ratio
SALI	solvent-assisted ligand incorporation
SET	single electron transfer



SM	surface modification
TFAH	trifluoroacetic acid
TGA	thermogravimetric analysis
tptc-(Me <sub>2</sub> )	2',5'-dimethyl-[1,1':4',1''-terphenyl],3,3'',5,5''-tetracarboxylate
TON	turnover number
UiO	University of Oslo

# List of Tables

3.1	TON for biaryl formation and isomer selectivity (%) towards the 3,3',4,4'-tetramethylbiphenyl in the homocoupling of <i>o</i> -xylene upon varying the weak acid. Reaction conditions: 0.05 mol% Pd(OAc) <sub>2</sub> , 0.5:1 Bi(OTf) <sub>3</sub> , 1:1 <sup>2</sup> Fpyr, <i>o</i> -xylene (2 mL), 95 °C, 16 bar O <sub>2</sub> , 17 hours.....	25
3.2	TON biaryl formation and isomer selectivity (%) towards the 3,3',4,4'-tetramethylbiphenyl in the homocoupling of <i>o</i> -xylene upon varying the concentration PivOH. Reaction conditions: Pd(OAc) <sub>2</sub> (0.05 mol%), 0.5:1 Bi(OTf) <sub>3</sub> , x eq. PivOH, 1:1 <sup>2</sup> Fpyr, 95 °C, 16 bar O <sub>2</sub> , 17 hours.....	28
3.3	TON for biaryl formation and isomer selectivity (%) towards the 3,3',4,4'-tetramethylbiphenyl in the homocoupling of <i>o</i> -xylene upon varying the temperature. Reaction conditions: Pd(OAc) <sub>2</sub> (0.05 mol%), 0.5:1 Bi(OTf) <sub>3</sub> , 250 eq. pivOH, 1:1 <sup>2</sup> Fpyr, 16 bar O <sub>2</sub> , 17 hours.....	29
3.4	TON for biaryl formation and isomer selectivity (%) towards the 3,3',4,4'-tetramethylbiphenyl in the homocoupling of <i>o</i> -xylene upon varying the triflate salt. Reaction conditions: Pd(OAc) <sub>2</sub> (0.05 mol%), 0.5:1 M(OTf) <sub>n</sub> , 50 eq. pivOH, 1:1 <sup>2</sup> Fpyr, 95 °C, 16 bar O <sub>2</sub> , 17 hours.....	30
3.5	TON for biaryl formation and isomer selectivity (%) towards the 3,3',4,4'-tetramethylbiphenyl in the homocoupling of <i>o</i> -xylene upon varying the amount of trifluoroacetic acid. Reaction conditions: Pd(OAc) <sub>2</sub> (0.05 mol%), 1:1 <sup>2</sup> Fpyr, 95 °C, 16 bar O <sub>2</sub> , 17 hours.....	31
3.6	TON for biaryl formation and isomer selectivity (%) towards the 3,3',4,4'-tetramethylbiphenyl in the homocoupling of <i>o</i> -xylene upon using other sources of TFAH. Reaction conditions: Pd-catalyst (0.05 mol%), 1:1 <sup>2</sup> Fpyr, co-cat, 95 °C, 16 bar O <sub>2</sub> , 17 hours.....	33
3.7	TON for biaryl formation and isomer selectivity (%) towards the 3,3',4,4'-tetramethylbiphenyl in the homocoupling of <i>o</i> -xylene upon varying the temperature. Reaction conditions: Pd(OAc) <sub>2</sub> (0.05 mol%), 2:1 TFAH, 1:1 <sup>2</sup> Fpyr, T(°C), 16 bar O <sub>2</sub> , 17 hours.....	34
3.8	Impact of MOF-808 as additive in the reaction after a washing procedure with salts on the TON for biaryl formation and isomer selectivity (%) towards 3,3',4,4'-tetramethylbiphenyl in the homocoupling of <i>o</i> -xylene. Reaction conditions: 0.05 mol%	

	Pd(OAc) <sub>2</sub> , 0.5 eq. Bi(OTf) <sub>3</sub> , 50 eq. PivOH, 1:1 <sup>2F</sup> pyr, 95 °C, 16 bar O <sub>2</sub> , 17 hours. *Washing procedure results in loss of MOF-808, less than 10 mg available for reaction.....	38
3.9	Impact of MOF-808, washed with strong acids, on the TON for biaryl formation and isomer selectivity (%) towards 3,3',4,4'-tetramethylbiphenyl in the homocoupling of <i>o</i> -xylene. Reaction conditions: 0.05 mol% Pd(OAc) <sub>2</sub> , 0.5 eq. Bi(OTf) <sub>3</sub> , 50 eq. PivOH, 1:1 <sup>2F</sup> pyr, 95 °C, 16 bar O <sub>2</sub> , 17 hours. *Washing procedure results in loss of MOF-808, less than 10 mg available for reaction.....	38
3.10	Scale up of washing procedures and synthesis procedure of MOF-808 and impact of 10 mg MOF-808 on the TON for biaryl formation and isomer selectivity (%) towards 3,3',4,4'-tetramethylbiphenyl in the homocoupling of <i>o</i> -xylene. Reaction conditions: 0.05 mol% Pd(OAc) <sub>2</sub> , 0.5 eq. Bi(OTf) <sub>3</sub> , 50 eq. PivOH, 1:1 <sup>2F</sup> pyr, 95 °C, 16 bar O <sub>2</sub> , 17 hours.....	39
3.11	Cluster composition determined by <sup>1</sup> H-NMR after the different washing procedures (Ca(OAc) <sub>2</sub> .H <sub>2</sub> O, propanesulfonic acid, sulfuric acid) or synthesis procedure from ZrO(NO <sub>3</sub> ) <sub>2</sub> .xH <sub>2</sub> O and after ligand incorporation with <sup>2F3C</sup> pyr .....	40
3.12	Influence of DMF on the TON for biaryl formation and isomer selectivity (%) towards 3,3',4,4'-tetramethylbiphenyl in the homocoupling of <i>o</i> -xylene. Reaction conditions: Pd(OAc) <sub>2</sub> (0.05 mol%), 1:1 <sup>2F</sup> pyr, 50 eq. PivOH, 0.5:1 Bi(OTf) <sub>3</sub> , 95 °C, 16 bar O <sub>2</sub> , 17 hours.....	40
3.13	Scale up of washing procedure and synthesis procedures of MOF-808 and impact of 10 mg MOF-808 on the TON for biaryl formation and isomer selectivity (%) towards 3,3',4,4'-tetramethylbiphenyl in the homocoupling of <i>o</i> -xylene. Reaction conditions: 0.05 mol% Pd(OAc) <sub>2</sub> , 0.5:1 Bi(OTf) <sub>3</sub> , 50 equivalent PivOH, 1:1 <sup>2F</sup> pyr, 95 °C, 16 bar O <sub>2</sub> , 17 hours.....	41
3.14	Cluster composition determined by <sup>1</sup> H-NMR after washing procedure with MeOH of MOF-808 synthesized from ZrO(NO <sub>3</sub> ) <sub>2</sub> .xH <sub>2</sub> O and after ligand incorporation with six <sup>2F3C</sup> pyr ligands per Zr <sub>6</sub> -cluster.....	42
3.15	TON for biaryl formation and isomer selectivity (%) towards 3,3',4,4'-tetramethylbiphenyl in the homocoupling of <i>o</i> -xylene. Introduction of 5 mg MOF-808 after washing procedure with methanol or after ligand incorporation with <sup>2F3C</sup> pyr. Reaction conditions: 5 mg MOF-808, A) or B), 95 °C, 16 bar O <sub>2</sub> , 17 hours.....	43
3.16	TON for biaryl formation and isomer selectivity (%) towards the 3,3',4,4'-tetramethylbiphenyl in the homocoupling of <i>o</i> -xylene upon varying the amount of ligand. Reaction conditions: A) 0.05 mol% Pd(OAc) <sub>2</sub> , 1:1 Sc(OTf) <sub>3</sub> , 50 eq. PivOH or B) Pd(TFA) <sub>2</sub> (0.05 mol%), 5 mg TiO <sub>2</sub> -ligand, 95 °C, 16 bar O <sub>2</sub> , 17 hours.....	46

3.17	TON for biaryl formation and isomer selectivity (%) towards the 3,3',4,4'-tetramethylbiphenyl in the homocoupling of <i>o</i> -xylene upon varying the amount of ligand. Reaction conditions: Pd(TFA) <sub>2</sub> (0.05 mol%), 5 mg TiO <sub>2</sub> -ligand, 95 °C, 16 bar O <sub>2</sub> , 17 hours...	47
3.18	TON for biaryl formation and isomer selectivity (%) towards the 3,3',4,4'-tetramethylbiphenyl in the homocoupling of <i>o</i> -xylene upon varying the amount of ligand. Reaction conditions: Poly(4-vinylpyridine) (1,2 or 4 eq.), A) 0,05 mol % Pd(TFA) <sub>2</sub> , B) 0,05 mol% Pd(OAc) <sub>2</sub> and 2:1 TFAH, C) 0,05 mol% Pd(OAc) <sub>2</sub> and 4:1 TFAH, 95 °C, 16 bar O <sub>2</sub> , 17 hours.....	49
3.19	TON for biaryl formation and isomer selectivity (%) towards 3,3',4,4'-tetramethylbiphenyl in the homocoupling of <i>o</i> -xylene upon varying the ratio of mixed ligand systems. Reaction conditions: 0.05 mol% Pd(TFA) <sub>2</sub> , x eq. pyridine + y eq. <sup>2F</sup> pyr (x+y=1), 95 °C, 16 bar O <sub>2</sub> , 17 hours.....	53
3.20	TON for biaryl formation and isomer selectivity (%) towards 3,3',4,4'-tetramethylbiphenyl in the homocoupling of <i>o</i> -xylene upon varying the amount of ligand. Reaction conditions: 4 eq. poly(4-vinylpyridine) and 0.5 eq. pyridine, A) 0.05 mol% Pd(TFA) <sub>2</sub> , B) 0.05 mol% Pd(OAc) <sub>2</sub> and 2:1 TFAH, C) 0.05 mol% Pd(OAc) <sub>2</sub> and 4:1 TFAH, 95 °C, 16 bar O <sub>2</sub> , 17 hours.....	54
3.21	Cluster composition determined by <sup>1</sup> H-NMR after washing procedure with MeOH of MOF-808 synthesized from ZrO(NO <sub>3</sub> ) <sub>2</sub> .xH <sub>2</sub> O and after ligand incorporation with isonicotinic, nicotinic and picolinic acid.....	58
3.22	TON for biaryl formation and isomer selectivity (%) towards 3,3',4,4'-tetramethylbiphenyl in the homocoupling of <i>o</i> -xylene upon using a mixed ligand system with pyridine. Reaction conditions: 0.05 mol% Pd(TFA) <sub>2</sub> , x eq. pyridine + y eq. (A, B or C), with x + y = 1, 95 °C, 16 bar O <sub>2</sub> , 17 hours.....	59
3.23	Cluster composition determined by <sup>1</sup> H-NMR after washing procedure with MeOH of MOF-808 synthesized from ZrO(NO <sub>3</sub> ) <sub>2</sub> .xH <sub>2</sub> O and after ligand incorporation with <sup>2F3C</sup> pyr and <sup>2F4C</sup> pyr.....	60

# List of Figures

1.1	Examples of relevant pharmaceuticals and agrochemicals. The coupled bond is marked with a thick line.....	1
1.2	The mechanism of the Ullmann reaction. The net reaction is shown in red and generates a stoichiometric amount of copper halide.....	2
1.3	General cycle of catalytic cross-coupling reactions. The reaction starts with the oxidative addition of the aryl halide or pseudohalide. The oxidative addition is followed by a transmetalation and subsequent reductive elimination.....	4
1.4	The most common synthesis routes towards pseudo(halides) (left) and borylated arenes (right).....	5
1.5	Direct biaryl coupling versus cross-dehydrogenative coupling.....	6
1.6	Coupling reaction between two different substrates ( $\text{Ar}_1\text{-H}$ and $\text{Ar}_2\text{-H}$ ) can result in the cross-coupling between $\text{Ar}_1\text{-H}$ and $\text{Ar}_2\text{-H}$ , but also in the homo-coupling between $\text{Ar}_1\text{-H}$ and $\text{Ar}_1\text{-H}$ or $\text{Ar}_2\text{-H}$ and $\text{Ar}_2\text{-H}$ . Furthermore, different regio-isomers can be formed, since the substrate can contain several C-H bonds which are all possible candidates for C-H activation.....	6
1.7	Examples of hetero-aromatic compounds, having directing groups, which result in C-H activation at predominantly the <i>ortho</i> position.....	7
1.8	Comparison of 'DG-assisted' C-H activation and C-H activation of simple arenes.....	7
1.9	Pd-catalyzed CDC consist out of (i) $\text{Pd}^{\text{III}}$ -mediated activation of two aryl C-H bond to produce a $\text{Pd}^{\text{III}}\text{Ar}_1\text{Ar}_2$ intermediate, (ii) reductive elimination of $\text{Ar}_1\text{Ar}_2$ from $\text{Pd}^{\text{III}}\text{Ar}_1\text{Ar}_2$ and (iii) aerobic oxidation of $\text{Pd}^{(0)}$ to $\text{Pd}^{\text{II}}$ .....	8
1.10	Several activation mechanisms by transition-metal complexes: (i) oxidative addition, (ii) electrophilic substitution, (iii) $\sigma$ -bond metathesis, (iv) concerted metalation deprotonation, (v) 1,2-addition.....	8
1.11	Two pathways for $\text{Pd}^{\text{III}}\text{ArAr}'$ formation: at a single $\text{Pd}^{\text{III}}$ center ("monometallic"), at two separate $\text{Pd}^{\text{III}}$ centers followed by transmetalation ("bimetallic").....	9
1.12	Formation of palladium nanoparticles by aggregation of $\text{Pd}^{(0)}$ centers. When these $\text{Pd}^{(0)}$ NPs keep growing, the catalyst deactivates due to the formation of 'Pd-black'.....	10
1.13	Hydrolysis of the palladium acetate precursor into monomeric palladium acetate. The presence of ligands can facilitate the breakup of the trimeric species into monomeric species.....	11
1.14	Current and proposed routes for the industrial synthesis of 4,4'-biphtalic anhydride.....	11

1.15	Rate law for the “monometallic” and “bimetallic” mechanism. The rate law in the bimetallic mechanism changes from first order dependence (in case of rate-limiting C-H activation) to second order dependence (in case of rate-limiting transmetalation).....	13
1.16	Structure of UiO-66 (a) tetrahedral cage, (b) octahedral cage and (c) two type of cages.....	16
1.17	12-connected cluster in fcu net (a), resulting in UiO-67 net structure with fcu topology (c), 8-connected cluster in bcu net (b), resulting in PCN-700 structure with bcu topology (d) and breathing behavior (e): flexible single bipyramid, shrinking along the c-axis while expanding within the ab-plane.....	16
1.18	Representation of spn topology (a) of MOF-808 which consist of tetrahedral cages (b) (orange) and large adamantane pores (c) (yellow).....	17
1.19	Use of tetratopic organic ligands bptc <sup>4-</sup> , abtc <sup>4-</sup> and tptc-(Me <sub>2</sub> ) <sup>4-</sup> result respectively in 12-, 8- and 4-connected Zr <sub>6</sub> -cluster with ftw, scu and lvt type structures.....	17
1.20	Proposed mechanism for the Pd NP-catalyzed Suzuki cross-coupling reaction involving both homogeneous and heterogeneous pathways.....	20
1.21	Schematic overview of the synthesis of UiO-66-TCATPd.....	21
1.22	Design of carboxylate ligands attached to the OCSs of a MOF.....	21
3.1	Different methods to obtain a heterogeneous support containing a pyridine-type of ligand. MOF-808 with pyridine ligands with a secondary carboxylate functionality (left), poly(4-vinylpyridine) (middle) and TiO <sub>2</sub> -functionalized nanoparticles with pyridine ligands with a secondary carboxylate or phosphonate functionality (right).....	25
3.2	The isomer selectivity (%) towards 3,3',4,4'-tetramethylbiphenyl in the homocoupling of <i>o</i> -xylene upon varying the amount of triflate salt (for Bi(III), Sc(III), Fe(III) and Mg(II)). Reaction conditions: Pd(OAc) <sub>2</sub> (0.05 mol%), 50 eq. PivOH, 1:1 <sup>2</sup> Fpyr, 95 °C, 16 bar O <sub>2</sub> , 17 hours.....	28
3.3	TON for biaryl formation in the homocoupling of <i>o</i> -xylene upon varying the amount of triflate salt (for Bi <sup>(III)</sup> , Sc <sup>(III)</sup> , Fe <sup>(III)</sup> and Mg <sup>(II)</sup> ). Reaction conditions: Pd(OAc) <sub>2</sub> (0.05 mol%), 50 eq. PivOH, 1:1 <sup>2</sup> Fpyr, 95 °C, 16 bar O <sub>2</sub> , 17 hours.....	29
3.4	TON for biaryl formation and isomer selectivity (%) towards 3,3',4,4'-tetramethylbiphenyl in the homocoupling of <i>o</i> -xylene upon varying the ligand. Reaction conditions: Pd(OAc) <sub>2</sub> (0.05 mol%), 0.5:1 M(OTf) <sub>n</sub> with M = Bi <sup>(III)</sup> , Sc <sup>(III)</sup> , Fe <sup>(III)</sup> and Mg <sup>(II)</sup> ; 50 eq. PivOH, 1:1 ligand (L1-L12) and no ligand, 95 °C, 16 bar O <sub>2</sub> , 17 hours.....	30
3.5	TON for the formation of a biaryl and isomer selectivity (%) towards 3,3',4,4'-tetramethylbiphenyl in the homocoupling of <i>o</i> -xylene upon varying the amount ligand	

	(for $^{2F}$ pyr, pyridine and methyl nicotinate). Reaction conditions: Pd(OAc) <sub>2</sub> (0.05 mol%), 50 eq. PivOH, 0.5:1 Bi(OTf) <sub>3</sub> , 1:1 $^{2F}$ pyr or pyridine, 95 °C, 16 bar O <sub>2</sub> , 17 hours.....	31
3.6	TON for biaryl formation and isomer selectivity (%) towards 3,3',4,4'-tetramethylbiphenyl in the homocoupling of <i>o</i> -xylene upon varying the ligand (L1-L12) and no ligand. . Reaction conditions: Pd-catalyst (0.05 mol%), 1:1 ligand, 95 °C, 16 bar O <sub>2</sub> , 17 hours, A) Pd(OAc) <sub>2</sub> + 2:1 TFAH, B) Pd(OAc) <sub>2</sub> + 4:1 TFAH and C) Pd(TFA) <sub>2</sub> .....	33
3.7	TON for biaryl formation and isomer selectivity (%) towards 3,3',4,4'-tetramethylbiphenyl in the homocoupling of <i>o</i> -xylene upon varying the amount of ligand. Reaction conditions: Pd(TFA) <sub>2</sub> (0.05 mol%), x:1 ligand ( $^{2F}$ pyr and pyridine), 95 °C, 16 bar O <sub>2</sub> , 17 hours.....	34
3.8	TON for biaryl formation and isomer selectivity (%) towards 3,3',4,4'-tetramethylbiphenyl in the homocoupling of <i>o</i> -xylene upon addition of an additive. Reaction conditions: 0.05 mol% Pd(OAc) <sub>2</sub> , 1:1 $^{2F}$ pyr, 0.5:1 Bi(OTf) <sub>3</sub> , 50 eq. PivOH, additive, 95 °C, 16 bar O <sub>2</sub> , 17 hours.....	35
3.9	Powder diffractograms of MOF-808: simulated, after synthesis from ZrO(NO <sub>3</sub> ) <sub>2</sub> .xH <sub>2</sub> O and washing procedure with methanol and after ligand incorporation with $^{2F3C}$ pyr.....	42
3.10	The difference in conformation of $^{2F3C}$ pyr and $^{2F4C}$ pyr (left) and MOF-808 with on average three $^{2F3C}$ pyr ligands per Zr <sub>6</sub> -cluster (right).....	44
3.11	TGA of sample TiO <sub>2</sub> functionalized with isonicotinic acid with an immersing solution of pH 4 before reaction. The TGA shows that ligands are present on the surface at low pH.....	47
3.12	TGA of sample TiO <sub>2</sub> functionalized with isonicotinic acid with an immersing solution of pH 4 after reaction. The TGA shows that part of the ligands are released from the support.	48
3.13	Addition homogeneous 'mobile' pyridine is required in order to obtain high isomer selectivity when a bimetallic mechanism takes place in a system with immobilized ligands	50
3.14	Kinetic dependence of the rate of Pd-catalyzed CDC of <i>o</i> -xylene on [Pd]. Reaction conditions: 16.6 mmol <i>o</i> -xylene, [Pd]: 1-60 mM, 1:1 pyridine, 16 bar O <sub>2</sub> , 95 °C, 0-4 hours....	51
3.15	Isomer selectivity (%) towards 3,3',4,4'-tetramethylbiphenyl in the homocoupling of <i>o</i> -xylene upon addition of 'mobile' $^{2F}$ pyr (0, 0.25, 0.50, 0.75 and 1 eq.). Reaction conditions: 0.05 mol% Pd(TFA) <sub>2</sub> , poly(4-vinylpyridine) (0, 1 or 4 eq.), 95 °C, 16 bar O <sub>2</sub> , 17 hours.....	52
3.16	TON for biaryl formation in the homocoupling of <i>o</i> -xylene upon addition of 'mobile' $^{2F}$ pyr (0, 0.25, 0.50, 0.75 and 1 eq.). Reaction conditions: 0.05 mol% Pd(TFA) <sub>2</sub> , poly(4-vinylpyridine) (0, 1 or 4 eq.), 95 °C, 16 bar O <sub>2</sub> , 17 hours.....	52
3.17	Isomer selectivity (%) towards 3,3',4,4'-tetramethylbiphenyl in the homocoupling of <i>o</i> -xylene upon addition of 'mobile' pyridine (0, 0.25, 0.50, 0.75 and 1 eq.). Reaction	

	conditions: 0.05 mol% Pd(TFA) <sub>2</sub> , poly(4-vinylpyridine) (0, 1 or 4 eq.), 95 °C, 16 bar O <sub>2</sub> , 17 hours.....	53
3.18	TON for biaryl formation in the homocoupling of <i>o</i> -xylene upon addition of 'mobile' pyridine (0, 0.25, 0.50, 0.75 and 1 eq.). Reaction conditions: 0.05 mol% Pd(TFA) <sub>2</sub> , poly(4-vinylpyridine) (0, 1 or 4 eq.), 95 °C, 16 bar O <sub>2</sub> , 17 hours.....	54
3.19	TiO <sub>2</sub> and CeO <sub>2</sub> NPs functionalized with 2-pyridine-phosphonate, either by one-pot reaction or SM.....	55
3.20	Isomer selectivity (%) towards 3,3',4,4'-tetramethylbiphenyl in the homocoupling of <i>o</i> -xylene upon addition of 'mobile' pyridine (0, 0.25, 0.50 and 0.75 eq.). Reaction conditions: 0.05 mol% Pd(TFA) <sub>2</sub> , TiO <sub>2</sub> -pyridine-onepot (0, 0.5, 1 and 2 eq.), 95 °C, 16 bar O <sub>2</sub> , 17 hours.....	56
3.21	TON for biaryl formation in the homocoupling of <i>o</i> -xylene upon addition of 'mobile' pyridine (0, 0.25, 0.50 and 0.75 eq.). Reaction conditions: 0.05 mol% Pd(TFA) <sub>2</sub> , TiO <sub>2</sub> -pyridine-onepot (0, 0.5, 1 and 2 eq.), 95 °C, 16 bar O <sub>2</sub> , 17 hours.....	56
3.22	Isomer selectivity (%) towards 3,3',4,4'-tetramethylbiphenyl in the homocoupling of <i>o</i> -xylene upon addition of 'mobile' pyridine (0, 0.25, 0.50 and 0.75 eq.). Reaction conditions: 0.05 mol% Pd(TFA) <sub>2</sub> , 0 and 0.5 eq. TiO <sub>2</sub> -pyridine-onepot, TiO <sub>2</sub> -pyridine-SM and CeO <sub>2</sub> -pyridine SM, 95 °C, 16 bar O <sub>2</sub> , 17 hours.....	57
3.23	TON for biaryl formation in the homocoupling of <i>o</i> -xylene upon addition of 'mobile' pyridine (0, 0.25, 0.50 and 0.75 eq.). Reaction conditions: 0.05 mol% Pd(TFA) <sub>2</sub> , 0 and 0.5 eq. TiO <sub>2</sub> -pyridine-onepot, TiO <sub>2</sub> -pyridine-SM and CeO <sub>2</sub> -pyridine SM, 95 °C, 16 bar O <sub>2</sub> , 17 hours.....	57
3.24	Isomer selectivity (%) towards 3,3',4,4'-tetramethylbiphenyl in the homocoupling of <i>o</i> -xylene upon addition of 'mobile' pyridine (0, 0.25, 0.50 and 0.75 eq.). Reaction conditions: 0.05 mol% Pd(TFA) <sub>2</sub> , 0 and 5 mg MOF-808 functionalized with 2 eq. of ligands (ligand = isonicotinic acid, nicotinic acid or picolinic acid), 95 °C, 16 bar O <sub>2</sub> , 17 hours.....	59
3.25	TON for biaryl formation in the homocoupling of <i>o</i> -xylene upon addition of 'mobile' pyridine (0, 0.25, 0.50 and 0.75 eq.). Reaction conditions: 0.05 mol% Pd(TFA) <sub>2</sub> , 0 and 5 mg MOF-808 functionalized with 2 eq. ligands (ligand = isonicotinic acid, nicotinic acid or picolinic acid), 95 °C, 16 bar O <sub>2</sub> , 17 hours.....	60
3.26	Isomer selectivity (%) towards 3,3',4,4'-tetramethylbiphenyl in the homocoupling of <i>o</i> -xylene upon addition of 'mobile' <sup>2F</sup> pyr (0, 0.25, 0.50 and 0.75 eq.). Reaction conditions: 0.05 mol% Pd(TFA) <sub>2</sub> , 0 and 5 mg of MOF-808 functionalized with x eq. of ligand (ligand = <sup>2F3C</sup> pyr or <sup>2F4C</sup> pyr, x=2 or 6 eq.), 95 °C, 16 bar O <sub>2</sub> , 17 hours.....	61



3.27	TON for biaryl formation in the homocoupling of <i>o</i> -xylene upon addition of 'mobile' $^{2F}$ pyr (0, 0.25, 0.50 and 0.75 eq.). Reaction conditions: 0.05 mol% Pd(TFA) <sub>2</sub> , 0 and 5 mg MOF-808 functionalized with x eq. ligand (ligand = $^{2F3C}$ pyr or $^{2F4C}$ pyr, x = 2 or 6 eq.), 95 °C, 16 bar O <sub>2</sub> , 17 hours.....	61
3.28	Yield for biaryl formation in the homocoupling of <i>o</i> -xylene at 4 hours reaction times and after filtration (dashed lines, end at 17 hours). In addition, normal kinetics are measured (full lines). Reaction conditions: 0.05 mol% Pd(TFA) <sub>2</sub> with 4 eq. poly(4-vinylpyridine) (or preloaded), with 0 or 0.5 eq. pyridine, 95 °C, 16 bar O <sub>2</sub> , 17 hours.....	64
3.29	Yield for biaryl formation in the homocoupling of <i>o</i> -xylene upon varying the reaction time. Reaction conditions: 0.05 mol% Pd(TFA) <sub>2</sub> with 4 eq. poly(4-vinylpyridine), with 0 or 0.5 eq. pyridine, 95 °C, 16 bar O <sub>2</sub> , 4, 6, 8, 10, 15 and 17 hours.....	65
3.30	Possible locations of palladium and the 'mobile' pyridine ligand: in solution (grey box), or at immobilized ligand (poly(4-vinylpyridine)). Pd is continuously interchanged between immobilized ligand and solution until all palladium is deactivated.....	65
3.31	Yield (%) and TON for biaryl formation in the homocoupling of <i>o</i> -xylene upon catalyst recycle. Reaction conditions: Heterogeneous reaction: 0.5 mol% Pd(TFA) <sub>2</sub> with 4 eq. poly(4-vinylpyridine) with 0.5 eq. pyridine and recycle. Homogeneous reaction: 0.5 mol% Pd(TFA) <sub>2</sub> with 1 eq. pyridine, 95 °C, 16 bar O <sub>2</sub> and 17 hours.....	66
3.32	TON for biaryl formation and average isomer selectivity (%) towards 3,3',4,4'-tetramethylbiphenyl in the homocoupling of <i>o</i> -xylene upon catalyst recycle. Reaction conditions: Heterogeneous reaction: 0.05 mol% Pd(TFA) <sub>2</sub> with 4 eq. poly(4-vinylpyridine) with 0.5 eq. pyridine and recycle: add 1.38 mg Pd to obtain 0.05 mol% and 0.5 eq. pyridine. Homogeneous reaction: 0.05 mol% Pd(TFA) <sub>2</sub> with 1 eq. pyridine, 95 °C, 16 bar O <sub>2</sub> and 17 hours.....	67
3.33	Possible locations of palladium and the 'mobile' pyridine ligand: in solution (grey box), at the immobilized ligands or at the open sites of the surface of a TiO <sub>2</sub> particle (left) or at the OCSs of MOF-808 (right).....	68
3.34	High throughput reactor system and high throughput filtration system, which can be immediately used in HT PXRD.....	69
3.35	Succeeded powder diffractograms of first HT synthesis and simulated powder diffractogram of zirconium formate.....	69
3.36	Succeeded powder diffractogram of second HT synthesis without methanol as additive and simulated powder diffractogram of PCN-700 (left) and the structure of PCN-700 (right).....	70

3.37	Succeeded powder diffractogram of second HT synthesis with methanol as additive and simulated powder diffractogram of UiO-67 (left) and the structure of UiO-67 (right).....	70
3.38	Le bial fits of PCN-700-BPHeC (left) and UiO-67-BPHeC (right) show structural agreement with PCN-700 and UiO-67. The black lines indicate the experimental data, while red lines represent the calculated data and vertical lines mark the allowed Bragg positions. The blue curves indicate the difference between the measured and the calculated pattern.....	71
3.39	The powder diffractograms of PCN-700-BPHeC immediately after synthesis and three days later.....	71
3.40	The powder diffractograms of UiO-67-BPHeC immediately after synthesis and three days later.....	72
3.41	The powder diffractogram of Fe-BPHeC, with acetic acid as modulator and 1:1 metal to linker ratio immediately measured and three days later.....	72
3.42	The powder diffractogram of Ce-BPHeC immediately measured. The pattern after three days was similar.....	73

# Table of Contents

Acknowledgment.....	i
Abstract .....	ii
Samenvatting.....	iv
List of Abbreviations.....	vi
List of Tables.....	viii
List of Figures.....	xi
Context and objectives.....	xix
Chapter 1: Literature study .....	1
I.    Historic overview of carbon-carbon cross-coupling of arenes.....	1
1.    Ullmann reaction.....	1
1.1.    Mechanism .....	2
1.2.    Catalytic system.....	2
2.    Catalytic cross-coupling.....	3
2.1.    Mechanism .....	3
2.2.    Catalytic system.....	4
2.3.    The Suzuki reaction .....	4
3.    Coupling of arenes <i>via</i> C-H activation .....	5
3.1.    Direct arylation .....	6
3.2.    Cross-dehydrogenative coupling.....	6
II.    Metal-organic frameworks.....	15
1.    Zirconium-MOFs with carboxylate linkers.....	15
2.    Synthesis.....	18
3.    Post-synthetic modification .....	18
III.    Immobilization of homogeneous catalyst on MOFs.....	19
1.    MOF as support for palladium NPs .....	20
2.    MOFs as support for palladium complexes.....	20
Chapter 2: Experimental procedures .....	22
I.    Materials and Methods .....	22
1.    Synthesis, washing procedure and ligand incorporation .....	22
1.1.    MOF-808.....	22
1.2.    TiO <sub>2</sub> nanoparticles.....	23
II.    Reaction procedure .....	23
III.    Analysis.....	23
1.    Gas chromatography (GC-FID).....	23

2.	High Throughput Powder X-ray Diffraction.....	24
3.	Thermogravimetric analysis.....	24
4.	Liquid $^1\text{H}$ Nuclear magnetic resonance .....	24
Chapter 3: Results and discussion .....		25
I.	<i>O</i> -xylene coupling – Homogeneous reactions.....	26
1.	Reported procedures .....	26
1.1.	Triflate .....	26
1.2.	Trifluoroacetate.....	32
1.3.	Conclusion .....	35
II.	<i>O</i> -xylene coupling – Heterogeneous reactions .....	36
1.	Metal-organic frameworks as support – MOF-808 .....	36
1.1.	Chloride removal MOF-808 from the $\text{ZrOCl}_2 \cdot 8\text{H}_2\text{O}$ salt to eliminate reaction inhibition..	37
1.2.	Tuning MOF-808 from the $\text{ZrO}(\text{NO}_3)_2 \cdot x\text{H}_2\text{O}$ salt .....	41
1.3.	Conclusion .....	44
2.	Other heterogeneous supports as alternatives for MOFs.....	46
2.1.	$\text{TiO}_2$ nanoparticles .....	46
2.2.	Poly(4-vinylpyridine).....	49
2.3.	Conclusion .....	49
3.	Mechanistical insights .....	50
3.1.	Poly(4-vinylpyridine).....	51
3.2.	$\text{TiO}_2$ and $\text{CeO}_2$ NPs .....	55
3.3.	MOF-808.....	58
3.4.	Conclusion .....	62
4.	Heterogeneity of the system.....	63
4.1.	Hot filtration tests .....	63
4.2.	Recycling tests .....	66
4.3.	Conclusion .....	68
III.	Side project Kiel – MOF synthesis with biphenylhexacarboxylic acid linker .....	69
1.	Zirconium MOFs .....	69
2.	Other metals MOFs .....	72
3.	Conclusion .....	73
General conclusion .....		74
Bibliography.....		75
Vulgariserende samenvatting .....		81

# Context and objectives

The cross-coupling methodology for the formation of aryl-aryl bonds is one of the most important and widely applied processes in organic chemistry.<sup>1</sup> These palladium or nickel catalyzed reactions require stoichiometric amounts of organohalide and organometallic species, in which the metal evolved over time from Mg or Li (Kumada coupling) to Al, Zn or Zr (Negishi coupling), Sn (Stille coupling) and B (Suzuki coupling), and resulted in a better functional group compatibility and expanded substrate scope.<sup>2</sup> Even though these reactions are very efficient and selective, they suffer from fundamental drawbacks. The organohalides and organometals originate from prior prefunctionalization steps and consequently bring along side-products and additional synthetic operations such as purification steps.<sup>3,4</sup> Moreover, stoichiometric amounts of salts are formed after the reaction, which also need to be removed from the product. Recently, the direct formation of aryl-aryl bonds *via* palladium catalyzed CDC has emerged as a very attractive, economic and sustainable alternative for traditional cross-coupling reactions, since non-prefunctionalized substrates are used and water is the only side-product if oxygen is used as the oxidant. However, the control over the regio-selectivity of the reaction remains challenging, since many C-H bonds are usually present in substrates which do not differ greatly in electronic properties, unless directing groups are used.

In this work, research towards a heterogeneous catalyst for *o*-xylene coupling is performed to develop a more economically viable process in which palladium can be recycled and re-used. Moreover, high isomer selectivity towards the 3,3',4,4'-tetramethylbiphenyl isomer (used for the production of heat resistant polymer Upilex®) is desired to compete with the currently existing selective homogeneous *o*-xylene coupling reactions. Firstly, the CDC of *o*-xylene was studied homogeneously, which indicated the importance of the presence of special type of pyridine ligands.<sup>5,6,7,8,9</sup> These ligands were heterogenized on MOF-808, TiO<sub>2</sub> and CeO<sub>2</sub> NPs and poly(4-vinylpyridine). Moreover, reaction conditions were selected based on homogeneous conditions by omitting the use of strong acids (which could give rise to leaching of the heterogenized ligand) and by making use of the salts of these acids. Secondly, reactions were performed with immobilized ligands under selected reactions conditions. The low isomer selectivities observed under these reaction conditions gave more insight in the reaction mechanism. The detailed understanding of the system gave opportunities to obtain very selective catalysts by using both immobilized ligands and small amounts of homogeneous 'mobile' ligands. However, the development of a complete heterogeneous catalyst was not possible.

In addition, new MOFs were synthesized by making use of a new biphenylhexacarboxylic acid linker. This special linker contains many functional groups on which catalytically active metal species can be attached.



# Chapter 1: Literature study

## I. Historic overview of carbon-carbon cross-coupling of arenes

The biaryl motif made *via* palladium-catalyzed coupling reactions plays a central role in the structure of many biologically active compounds, like pesticides, anti-oxidants, drugs, agrochemicals, etc.<sup>11,12</sup> The stable carbon-structure of the biaryl motif makes it suitable for many applications since this motif is not readily metabolized or degraded in living organisms.<sup>13</sup> Biaryls can be found for example in 4,4'-biphtalic anhydride<sup>14</sup>, which is a monomer for the synthesis of the high-performance polyimide resin Upilex®, in agrochemicals such as the fungicide Boscalid<sup>11</sup> and in pharmaceuticals like Odanacatib, a Cathepsin K inhibitor<sup>15</sup> for osteoporosis and Losartan for the treatment of hypertension (Figure 1.1).<sup>16</sup>

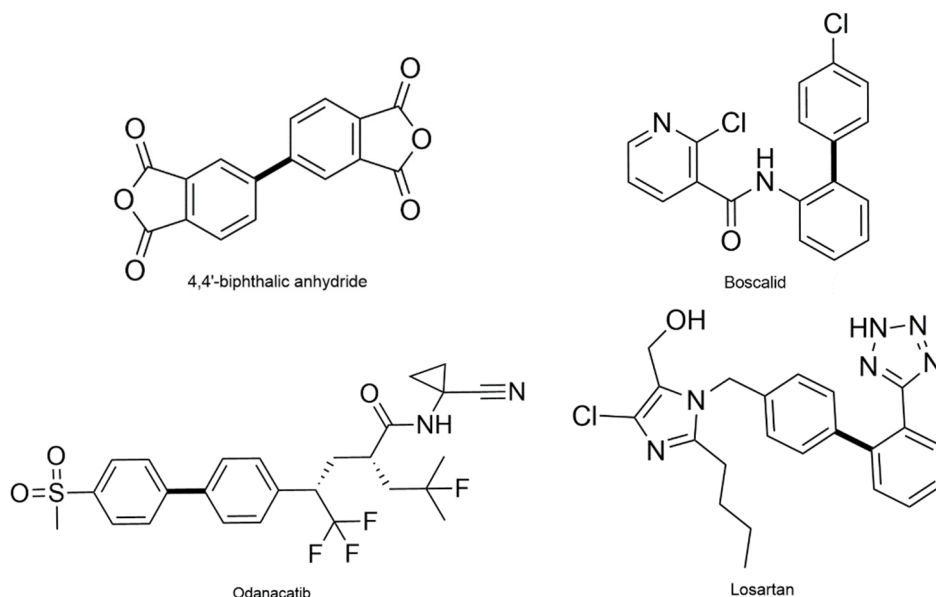


**Figure 1.1:** Examples of relevant polymers, pharmaceuticals and agrochemicals. The coupled bond is marked with a thick line.

### 1. Ullmann reaction

The first reaction procedure to produce biaryl compounds in decent yields was reported in 1901 by Fritz Ullmann, who observed that two aryl halides in the presence of excess copper powder give rise to the homo-coupled symmetric product at high temperatures (> 200 °C) and long reaction times.<sup>17–20</sup> Hence, the “Ullmann reaction” results in the formation of biaryl products and a stoichiometric amounts of copper halide. Furthermore, Cu-mediated reactions with amines, phenol or thiophenol and arylhalides are also possible and are referred to as “Ullmann condensation reactions”.<sup>21</sup>

### 1.1. Mechanism

The mechanism of the Ullmann reaction is highly debated in literature.<sup>18,19,22</sup> Quite a number of possible mechanisms are proposed, such as oxidative addition/reductive elimination, single electron transfer (SET),  $\sigma$ -bond metathesis and halogen atom transfer.<sup>17,22,23</sup> The most widely accepted mechanism is the oxidative addition/reductive elimination. This mechanism involves the formation of an organocuprate(II) intermediate coming from the oxidative addition of an aryl halide, which is followed by a SET to form an organocuprate(I) reagent (Figure 1.2). This organocuprate(I) reacts with a second aryl halide by oxidative addition resulting in a biaryl copper(III) halide complex. Steric hindrance plays an important role in this step, since this intermediate is inhibited by bulky groups in *ortho* position.<sup>19</sup> The final biaryl product is formed after reductive elimination.<sup>17,24</sup> The activation of the aryl halide is considered to be the most problematic step of the mechanism. Therefore, aryl iodides and bromides are preferred over aryl chlorides. The presence of electron withdrawing groups (e.g. nitro, carboxymethyl, etc.) in *ortho* position to the halogen atom has an activating effect.

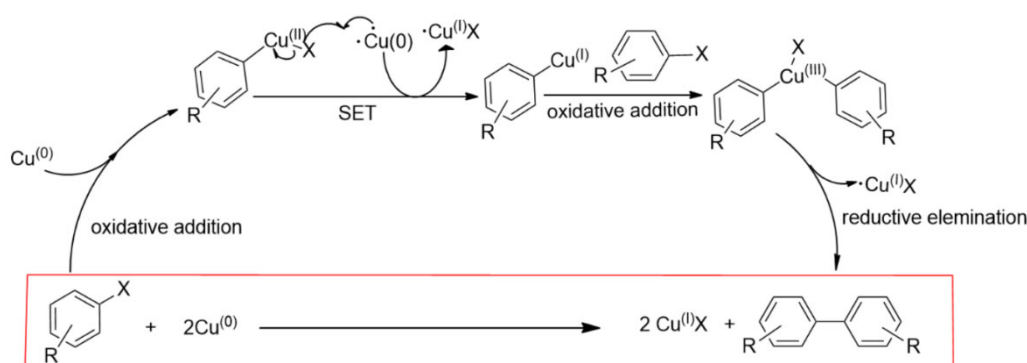


**Figure 1.2:** The mechanism of the Ullmann reaction. The net reaction is shown in red and generates a stoichiometric amount of copper halide.

The Ullmann coupling is extensively studied to produce symmetric compounds (i.e. homo-coupling). When unsymmetrical coupling is preferred (i.e. the product of two different aryl halides), coupling occurs also between two molecules of the same aromatic reagent, resulting in both homo-coupled and cross-coupled products.<sup>4,25,26</sup>

### 1.2. Catalytic system

Many different copper precursors (e.g.  $\text{Cu}^{(0)}$ ,  $\text{Cu}^{(I)}$  and  $\text{Cu}^{(II)}$ ) can be used for Ullmann-type reactions, both copper salts and oxides perform well. This suggests that different sources of Cu give rise to the same Cu species formed during the reaction. It was proposed that  $\text{Cu}^{(I)}$  is the most common intermediate, since it seemed to have a slightly higher reaction rate. It was shown that indeed  $\text{Cu}^{(II)}$  species are reduced to  $\text{Cu}^{(I)}$  in presence of coordinating molecules (e.g. phenoxides, amines, etc.).<sup>18</sup>



The inability to distinguish between two aromatic compounds, and thus the competition from homo-coupling reactions restricts the applicability of the Ullmann coupling in many industrial applications. However, large efforts were made to obtain the cross-coupled product selectively. Researchers found that the cross-coupling performs best when one aryl halide is very reactive and the other one is relatively unreactive. Temperature plays a crucial role; below or above the optimal temperature, the cross-coupling becomes less competitive and the homo-coupling is predominant.<sup>19</sup> Other drawbacks are the need for aggressive reaction conditions, limited substrate scope and high copper loadings. In order to apply the Ullmann reaction under milder conditions (typical temperatures < 100 °C), ligands can be introduced.<sup>17,18</sup>

## 2. Catalytic cross-coupling

One of the major breakthroughs in the field of coupling reactions was the use of nickel instead of copper in Ullmann-type procedures. Later, Kumada discovered that a bidentate phosphine complex in combination with a Grignard reagent results in a catalytic reaction instead of a stoichiometric reaction.<sup>19,27</sup> However, these Grignard reagents are highly reactive due to their anionic character and cannot be used in reactions with substrates containing ketones, esters and nitrile functional groups. This method gave a boost to research, resulting in more efficient catalysts, including palladium complexes, and less reactive but more selective nucleophilic reagents. Many organometallic reagents were explored. Negishi studied organoaluminium and organozirconium compounds in combination with organozinc compounds.<sup>19</sup> These zinc derivatives were much more compatible with functional groups compared to magnesium, resulting in a broader substrate scope.<sup>27</sup> Further research was done by Stille and Suzuki using organotin and organoboron compounds, respectively, which have an electronegativity close to carbon, resulting in tolerance of almost any functional group.<sup>3,19,28</sup> The disadvantage of the Stille reaction is the toxicity of the organotin materials, limiting its industrial use.<sup>27</sup> In 2010, R.F. Heck, A. Suzuki and E. Negishi obtained the Nobel Prize in Chemistry for developing these cross-coupling reactions.<sup>29</sup>

### 2.1. Mechanism

In traditional Pd-based cross-coupling reactions, one or both coupling partners need to be preactivated (e.g. organotin, organoboron, etc.) compared to simple arenes. Common to this type of coupling reactions is the oxidative addition of the aryl halide (or pseudohalide) to the catalytically active  $L_nPd^{(0)}$  complex (Figure 1.3). The next step is a transmetalation of the organometallic reagent to the previously formed  $Pd^{(II)}$  species. Subsequent reductive elimination results in the C-C bond formation and regeneration of the  $L_nPd^{(0)}$  complex.<sup>28,30,31,32</sup>

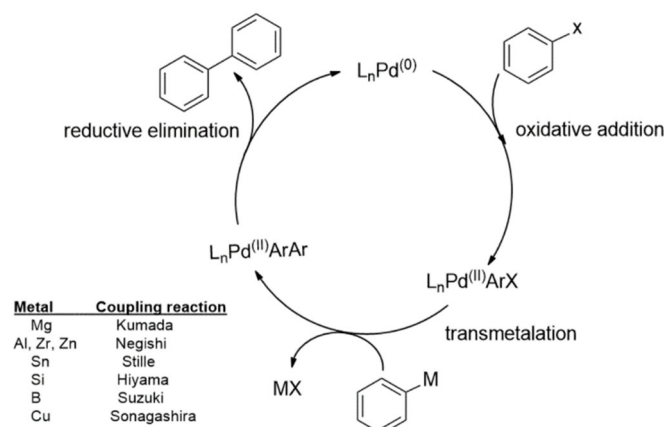


**Figure 1.3:** General cycle of catalytic cross-coupling reactions. The reaction starts with the oxidative addition of the aryl halide or pseudohalide. The oxidative addition is followed by a transmetalation and a subsequent reductive elimination step.

## 2.2. Catalytic system

Although Cu, Ni, Fe and other d-block transition metals can catalyze C-C cross-coupling reactions, it is Pd that represents the most widely applied catalyst in cross-couplings. Palladium catalysts show higher activity than other alternatives, which results in the efficient conversion of less reactive substrates at lower temperatures and also enables higher catalyst turnover numbers (TONs).<sup>2,26,33</sup> In traditional cross-coupling reactions, phosphine ligands have a significant positive effect on the reaction by stabilizing  $\text{Pd}^{(0)}$  (preventing the formation of Pd black), by promoting the oxidative addition and the reductive elimination (e.g. the larger P-Pd-P bite angle results in an acceleration of the reductive elimination) and by providing chiral scaffold for asymmetric processes.<sup>34</sup> In addition, N-heterocyclic carbene (NHC) ligands are very powerful in cross-coupling reactions. Compared to the phosphine ligands, the  $\pi$ -back donation from Pd to the NHC  $\pi^*$ -orbitals is negligible and the NHC ligands make stronger  $\sigma$ -bonds. This results in a lower amount of ligand required to prevent aggregation of the catalyst.<sup>35</sup>

## 2.3. The Suzuki reaction

In general, the Suzuki-Miyaura reaction is the most efficient method to synthesize biaryl products.<sup>28,31,36</sup> The easily handling of air- and moisture stable organoboron starting materials, mild and convenient reaction conditions, high yields and facile removal of the non-toxic byproducts make this reaction extremely useful for industrial applications.<sup>3,28</sup>

Typically, (pseudo)halides are synthesized *via* electrophilic aromatic substitution of simple benzene derivatives and require bromine ( $\text{Br}_2$ ), iodine ( $\text{I}_2$ ) or chlorine ( $\text{Cl}_2$ ) as electrophilic reagents and a Lewis acid (e.g.  $\text{FeCl}_3$ ,  $\text{AlCl}_3$ ,  $\text{SbCl}_3$ ,  $\text{MnCl}_2$ ,  $\text{MoCl}_3$ ,  $\text{SnCl}_4$ ,  $\text{TiCl}_4$ ) as catalyst.<sup>37</sup> These reactions proceed by activation of the electrophile by the Lewis acid, followed by the attack of the activated electrophile by benzene derivative and finally deprotonation to restore the aromatic ring. However, mixtures of isomers and compounds with varying degrees of halogenation are generally obtained and an extra

separation step is required. Furthermore, it is possible to vary the ratios of halogenated products by changing the reaction conditions and the catalyst.<sup>38</sup> Alternatively, (pseudo)halides can be synthesized *via* the Sandmeyer reaction, in which an aryl amine (e.g. aniline) is converted into an aryl halide.<sup>21,39</sup> In this type of reaction, the aryl amine reacts with a stoichiometric amount of nitrous salt (e.g.  $\text{NaNO}_2$ ) to produce a diazonium salt intermediate. Then a SET results in the decomposition of the diazonium intermediate and formation of  $\text{N}_2$  and an aryl radical, which subsequently abstracts a halide from the halogen source (Figure 1.4).<sup>39,40</sup>

For the synthesis of arylboronates, haloarenes are most commonly used as precursors.<sup>41,42</sup> The conventional method is metalation of the haloarene and formation of arylmagnesium or aryllithium that subsequently reacts with trialkyl borates ( $\text{B(OR)}_3$ ) *via* nucleophilic substitution. However, these reactions require anhydrous conditions and flammable solvents under inert atmosphere. Alternatively, transition-metal-catalyzed borylation of aryl C-H bonds (Rh, Ir, Pd, Pt, etc.) with a diboron compound can be used. However, most catalysts are very expensive and sensitive to oxygen and moisture.<sup>42,43</sup> Recently, more and more research is conducted to avoid the intermediacy of aryl halides. Direct borylation of arenes has evolved from stoichiometric reactions with transition-metal boryl reagents. Hartwig, Miyaura and Ishiyama developed a  $[\text{Ir(OMe)(cod)}]_2$  catalyst as precursor, where the regioselectivity was governed by steric factors of the substituted arenes. Furthermore, bidentate ligands are added (e.g. bipyridine ligands), which were essential for the desired reactivity (Figure 1.4).<sup>44</sup>

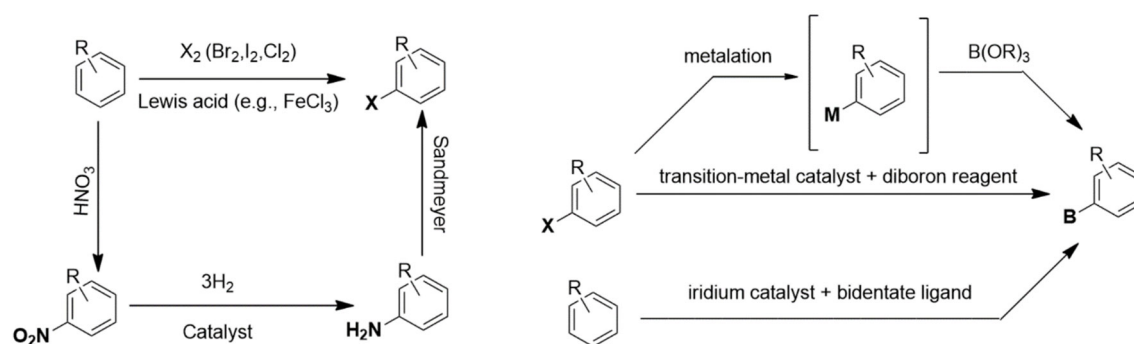


**Figure 1.4:** The most common synthesis routes towards (pseudo)halides (left) and borylated arenes (right).

### 3. Coupling of arenes *via* C-H activation

Although the Suzuki reaction is the most efficient coupling reaction used in industry, it suffers from drawbacks like prefunctionalization of both coupling partners, which generates a lot of waste coming from solvents, reagents and purifications. Moreover, a stoichiometric amount of salt waste is produced after completion of the coupling reaction, which is difficult to separate from the final product. Nowadays, more and more research focuses on the synthesis of biaryl compounds *via* C-H activation, which avoids the use of expensive prefunctionalized substrates and reduces the amount of waste produced, resulting in overall reduction of the environmental impact of traditional organic syntheses.<sup>45</sup>

### 3.1. Direct arylation

In synthesis of biaryl compounds *via* C-H activation reactions, one of the prefunctionalized arenes can be replaced by a simple arene (Figure 1.5 method 1). In this case, coupling occurs between a simple arene and an aryl halide (Ar-H and Ar-X) or between a simple arene and an organometallic arene (Ar-H and Ar-M).<sup>27</sup> The latter reaction is oxidative and requires a terminal oxidant to regenerate the reduced metal.<sup>27</sup> These reactions are usually referred to as “direct arylation reactions” and serve as alternative to Suzuki-Miyaura reactions. The most attractive option is to replace the organometallic arene, which is the less stable compound and the most challenging to prepare.<sup>15,46</sup> This part is not discussed in more detail in this literature study, since no prefunctionalized substrates are used in this master thesis.

### 3.2. Cross-dehydrogenative coupling

An even more environmental benign and possibly cheaper method to synthesize biaryl products is the direct coupling of two simple arenes *via* dual C-H activation (Figure 1.5 method 2). This strategy is usually referred to as “CDC” and has several advantages, such as cheaper substrates, less waste, a shortening of synthesis steps and an overall increased efficiency of the chemical process.<sup>27,32,47,48</sup>

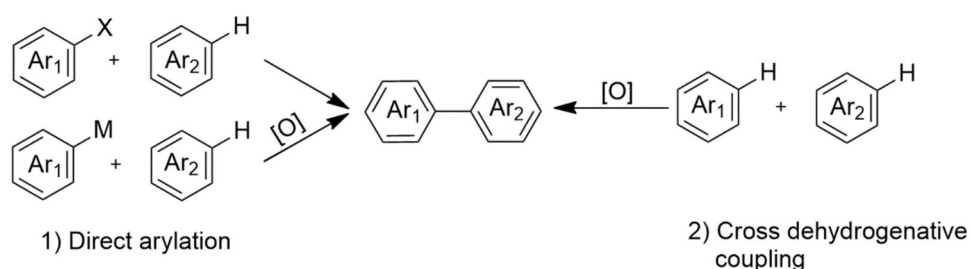


**Figure 1.5:** Direct biaryl coupling versus cross-dehydrogenative coupling.

The C-H activation step faces two challenges. The first challenge is the inert nature of most C-H bonds, resulting from the large dissociation energy of the covalent C-H bond. The second challenge is to control the selectivity towards the cross-coupled product (see also Ullmann reaction). In addition, regioselectivity is an extra challenge in molecules with various C-H bonds, since these molecules can undergo various C-H activations. In order to make the reaction regioselective, site-selective C-H activation is required to obtain the desired regio-isomer (this was not the case in the Ullmann reaction) (Figure 1.6).<sup>14,26,32,49</sup>

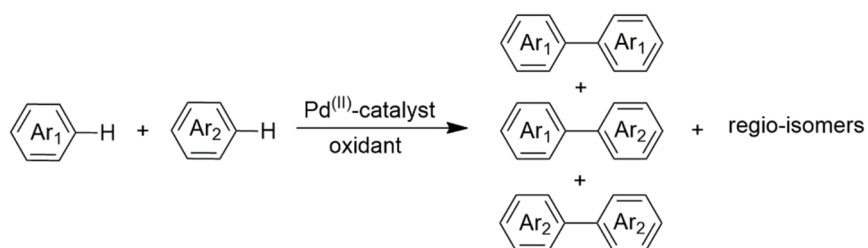


**Figure 1.6:** Coupling reaction between two different substrates ( $\text{Ar}_1\text{-H}$  and  $\text{Ar}_2\text{-H}$ ) can result in the cross-coupling between  $\text{Ar}_1\text{-H}$  and  $\text{Ar}_2\text{-H}$ , but also in the homo-coupling between  $\text{Ar}_1\text{-H}$  and  $\text{Ar}_1\text{-H}$  or  $\text{Ar}_2\text{-H}$  and  $\text{Ar}_2\text{-H}$ . Furthermore, different regio-isomers can be formed, since the substrate can contain several C-H bonds which are all possible candidates for C-H activation.

A possible solution to overcome the challenge of regioselectivity is the use of directing groups (DG), such as phenols, amides, ketones, imines and pyridines (figure 1.7).<sup>46</sup> The role of the DG is twofold. The DG directs the transition metal into close proximity of the C-H bond which need to be activated, resulting in higher regioselectivity but also in an increase in reactivity due to the higher concentration of catalyst at the site of interest. However, the use of a DG is often limited to selectivity in *ortho* position of the DG and limits the scope of possible products. Moreover, additional synthetic steps are often required to install and remove the DG (Figure 1.8).<sup>14,27</sup>

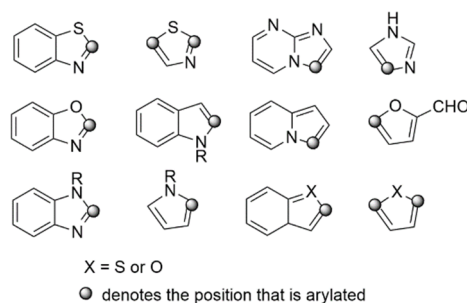


**Figure 1.7:** Examples of hetero-aromatic compounds, having directing groups, which result in C-H activation predominantly at the *ortho*-position.

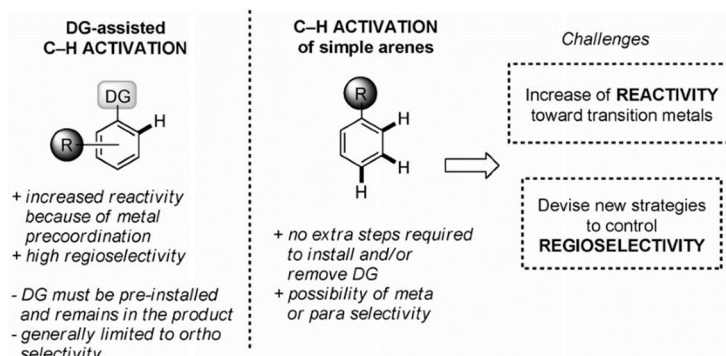


**Figure 1.8:** Comparison of 'DG-assisted' C-H activation and C-H activation of simple arenes.<sup>26</sup>

### 3.2.1. Mechanism

The Pd-catalyzed CDC of arenes consist of a  $\text{Pd}^{\text{III}}/\text{Pd}^{(0)}$  catalytic cycle with 3 general steps: (i) the  $\text{Pd}^{\text{III}}$ -mediated activation of two aryl C-H bonds to produce a  $\text{Pd}^{\text{III}}\text{Ar}_1\text{Ar}_2$  intermediate, (ii) the reductive elimination of  $\text{Pd}^{\text{III}}\text{Ar}_1\text{Ar}_2$  to form the coupled  $\text{Ar}_1\text{-Ar}_2$  product and (iii) the reoxidation of  $\text{Pd}^{(0)}$  to regenerate the active  $\text{Pd}^{\text{III}}$  species (Figure 1.9).<sup>50</sup> A number of variables must be considered in the study of this palladium-mediated reaction: choice of the ligand, solvent used, additives present in the reaction mixtures, etc. All these variables have their influence on the activity and selectivity.<sup>14</sup>

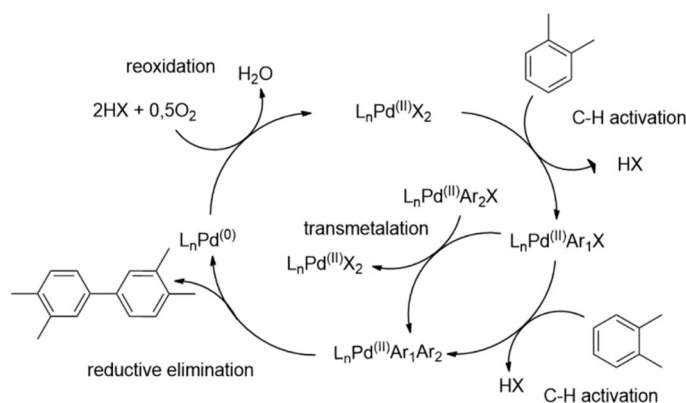


**Figure 1.9:** Pd-catalyzed CDC consist out of (i)  $\text{Pd}^{(II)}$ -mediated activation of two aryl C-H bond to produce a  $\text{Pd}^{(II)}\text{Ar}_1\text{Ar}_2$  intermediate, (ii) reductive elimination of  $\text{Ar}_1\text{Ar}_2$  from  $\text{Pd}^{(II)}\text{Ar}_1\text{Ar}_2$  and (iii) aerobic oxidation of  $\text{Pd}^{(0)}$  to  $\text{Pd}^{(II)}$ .

The C-H activation step involves a C-H to C-Pd refunctionalization, which generates a reactive aryl-palladium intermediate.<sup>30</sup> There are several possible mechanisms for the C-H bond cleavage: (i) oxidative addition, (ii) electrophilic substitution, (iii)  $\sigma$ -bond metathesis, (iv) concerted metalation deprotonation (CMD) and (v) 1,2 addition (Figure 1.10).<sup>48,49</sup>

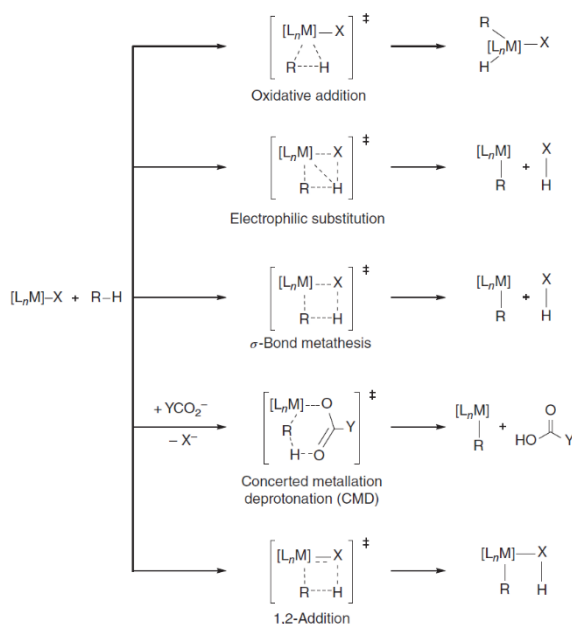


**Figure 1.10:** Several activation mechanisms by transition-metal complexes: (i) oxidative addition, (ii) electrophilic substitution, (iii)  $\sigma$ -bond metathesis, (iv) concerted metalation deprotonation, (v) 1,2-addition.<sup>47</sup>

For the oxidative addition mechanism, transition metals which can increase their oxidation state by two units are preferred. This is the case for several low-valency transition metals, such as  $\text{Pd}^{(0)}$ ,  $\text{Ru}^{(0)}$ ,  $\text{Pt}^{(0)}$ ,  $\text{Rh}^{(I)}$ ,  $\text{Ir}^{(I)}$  and  $\text{Pt}^{(III)}$ .<sup>49</sup> Electrophilic substitution, on the other hand, occurs between C-H bonds of arenes (or alkenes) and high valent, electrophilic transition metal species (e.g.  $\text{Hg}^{(II)}$ ,  $\text{Pd}^{(II)}$ ,  $\text{Pt}^{(II)}$ ,  $\text{Rh}^{(III)}$ ,  $\text{Au}^{(III)}$  and  $\text{Pt}^{(IV)}$ ). Since alkyl-metal intermediates are often not stable, electrophilic substitution mostly refers to electrophilic aromatic substitution.<sup>49</sup> Furthermore,  $\sigma$ -bond metathesis is the addition of a C-H bond to an activated M-C or M-H bond, which is a typical mechanism for early transition metals (scandium, lanthanides and actinides). In the CMD mechanism, an external base (e.g. carboxylate

attached to the transition metal) helps in the deprotonation of the C-H bond.<sup>30</sup> Finally, the 1,2-addition mechanism is the addition of a C-H bond to an unsaturated bond (e.g. C=M), which generates a C-M bond. This type of reaction occurs rarely and is mostly observed when early and middle transition metal are used (Zr<sup>(IV)</sup>, Ti<sup>(IV)</sup> and W<sup>(VI)</sup>).<sup>48,49</sup>

The most common mechanism of C-H bond cleavage in direct arylation reactions is the electrophilic aromatic substitution, and thus the reaction between an electrophilic Pd-species and an electron-rich nucleophilic aromatic ring. However, this pathway is commonly not suitable for simple and electron-deficient arenes in CDC reactions. The most typical pathway for simple arenes is considered to be the CMD mechanism, which is mainly catalyzed by metals such as Pd<sup>(II)</sup>, Ru<sup>(II)</sup> and Rh<sup>(III)</sup>. This mechanism depends not only on the electrophilicity of the Pd-complex and the electron density of the arene, but also on the acidity of the C-H bond being cleaved.<sup>48,49</sup>

The dual C-H activation can occur sequentially at one single Pd<sup>(II)</sup> center ("monometallic pathway") or *via* a parallel C-H activation at two separate Pd<sup>(II)</sup> centers followed by a transmetalation step between the two Pd<sup>(II)</sup>-aryl intermediates ("bimetallic pathway") (Figure 1.11).<sup>50</sup>

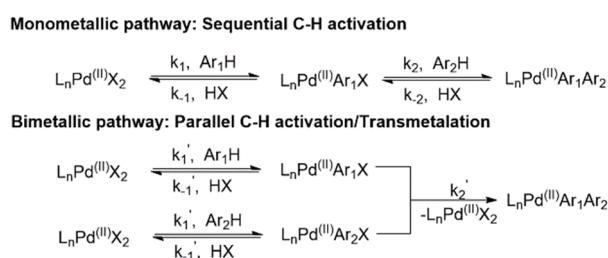


**Figure 1.11:** Two pathways for Pd<sup>(II)</sup>ArAr' formation: at a single Pd<sup>(II)</sup> center ("monometallic"), at two separate Pd<sup>(II)</sup> centers followed by transmetalation ("bimetallic").

In the next step, the biaryl product is formed during the reductive elimination, leaving a reduced Pd<sup>(0)</sup> center. In order to close the catalytic cycle, the Pd<sup>(0)</sup> center needs to be reoxidized to the active Pd<sup>(II)</sup> complex, which requires a terminal oxidant, such as K<sub>2</sub>S<sub>2</sub>O<sub>8</sub>, benzoquinone, Cu<sup>(II)</sup>, Ag<sup>(I)</sup>, peroxides or O<sub>2</sub>.<sup>51</sup> The Pd<sup>(0)</sup> center is susceptible for aggregation into Pd<sup>(0)</sup> NPs. These Pd<sup>(0)</sup> NPs are difficult to reoxidize, which eventually leads to catalyst deactivation.<sup>14</sup>

### 3.2.2. Catalytic system

The electronic and steric nature of the ligand, as well as the coordination number of Pd, have an influence on the different steps in the catalytic cycle and can affect the activity and selectivity of the CDC reaction. The phosphine ligands and NHC ligands used in the traditional catalytic cross-coupling reactions (e.g. Suzuki reaction) are not stable under oxidative conditions due to their susceptibility to form phosphine oxides or ureas under these conditions.<sup>29,34</sup> Hence, the oxidative systems make use of different ligand classes, such as sulfoxides, amines, pyridines and carbene derivatives.<sup>34,52,53</sup> For a ligand-controlled metal-catalyzed reaction, the selection and design of the ligand needs to be adapted

to the properties of the substrate and the metal.<sup>29,54</sup> The first problem of the Pd-catalyzed CDC is that the  $\pi$ -systems of the electron-deficient arenes are rather poor  $\sigma$ -donors, which means that they are unable to form a stable bond with Pd<sup>(II)</sup>. A second problem is that high reactivity of electron-poor arenes can only be achieved when the electrophilicity of the Pd<sup>(II)</sup> catalyst is greatly enhanced to favor the C-H activation step. Addition of strong acids (e.g. trifluoroacetic acid (TFAH)) can increase the electrophilicity of the Pd<sup>(II)</sup> catalyst and thus facilitate the C-H activation step.<sup>54</sup> Moreover, the anionic ligands of the active Pd<sup>(II)</sup> complex (e.g. acetate in Pd(OAc)<sub>2</sub>, carbonate, etc.) play an important role in the CMD mechanism. Due to the presence of a basic ligand, the C-H bond is readily deprotonated and the formation of the Pd-Ar intermediate is facilitated.<sup>8,14</sup>

The coordination of ligands has an impact on the structure and thus performance of the metal catalyst. The ligand can change the activation energy of the elementary steps in a given catalytic process, resulting in a change in kinetic activity of the catalyst. In addition, ligands can influence (increase or decrease) the selectivity (enantioselectivity, diastereoselectivity, regioselectivity and chemoselectivity) towards the preferred product.<sup>14,55,56</sup> In order to obtain a high selectivity, the catalyst must be able to recognize minor differences in steric and electronic environments of the different C-H bonds, promoting selective C-H cleavage.

Besides increasing the activity and selectivity of the catalyst, ligands can also extend the catalyst lifetime by stabilizing the Pd<sup>(0)</sup> centers and promoting the reoxidation step. The agglomeration of the Pd<sup>(0)</sup> atoms results in less catalytically active Pd<sup>(0)</sup> NPs and finally in a complete deactivation of the catalyst, since these large Pd<sup>(0)</sup> NPs cannot easily be reoxidized (Figure 1.12).<sup>57</sup> Generally, there are two strategies to increase the TON per palladium atom in oxidative coupling reactions. First, the addition of ligands which stabilize the Pd<sup>(0)</sup> centers and, secondly, by isolating the Pd centers on a heterogeneous support, which limits aggregation into large Pd<sup>(0)</sup> NPs (see III).<sup>58</sup>

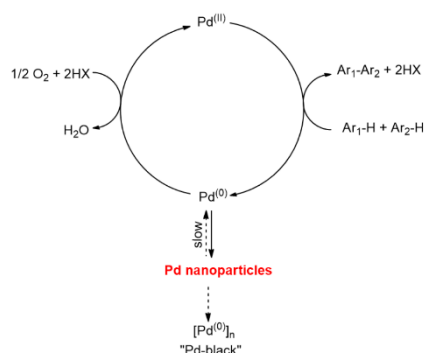


**Figure 1.12:** Formation of palladium nanoparticles by aggregation of Pd<sup>(0)</sup> centers. When these Pd<sup>(0)</sup> NPs keep growing, the catalyst deactivates due to the formation of 'Pd-black'.



The most popular palladium species to catalyze CDC reactions is palladium acetate. This complex occurs, in absence of ligands, predominantly as a trimer ( $\text{Pd}_3(\text{OAc})_6$ ) and all three palladium atoms have a square planar environment (Figure 1.13). However, two common impurities are often present in the commercially available trimeric palladium acetate samples, including  $\text{Pd}_3(\text{OAc})_5(\text{NO}_2)$  and the insoluble polymeric species  $[\text{Pd}(\text{OAc})_2]_n$ .<sup>59</sup> Fortunately, these impurities have usually only limited impact on the catalytic performance.<sup>60,61</sup>

The precise nature of the active palladium acetate species in the reaction mixture depends on several factors, such as the solvent, additives, ligands, substrate and relative Pd concentration. It is possible to break up the trimeric species into monomeric species by addition of a ligand, even in non-polar solvents such as benzene or toluene (Figure 1.13).<sup>62</sup> In general, the dimeric and polymeric Pd species have a higher energy barrier for the C-H activation than the mononuclear Pd complexes.<sup>61,62</sup>

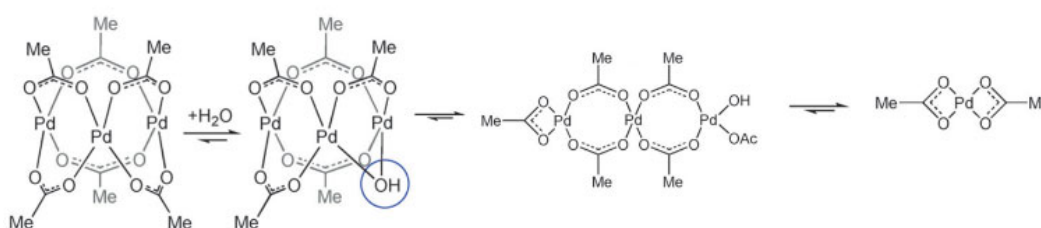


**Figure 1.13:** Hydrolysis of the palladium acetate precursor into monomeric palladium acetate. The presence of ligands can facilitate the breakup of the trimeric species into monomeric species.<sup>61</sup>

### 3.2.3. Oxidative coupling of *o*-xylene as model reaction

The homo-coupling of *o*-xylene is an interesting model reaction, since no problems of cross-coupling are present and only three regio-isomers can be formed. Moreover, the homocoupling of *o*-xylene is also industrially relevant for the production of high-performance polyimide (Upilex®). Industrially, Upilex® is synthesized *via* a Pd/Cu catalyzed oxidative CDC of phthalate to produce the 4,4'-biphtalic anhydride monomer, which takes 5 steps in total (Figure 1.14, route A). However, the reaction route towards the 4,4'-biphtalic anhydride monomer could potentially be shortened to a 2 step process. This reaction route consists of a homocoupling of *o*-xylene followed by the oxidation of the 3,3',4,4'-tetramethylbiphenyl product into the 4,4'-biphtalic anhydride monomer (Figure 1.14, route B).<sup>55</sup>

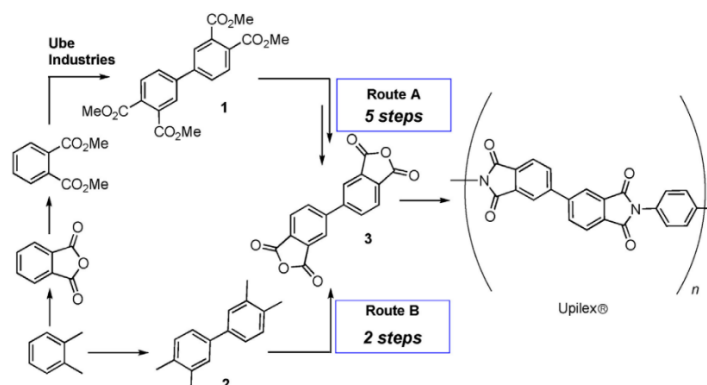


**Figure 1.14:** Current and proposed routes for the industrial synthesis of 4,4'-biphtalic anhydride.<sup>54</sup>

The homocoupling of simple arenes (e.g. toluene, *o*-xylene, etc.) is generally associated with low regioselectivity, since several C-H bonds can be activated. For *o*-xylene, the low regioselectivity results in a mixture of three bixylyl isomers (2,2',3,3'-tetramethylbiphenyl (A), 2,3,3',4'-tetramethylbiphenyl (B) and 3,3',4,4'-tetramethylbiphenyl (C)). However, only the *para*-isomer (C) is useful for the synthesis of Upilex®. Furthermore, oxidation and oligomerization of the bixylyl products result often in rather low chemoselectivity.<sup>8</sup> To avoid oligomerization of the bixylyl products, these reactions are typically halted at low conversions and the remaining feedstock is recycled.<sup>53</sup>

The TON can be defined as the amount of moles formed (yield) of the products (bixylyl isomers) divided by catalyst loading.<sup>53,63</sup>

$$TON = \frac{\% \text{ yield}}{\% Pd} = 2 * \frac{n_A + n_B + n_C}{n_{Pd}}$$

With  $n_A$ ,  $n_B$  and  $n_C$  the molar amounts of the three bixylyl isomers (A), (B) and (C) and  $n_{Pd}$  the molar amount of palladium used in the reaction. The multiplication by 2 in the numerator arises from the fact that two *o*-xylene molecules are required to form only one bixylyl product.

The chemoselectivity can be defined as the amount of bixylyl isomers formed (yield) divided by the amount of *o*-xylene reacted.

$$S_C = 100\% * \frac{2 * (n_A + n_B + n_C)}{n_{o-xylene, initial} - n_{o-xylene, final}}$$

The regioselectivity can be defined as the amount of the desired isomer divided by all bixylyl products.

$$S_R = 100\% * \frac{n_C}{n_A + n_B + n_C}$$

To activate the inert C-H bonds of *o*-xylene efficiently, highly electrophilic Pd<sup>(II)</sup> centers are required.<sup>7,8,64</sup> It was proven by the group of Stahl that the combination of palladium acetate as precursor, TFAH as strongly acidic additive and a special type of pyridine ligand (e.g. 2-fluoropyridine (<sup>2F</sup>pyr) or pyridine), resulted in an active and selective Pd complex for the formation of the 3,3',4,4'-tetramethylbiphenyl isomer.<sup>7,8,14,65,66,67</sup>

Stahl and coworkers showed in 2010 that the addition of special pyridine-type ligand can increase the selectivity, without decreasing the activity.<sup>8</sup> Very recently, Fernández-Ibáñez and coworkers studied the exact effect of the pyridine-type ligands in more detail. It is important to ascertain that the pyridine-type ligands itself cannot undergo a cyclopalladation, but also proper design of electronic and steric features is important, which not only controls the chemo- and regioselectivity but also the

activity. Due to their electron donative character, pyridines are expected to coordinate rather strongly to the palladium catalyst, resulting in a less active catalyst complex. However, due to their strong coordination to Pd, they affect the steric features of the catalyst complex, resulting in a higher regioselectivity towards the 3,3',4,4'-tetramethylbiphenyl isomer. In contrast, more electron poor pyridines (e.g. <sup>2</sup>Fpyr) are expected to coordinate less strongly to palladium, which results in a more active catalyst, but in a slightly lower regioselectivity, since the steric features are only operative when palladium is coordinated by the pyridine-type ligand.<sup>55</sup>

Stahl *et al.* showed in a later report that the aforementioned system, using TFAH and a pyridine-type ligand, can be improved by addition of Cu(OTf)<sub>2</sub> (OTf = trifluoromethanesulfonate) instead of TFAH, which results in a significant beneficial impact on the TON.<sup>7</sup> It was proposed that the addition of Cu(OTf)<sub>2</sub> results in the formation of another major species, where <sup>-</sup>OAc is replaced by <sup>-</sup>OTf in the coordination sphere of palladium. It was also shown that the mixed-anion Pd(OTf)(OAc) complex is more active than Pd(TFA)(OAc), due to a lower activation barrier for the C-H activation, but also more active than Pd<sup>(III)</sup> species with other combinations of <sup>-</sup>OAc, TFA and <sup>-</sup>OTf anionic ligands. These results are in accordance with the CMD mechanism, in which both a weakly coordinating anion is necessary to enhance the electrophilicity of the Pd<sup>(III)</sup> intermediate and a basic carboxylate group to take up the proton.<sup>7,14</sup> Cu<sup>(III)</sup> is typically assumed to serve as an oxidant or redox-active co-catalyst. However, it was proven that Cu(OTf)<sub>2</sub> plays a non-redox role in this catalytic reaction and Cu(OTf)<sub>2</sub> could be replaced by other triflate salts (e.g. Zn<sup>(III)</sup>, Al<sup>(III)</sup>, Bi<sup>(III)</sup>) with non-redox active cations. Moreover, it was shown that the Lewis acidity of the cation appears to be important, since monovalent cations like Ag<sup>(I)</sup> and Na<sup>(I)</sup> are less effective compared to di- and trivalent cations.<sup>7</sup>

In another publication by the group of Stahl, it was evidenced that the C-H activation step in the CDC of *o*-xylene occurs *via* the bimetallic pathway with transmetalation rather than *via* the monometallic pathway (see *supra* for derivation Figure 1.11). The monometallic pathway always exhibits a first order dependence on [Pd], while the bimetallic pathway can have a first order dependence (in case of rate-limiting C-H activation) or a second order dependence (in case of rate-limiting transmetalation) (Figure 1.15).<sup>50</sup>

**Rate law monometallic pathway:**

$$\frac{d[\text{ArAr}]}{dt} = \frac{k_1 k_2 [\text{Pd}][\text{ArH}]^2}{k_{-1} [\text{HX}] + k_2 [\text{ArH}]} \sim k_{\text{obs}} [\text{Pd}]$$

**Rate law bimetallic pathway (rate-limiting C-H activation):**

$$\frac{d[\text{ArAr}]}{dt} = \frac{k_1}{2} [\text{Pd}][\text{ArH}] \sim k_{\text{obs}} [\text{Pd}]$$

**Rate law bimetallic pathway (rate-limiting transmetalation):**

$$\frac{d[\text{ArAr}]}{dt} = \frac{k_1^2 \cdot k_2 [\text{Pd}]^2 [\text{ArH}]^2}{k_{-1}^2 [\text{HX}]^2} \sim k_{\text{obs}} [\text{Pd}]^2$$

**Figure 1.15:** Rate law for the “monometallic” and “bimetallic” mechanism. The rate law in the bimetallic mechanism changes from first order dependence (in case of rate-limiting C-H activation) to second order dependence (in case of rate-limiting transmetalation).

At low [Pd], a lower steady-state concentration of  $[L_nPd^{(II)}ArX]$  is formed and the transmetalation is rate-limiting. Additionally, the C-H activation is reversible ( $k_{-1}'$  term present in the denominator) under these conditions, which also results in a lower concentration of  $[L_nPd^{(II)}ArX]$ . In contrast, at higher [Pd], the bimetallic transmetalation rate increases and becomes faster than the unimolecular C-H activation, which causes a rate-limiting C-H activation.<sup>50</sup>

Both the group of Stahl and the group of Fernández-Ibáñez revealed that the rate-limiting step in the CDC of *o*-xylene can be identified by evaluation of the deuterium kinetic isotope effect (KIE) with the use of *o*-xylene- $d_{10}$ . Moreover, it was found the reaction conditions (catalyst concentration, solvent, etc.) determine which step of the catalytic cycle will be rate-limiting step.<sup>5,6,55</sup>

In case of a rate-limiting C-H activation step, a moderate substrate KIE of  $k_H/k_D \sim 3-5$  is observed. The theoretical 1/solvent KIE is 1 in this case, this arises from the fact that no  $k_{-1}'$  term is present in the equation of the rate law (Figure 1.15). When acetic acid was used as solvent, Stahl observed higher substrate KIE's, reaching values of  $k_H/k_D \sim 9-25$ . This is due to protonolysis (or reversible C-H activation), which occurs faster in acetic acid compared to other solvents, such as weaker acids. The faster protonolysis results in a lower steady-state concentration of  $[L_nPd^{(II)}ArX]$  and transmetalation becomes rate-limiting. Furthermore, the 1/solvent KIE reaches also values of  $\sim 9-25$  in transmetalation rate-limiting conditions due to the presence of the squared  $k_{-1}'$  term in the rate equation (Figure 1.15).<sup>5,6</sup> Fernández-Ibáñez discovered the near absence of a substrate KIE ( $k_H/k_D \sim 1$ ) when a non-polar solvent is used or without the use of any solvent. This might point at a rate-limiting dissociation of a carboxylate-bridged palladium dimer into two monometallic species. Arene C-H activation only takes place after formation of an adequate amount of monometallic  $Pd^{(II)}$  species with weakly bounded solvent-molecule (which is promoted by use of coordinating solvents such as acetic acid or propylene carbonate). When polar solvents (e.g. propylene carbonate) are used, the dissociation of the carboxylate-bridged dimer is no longer rate-limiting and C-H activation becomes rate-limiting again.<sup>5,6,55</sup>

## II. Metal-organic frameworks

MOFs are a class of porous, crystalline materials with an extended polymeric structure. These materials are constructed by connecting inorganic nodes (metal clusters or metal ions) and organic linkers through coordination bonds. The applicability of the MOF is mostly determined by the organic linkers due to impact on the pore size, the geometry and the functional groups, while the inorganic nodes mainly define the chemical and thermal stability, since the most vulnerable sites of the framework are the metal-ligands bonds.<sup>68</sup>

The stability of MOFs is influenced by several factors, such as the  $pK_a$  of the ligands, oxidation state of the metal, metal-linker geometry, hydrophilicity of the pores, operating environment, defects, etc. One way to increase the stability of MOFs, is the use of high valent metals (e.g. Zr-MOFs) in combination with carboxylate linkers. The high valent metals cause a high charge density and bond polarization which results in a strong affinity between the  $Zr^{(IV)}$  metal ions and carboxylate O atoms of the organic linkers. This is in line with Pearson's hard/soft acid/base principle, which predicts strong coordination bonds between hard Lewis acids (e.g. the  $Zr^{(IV)}$  ions) and hard Lewis bases (e.g. the carboxylate linkers) or soft Lewis acids and bases. In addition, high valent metals require generally more linkers to balance the charge, resulting in a higher coordination number and a more rigid framework structure.<sup>68,69</sup>

The stability of the MOF is also influenced by the operating environment. MOFs consisting of high-valent metal ions and carboxylate-based linkers are usually stable under acidic conditions, but not under basic conditions. The strong affinity between hydroxyl ions ( $OH^-$ ) and the high-valent metal ion results in the replacement of the linker by  $OH^-$  and, ultimately, in the decomposition of the MOF.<sup>68,69</sup>

### 1. Zirconium-MOFs with carboxylate linkers

Many zirconium-based MOFs contain an octahedral  $Zr_6$ -cluster  $[Zr_6(\mu_3-O)_4(\mu_3-OH)_4]$  and are especially stable to high temperatures, a wide pH range in aqueous solutions and also represent high mechanical stability.<sup>70</sup> These  $Zr_6$ -clusters can be 12-, 10-, 8-, or 6-connected, which refers to the amount of carboxylate linkers attached to each  $Zr_6$ -cluster. Each missing carboxylate can be replaced by a charge balancing labile  $OH^-/H_2O$  group, which is susceptible for substitution (e.g. by ligands or metals).<sup>69,71</sup>

The combination of different organic linkers with Zr-salts has led to the synthesis of many Zr-MOFs. Aromatic polycarboxylates are most commonly used and are classified based on the amount of carboxylate groups: (1) ditopic, (2) tritopic and (3) tetratopic carboxylate linkers.<sup>69</sup> Linear ditopic carboxylate linkers have been widely exploited in the synthesis of Zr-MOFs. Commonly used ditopic carboxylate linkers are terephthalate ( $bdc^{2-}$ ) or biphenyl-4,4'-dicarboxylate ( $bpdc^{2-}$ ). These linkers are used for synthesis of UiO-66 and UiO-67, respectively. In UiO-66, all twelve edges of the  $Zr_6$ -cluster are

occupied by the carboxylates of the  $\text{bdc}^{2-}$  linkers, resulting in the **fcu** topology. An open framework with tetrahedral and octahedral cages is formed (figure 1.16). When the length of the linkers is increased, several isorecticular (see further) Zr-MOFs are established, such as UiO-67 and UiO-68.<sup>69,71</sup>

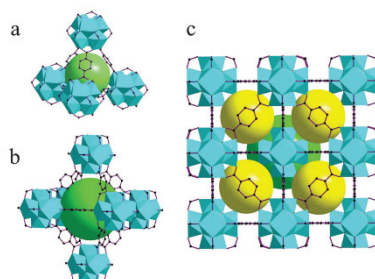


**Figure 1.16:** Structure of UiO-66 (a) tetrahedral cage, (b) octahedral cage and (c) two type of cages.<sup>68</sup>

Another interesting example of a MOF consisting of a ditopic linker is PCN-700 (PCN = porous coordination network). In this case 2,2'-dimethylbiphenyl-4,4'-dicarboxylate ( $\text{Me}_2\text{-bpd}^{2-}$ ) is used as linker, which results in an 8-connected Zr-cluster with **bcu** topology. A flexible net with breathing behavior is created, which can shrink along the c-axis while expanding within the ab-plane. This breathing behavior occurs upon introduction or removal of guest molecules. The PCN-700 ( $\text{Me}_2\text{-bpd}^{2-}$  linker) can be regarded as a structural derivative of UiO-67 ( $\text{bpd}^{2-}$  linker). The symmetry of the crystal is reduced from cubic to tetragonal, resulting in the change from **fcu** to **bcu** topology (Figure 1.17).<sup>69,72,73,74</sup>

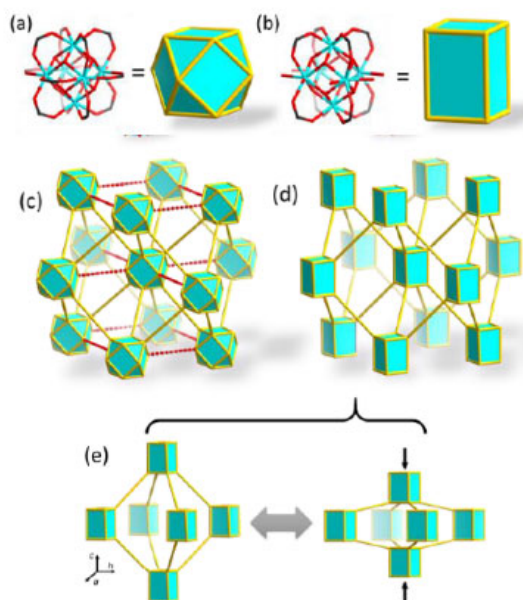


**Figure 1.17:** 12-connected cluster in **fcu** net (a), resulting in UiO-67 net structure with **fcu** topology (c), 8-connected cluster in **bcu** net (b), resulting in PCN-700 structure with **bcu** topology (d) and breathing behavior (e): flexible single bipyramid, shrinking along the c-axis while expanding within the ab-plane.<sup>73</sup>

For the tritopic carboxylate linkers, benzenetricarboxylate ( $\text{btc}^{3-}$ ) is a commonly used example of organic linker. The combination of this linker with a Zr-salt results in MOF-808, which consist of a 6-connected  $\text{Zr}_6$ -cluster with **spn** topology. The terminal ligands at the  $\text{Zr}_6$ -cluster are located equatorially and are generally formate or acetate ions. The framework of MOF-808 consists of tetrahedral cages with an internal pore diameter of 4.8 Å. Furthermore, a large adamantane-like cage is formed with an internal pore diameter of 18.4 Å by connection of the tetrahedral cages (Figure 1.18).<sup>69,75</sup>

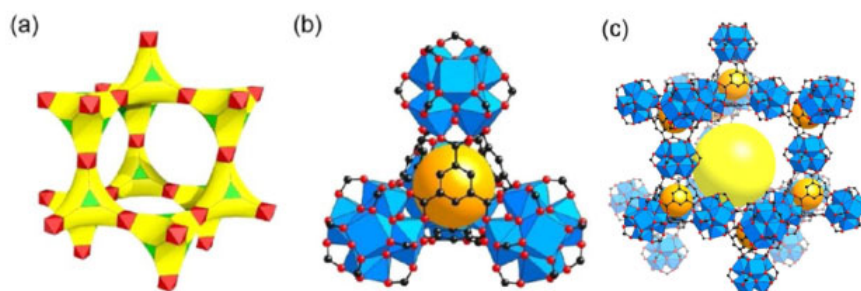


**Figure 1.18:** Representation of **spn** topology (a) of MOF-808 which consist of tetrahedral cages (b) (orange) and large adamantine pores (c) (yellow).<sup>74</sup>

Commonly used tetratopic linkers are 3,3',5,5'-biphenyltetracarboxylate ( $\text{bptc}^{4-}$ ) or 3,3',5,5'-azobenzene-tetracarboxylate ( $\text{abtc}^{4-}$ ), which respectively result in a 12-connected  $\text{Zr}_6$ -cluster with octahedral symmetry, cage-like pores and **ftw** topology and a 8-connected  $\text{Zr}_6$ -cluster with  $\text{D}_{4h}$  symmetry and **scu** topology. The connectivity of the  $\text{Zr}_6$ -cluster can be further reduced by changing the linker to 2',5'-dimethyl-[1,1':4',1''-terphenyl],3,3'',5,5''-tetracarboxylate ( $\text{tptc}-(\text{Me}_2)$ ), resulting in a 4-connected  $\text{Zr}_6$ -cluster with **lvt** topology (Figure 1.19).<sup>76</sup>

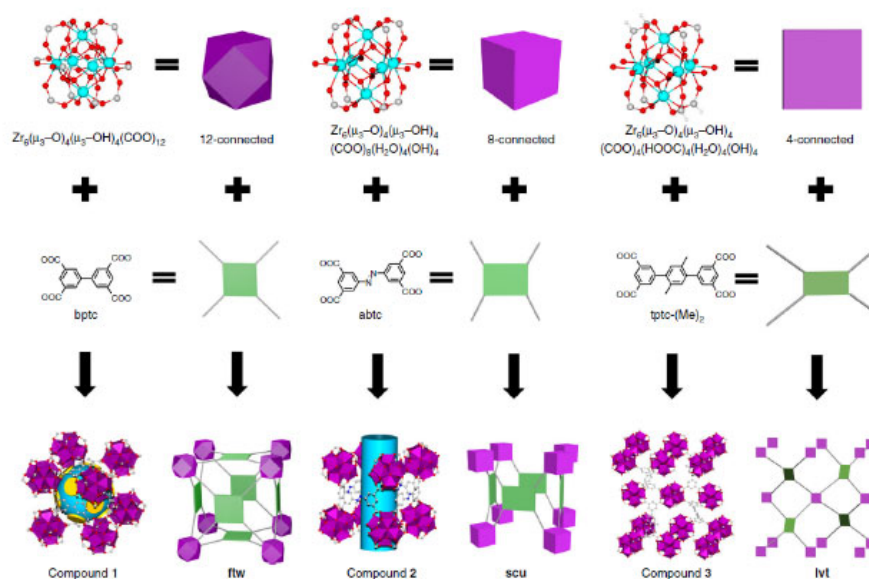


**Figure 1.19:** Use of tetratopic organic ligands  $\text{bptc}^{4-}$ ,  $\text{abtc}^{4-}$  and  $\text{tptc}-(\text{Me}_2)^{4-}$  result respectively in 12-,8- and 4-connected  $\text{Zr}_6$ -cluster with **ftw**, **scu** and **lvt** type structures.<sup>75</sup>

## 2. Synthesis

Conventionally, MOF synthesis occurs under solvothermal conditions. However, many alternative synthesis routes have appeared, such as microwave-assisted synthesis, electrochemical synthesis, sonochemical synthesis, mechanochemical synthesis and spray-dry synthesis.<sup>77</sup> The synthesis of MOFs by only making use of metal salts and organic linkers usually leads to quick precipitation of low crystalline powders, since the conditions are unfavorable for defect repair during the crystallization process.<sup>69,71</sup> In modulated synthesis, the coordination equilibrium is controlled by the introduction of modulators with similar chemical functionalities as the organic linkers. This results in a competitive interaction of the modulator and the organic linker for coordination with the metal ions, slowing down the rate of nucleation and crystal growth, allowing the formation of highly crystalline products.<sup>69</sup>

Isorecticular expansion can be used to increase the pore size and surface areas by expanding the structure of an already existing MOF. The surface area can be increased by making use of larger linkers, but the framework stability is not guaranteed and is mostly inversely correlated. This is for example the case for UiO-66 (bdc<sup>2-</sup> linker) and UiO-67 (bpdc<sup>2-</sup> linker).<sup>10,69</sup>

Another special feature of several Zr-MOF is the possibility to introduce defects. Due to the high connectivity of the Zr<sub>6</sub>-cluster, it is possible to introduce defects without severe loss in crystallinity or stability. There are two different types of defects: missing-linker and missing-cluster defects. In the former case, the organic linker is removed from a pair of neighboring Zr<sub>6</sub>-clusters, leaving unsaturated Zr<sub>6</sub>-clusters in which the coordination vacancy is usually terminated by –OH<sup>+</sup>/H<sub>2</sub>O or a monocarboxylate to balance the charge. In the case of missing cluster defects, entire Zr<sub>6</sub>-clusters are missing. These missing linker and missing cluster defects are generally distributed randomly in the MOF particle. Moreover, the amount and the nature of defect sites can be controlled by synthetic conditions like metal to linker ratio, the selection of a modulator (type and concentration), reaction temperature, etc.<sup>71</sup>

## 3. Post-synthetic modification

The functional groups of the organic linkers and metal clusters in Zr-MOFs can be tailored *via* post-synthetic modification (PSM). PSM embodies various ways of modification, such as covalent modification, surface functionalization, post-synthetic metalation and solvent assisted ligand incorporation (SALI).<sup>70</sup>

In covalent modification, a variety of functional groups are anchored onto the pore walls with control of loading, density and functionality.<sup>69,71</sup> Covalent modification is based on the reactivity of pendant or integral functional moieties on the organic linker of the MOF. Amine groups (e.g. UiO-66-NH<sub>2</sub> with NH<sub>2</sub>-bdc linkers) are often used as pendant functional moieties due to the large variety of possible



chemical transformations. An example of pendant covalent modification is the subsequent reaction of UiO-66-NH<sub>2</sub> with acid anhydrides, salicylaldehyde or 2-methyl-aziridine, resulting in amide, imine or alkyl-amine functionalized pores, respectively. Examples of PSM at pendant functional groups are more abundant than examples of integral covalent modification as a consequence of the lower reactivity of structural components (e.g. integral linker sites).<sup>70</sup>

In surface functionalization, the PSM is limited to the outer surface of the MOF, by employing modifying agents which are too large to penetrate the pores of the MOF. In this way, interesting properties can be induced (e.g. tuning of the hydrophobicity of the surface), which can be exploited in a wide range of applications (e.g. removal of organic compounds from water).<sup>70</sup>

In PSM, free chelating groups of the linker can coordinate with metals or the Zr<sub>6</sub>-cluster itself can act as an acid to bind metal cations as a base when coordinatively unsaturated sites are present. It is not always necessary to have an unsaturated Zr<sub>6</sub>-cluster, in fact, the  $\mu_3$ -OH groups of 12-connected Zr<sub>6</sub>-cluster can be deprotonated by a strong base (e.g. AuMe(PMe<sub>3</sub>), CH<sub>3</sub>MgBr, etc.), which results in replacement of protons by metal cations.<sup>69,71,77</sup>

Finally, SALI makes it possible to incorporate ligands coordinatively to unsaturated Zr<sub>6</sub>-clusters. These attached ligands are believed to coordinate to the Zr<sub>6</sub>-cluster by replacement of the -OH<sup>-</sup>/H<sub>2</sub>O pairs. In this way, the pore sizes and functionality can easily be tuned by making use of a different set of ligands of various lengths and with several functional groups.<sup>71,77,78</sup>

### III. Immobilization of homogeneous catalyst on MOFs

In homogeneous CDC, Pd complexes can decompose during the catalytic cycle by the formation of Pd<sup>(0)</sup> NPs, resulting in a decrease in activity.<sup>58</sup> This problem can be solved by the use of specific ligands with P, N or electron rich C atoms as binding sites, which can result in very stable and active Pd. Moreover, they can also give rise to high selectivity.<sup>34,48,52,79,80</sup> In addition, the Pd content in the final product has to be below a certain ppm level for many drugs and other fine chemicals.<sup>81</sup> In order to achieve this, the homogeneous catalyst need to be separated from the product solution, which requires the use of expensive nanofiltration membranes or extensive column chromatography separation.<sup>47</sup> These drawbacks have triggered research to convert homogeneous systems into heterogeneous systems, in which the catalyst can easily be recovered from the reaction medium and readily reused.<sup>53,58,80</sup>

Porous materials on which the Pd complex can be anchored are preferred, since they have high surface areas and good access to the active sites. In this context, MOFs are materials of high interest to attach Pd-complexes on.<sup>38-40,64,80,82-85</sup> MOFs are enormously versatile materials in the field of heterogeneous materials with important properties for catalysis, such as their high surface areas and open porosity,

which reduces mass transfer limitations.<sup>86</sup> However, there are more conditions to be met in order to obtain a good heterogeneous catalyst such as structural stability under reaction conditions (reagents, solvents, temperature, pressure, etc.).<sup>81</sup>

## 1. MOF as support for palladium NPs

Due to their large pore volume, several MOFs can serve as host material to incorporate metal NPs. The support plays an important role in preventing the aggregation of the NPs by controlling the dimension, dispersion and stability of the metal NPs and avoids their growth under the reaction conditions.<sup>57,80</sup> This approach has the advantage of eliminating the synthesis of organic ligands.<sup>57,81</sup> Moreover, the uniformity of pores in MOFs allows channels with a strict geometry which can be used for size and shape-selective catalysis. In order to obtain a MOF with size and shape-selectivity, it is important to select the proper inorganic nodes and organic linker to ensure enough free internal space.<sup>86</sup>

An example is the use of MOFs as support for nanosized catalysts for Suzuki cross-coupling reactions. However, the nature of the true catalytic species is controversial, since Ostwald ripening of these Pd<sup>(0)</sup> NPs occurs during the reaction and results in an important degree of atomic species in solution, which can also catalyze the reaction (Figure 1.20).<sup>29,47,57,82</sup> Fast redeposition of these atomic Pd species under properly chosen reaction conditions may eliminate leaching and makes reuse feasible. In this way, it is possible to obtain a high cumulative TON.<sup>82</sup>

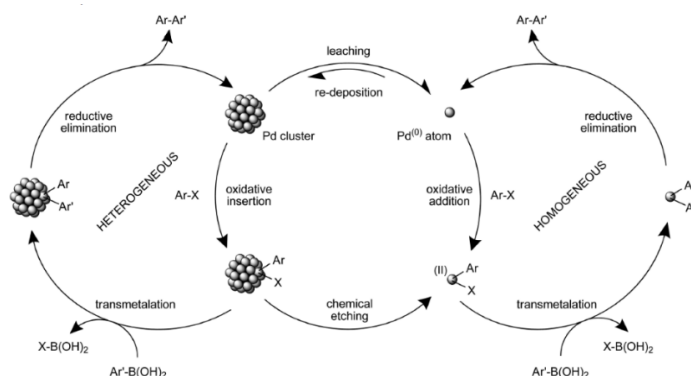


**Figure 1.20:** Proposed mechanism for the Pd NP-catalyzed Suzuki cross-coupling reaction involving both homogeneous and heterogeneous pathways.<sup>82</sup>

## 2. MOFs as support for palladium complexes

Anchoring organometallic complexes on a porous solid is a promising way to combine the unique properties of both homo- and heterogeneous systems.<sup>80</sup> The immobilization of the Pd complexes results in a single-site catalyst and may allow for the tuning of the catalytic activity in a similar fashion as ligand modification in a homogeneous system.<sup>87</sup> However, the main challenge is to overcome the lack of stability of the Pd complexes under the harsh reaction conditions, leading to the formation of larger Pd<sup>(0)</sup> NPs.<sup>29,53</sup>

MOFs are suitable for immobilizing the catalytically active metal species since they can have attachment sites on the metal nodes or pendant functional groups on the organic linkers. The attachment sites on the metal nodes of MOFs are geometrically undercoordinated and commonly referred to as Open Coordination Sites (OCSs).<sup>57,69,87</sup> The OCSs can be generated during the synthesis of the MOF or by PSM and are prompt to interact with electron-rich substituents.<sup>87</sup> Isolation of palladium on the MOF OCSs can inhibit aggregation of Pd<sup>(0)</sup> and thus catalyst deactivation.<sup>88</sup> An example of a MOF with pendant functionalities for Pd immobilization is thiocatechol functionalized UiO-66, formed after solvent assisted linker exchange to obtain UiO-66-TCAT. After addition of Pd(OAc)<sub>2</sub>, a catalytically active MOF is obtained, which is efficient for regioselective sp<sup>2</sup> functionalization of C-H bonds (Figure 1.21).<sup>89</sup>

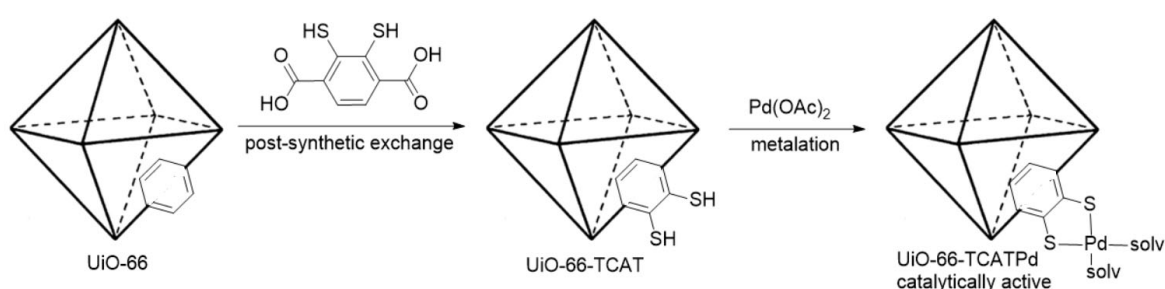


**Figure 1.21:** Schematic overview of the synthesis of UiO-66-TCATPd.

Another approach could be the design of a MOF material with adequate ligands (e.g. ligands similar as under homogeneous condition) attached to OCSs, which can fine-tune the activity and selectivity of the active Pd complex. The OH<sup>-</sup>/H<sub>2</sub>O groups on coordinative unsaturated metal centers can be displaced by ligands *via* SALI (Figure 1.22). In order to do this, the ligands need to have at least two functionalities. Firstly, a charge compensating carboxylate, phosphonate or similar groups, to attach it to the heterogeneous support. Secondly, another functionality like an amine, hydroxyl, pyridine, aromatic halide, etc. to interact with the Pd<sup>(II)</sup> complex in a similar fashion as under homogeneous conditions. The trapping of the palladium atom through coordination, can prevent the agglomeration of Pd<sup>(0)</sup> during the catalytic cycle.<sup>78,90</sup>

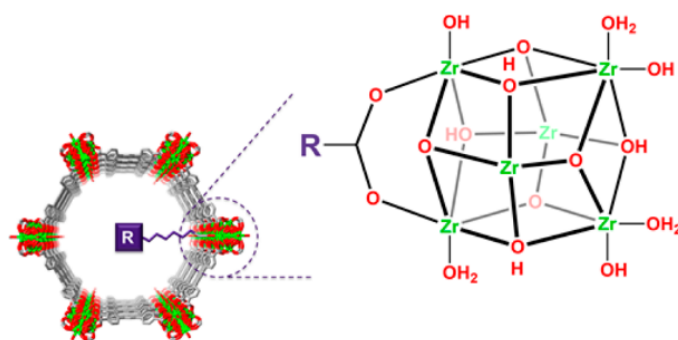


**Figure 1.22:** Design of carboxylate ligands attached to the OCSs of a MOF.<sup>78</sup>

# Chapter 2: Experimental procedures

## I. Materials and Methods

### 1. Synthesis, washing procedure and ligand incorporation

#### 1.1. MOF-808

MOF-808 was synthesized in a 250 mL Teflon lined stainless steel autoclave by dissolving 0.706 g (3.36 mmol) trimesic acid (98 %, Acros) and 3.220 g (10.00 mmol) zirconyl chloride octahydrate (>98 %, Acros) in 100 mL dimethylformamide (DMF) (>99 %, Acros). Subsequently, 56 mL acetic acid (glacial, Fisher), which acts as modulator, was added. The resulting solution was placed in a synthesis oven at 135 °C for 24 hours. Other Zr-salts such as zirconyl nitrate hydrate can also be used for the synthesis of MOF-808, which occurs in 10 mL crimp cap vials by dissolving 67.2 mg trimesic acid (98 %, Acros) and 147.9 mg zirconyl nitrate hydrate (%Zr-25.8, strem chemicals) in 1.6 mL DMF (>99 %, Acros). Furthermore, 1.2 mL milliQ water was added followed by 4.12 mL formic acid (>98 %, Carl Roth). The resulting mixture was placed in a heating block at 100 °C for 20 minutes.<sup>91</sup> After synthesis, the mixture was cooled and transferred to a 50 mL centrifuge tube and centrifuged at 5000 RPM in a fixed angle rotor centrifuge for 10 minutes. The solvent was decanted and the solids were washed three times with DMF to remove the excess of linker and Zr-salt from the pores and three times with ethanol to remove the remaining DMF. The supernatants was replaced by centrifugation and decantation after 15 minutes of sonication. The resulting solids were dried in air, and finally dried in the vacuum oven for 24 hours at 115 °C. Additional wash steps might be necessary before using MOF-808 in a catalytic reaction.

Washed MOF-808, synthesized from zirconyl nitrate hydrate or zirconyl chloride octahydrate, can be used in a next step for ligand incorporation. The special ligand with carboxylic acid group was dissolved in a proper solvent. MilliQ water was used for water-soluble ligands and methanol for non-water soluble ligands. Next, a predetermined amount of MOF-808 was added to obtain a predetermined amount of ligands per  $Zr_6$ -cluster. This mixture was stirred during 24 hours at 100 RPM. Next, the mixture was centrifuged at 5000 RPM for 10 minutes in a fixed rotor centrifuge. Afterwards, MOF-808 with ligands was washed six times to remove the physisorbed ligands (when milliQ was used as solvent, MOF-808 is washed three times with milliQ and three times with ethanol; in case of methanol as solvent, six washing steps with ethanol were performed). The washing solution was replaced every 15 minutes after sonication by centrifugation. After this, MOF-808 with ligand was dried in air and placed in the vacuum oven for 24 hours at 115 °C.

## 1.2. TiO<sub>2</sub> nanoparticles

Titanium(IV) oxide nanopowder of 21 nm primary particles (Sigma Aldrich, >99.5 %), was used for ligand incorporation. The TiO<sub>2</sub> NPs were suspended in a proper solvent, followed by addition of a predetermined amount of ligand. The pH of the immersion solution was adjusted to the desired value with tri-ethylamine. Afterwards, the TiO<sub>2</sub> NPs were washed two times with water and two times with ethanol. The functionalized TiO<sub>2</sub> NPs were dried in air and placed in the vacuum oven for 24 hours at 115 °C. The washing solution was replaced every 15 minutes after sonication by centrifugation. The functionalized TiO<sub>2</sub> NPs were dried in air and placed in the vacuum oven for 24 hours at 115 °C.

## II. Reaction procedure

All chemicals were purchased from conventional suppliers (Sigma-Aldrich, Strem Chemicals, Acros Organics, etc.) and used without further purification. For the experimental procedure of standard reactions, the desired quantity of palladium catalyst and/or other solids were weighed on a microbalance in a 5 mL glass liner. Afterwards, the solvent was added followed by other liquid reagents. In addition, a small quantity of hexadecane was added as internal standard. Reactions were performed in glass lined autoclaves, which contain the glass liners (5 mL), closed with Teflon stoppers containing a hole. The reactors were purged twice with approximately 10 bars of oxygen before pressurizing the autoclave at the desired pressure. The reactions were performed at the desired temperature and at a stirring rate of 750 RPM using a magnetic stirrer. After reaction, the reactor was cooled in an ice bath. When solids were present, the glass liners were centrifuged at 4000 RPM for 10 minutes in a fixed angle rotor centrifuge. The organic solution was analyzed by GC-FID.

## III. Analysis

### 1. Gas chromatography (GC-FID)

Products were analyzed by a Shimadzu 2010 gas chromatograph equipped with a DB-1HT column (Agilent, 100 % PDMS, 30 meters, 0.32 mm diameter, 1.00 µm film thickness) which is coupled to a flame ionization detector (FID), heated to 420 °C. Samples of 1 µL were injected with an AOC-20i auto-injector. An injection temperature of 400 °C was used, the split ratio was set to 1:30 and N<sub>2</sub> was used as carrier gas at a constant linear velocity of 31.5 cm/s. The temperature profile consists of holding the column at 80 °C for 1 minute, followed by increasing the temperature by 10 °C/min until 400 °C. This temperature was kept steady for 4 minutes.

## 2. High Throughput Powder X-ray Diffraction

High throughput powder X-ray diffraction (HT PXRD) patterns were recorded to confirm the crystal structure of the synthesized and modified materials. Measurements were carried out in Debye-Scherrer transmission geometry, operating at 45 kV and 40 mA. The X-rays were focused on the sample by means of a curved mirror, which removes all Cu K $\beta$  radiation and only leaves a beam which consist mainly (2/3<sup>rd</sup>) of Cu K $\alpha$ 1 ( $\lambda$ =1.5406 Å) and to a lesser extent of Cu K $\alpha$ 2. A solid state PIXcel 3D detector records data between a 2 $\theta$ -range of 1.3° and 45°, using a step size of 0.013° and counting 79 seconds per step (scan speed of 0.042° per second). Mercury 3.6 was used to simulate theoretical patterns of the materials based on CIF-files derived from the CCDC database.

## 3. Thermogravimetric analysis

Analysis of the amount of linkers per TiO<sub>2</sub> particle was performed by thermogravimetric analysis (TGA). TGA experiments were performed on a TGA Q500 (TA Instruments) under 10 mL per min O<sub>2</sub> flow and 40 mL per minute N<sub>2</sub> flow over a temperature range of 35 °C to 650 °C at a ramp of 5 °C per minute. The number of carboxylate linkers (n) per TiO<sub>2</sub> NP was calculated by:

$$\text{relative weight} = \frac{M_w((\text{TiO}_2)(\text{linker})_n)}{M_w(\text{TiO}_2)}$$
$$n = \frac{\text{relative weight} * M_w(\text{TiO}_2) - M_w(\text{TiO}_2)}{M_w(\text{linker})}$$

The relative weight is defined as the ratio of the weight at the temperature of minimal weight loss (where the first order derivative of the weight is zero and below the decomposition temperature) and the weight of the material after full decomposition. For TiO<sub>2</sub>, the relative weight can be calculated at 150 °C. In this case all water and other substances are evacuated from the surface.

## 4. Liquid <sup>1</sup>H Nuclear magnetic resonance

Liquid phase <sup>1</sup>H nuclear magnetic resonance (NMR) was used to determine the amount of ligands (isonicotinic acid, picolinic acid, nicotinic acid, etc.) relative to the amount of btc-linkers in MOF-808 samples. In order to dissolve the material, 25 µL of a 40 wt% hydrofluoric acid solution was added to 600 µL of deuterated dimethylsulfoxide and 5 mg MOF-808. After decomposing the samples for 24 hours, a Bruker AMX-300 spectrometer at 300 MHz (64 scans) was used to record the <sup>1</sup>H-NMR spectra. The data was analyzed with the software packet MestReNova 12.0.2.

# Chapter 3: Results and discussion

The goal of this master thesis is to develop a heterogeneous catalyst for the CDC of *o*-xylene. It was shown in the literature study that special types of pyridine ligands are absolutely necessary to obtain a high isomer selectivity (see Chapter 1 Literature).<sup>50,55</sup> Furthermore, a strong interaction of palladium with the pyridine ligand is expected, resulting in supported palladium centers on the immobilized ligands, which should make reuse possible. MOF-808 shows high potential for its use as heterogeneous support due to its large pore size (18.4 Å diameter) and the under-coordinated  $Zr_6$ -cluster which can be used for PSM (e.g. SALI or metalation).<sup>88</sup> The pyridine ligands require a secondary functionality (e.g. carboxylic acid) to coordinate with the  $Zr_6$ -cluster at the OCSs and replace the weakly coordinating ligands present after synthesis and washing procedures (e.g. formate or  $OH^-/H_2O$ ). Other supports, like  $TiO_2$  functionalized NPs and poly(4-vinylpyridine), were also tested (Figure 3.1).<sup>92,93,94,95</sup>

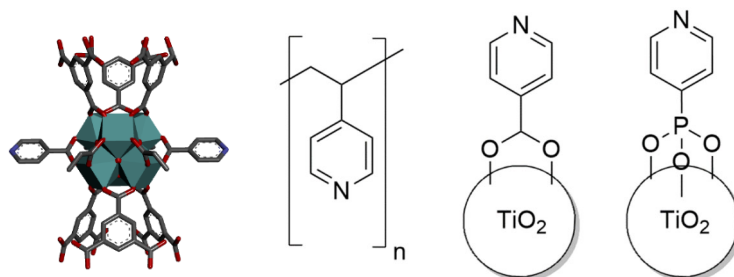


**Figure 3.1:** Different methods to obtain a heterogeneous support containing a pyridine-type of ligand. MOF-808 with pyridine ligands with a secondary carboxylate functionality (left), poly(4-vinylpyridine) (middle) and  $TiO_2$  functionalized nanoparticles with pyridine ligands with a secondary carboxylate or phosphonate functionality (right).

Reaction conditions were selected based on the optimal homogeneous conditions (see Chapter 1 Literature). In homogeneous conditions, a 1:1 ligand/Pd ratio was mainly explored, since in heterogeneous conditions, more ligands per Pd atom can be present but only one ligand can approach one Pd atom at the same time, since the ligands are distributed over the support. It is hypothesized that the ligands at the heterogeneous support increase the isomer selectivity towards the 3,3',4,4'-tetramethylbiphenyl isomer in a similar way as in the homogeneous reaction conditions. There are several considerations to take into account for selection of the right reaction conditions: (i) additional coordinating ligands need to be chosen properly to obtain an active system (e.g.  $Pd(OAc)_2$  as palladium source to support the CMD pathway and a weakly coordinating anionic ligand which makes the palladium more electrophilic to stimulate the C-H activation step, like triflate ( $OTf$ ) or trifluoroacetate ( $TFA^-$ )); (ii) the use of strong Brønsted acids ( $TFAH$ , triflic acid) needs to be avoided if possible, since they can give rise to leaching of the ligands, or of the palladium centers. Systems which use the salts of these strong acids are preferred.

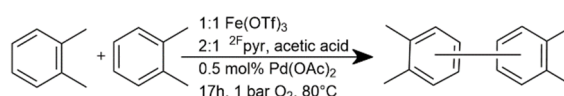
## I. *O*-xylene coupling – Homogeneous reactions

### 1. Reported procedures

#### 1.1. Triflate

The majority of oxidative aryl-aryl couplings described in the literature are performed homogeneously.<sup>5,6,7,8,9</sup> Therefore, the coupling of *o*-xylene was first investigated under homogeneous conditions.

Reactions were performed based on the conditions described by the group of Stahl. They made use of 2:1 <sup>2F</sup>pyr, 0.1 mol% Pd(OAc)<sub>2</sub> and a 1:1 M(OTf)<sub>n</sub> (with M=metal and n=valance metal) in acetic acid. The reaction was performed at 80 °C, during 17 hours at 1 bar O<sub>2</sub>. With the use of Fe(OTf)<sub>3</sub> as additive, a TON of 150 and an isomer selectivity of 90 % towards the 3,3',4,4'-tetramethylbiphenyl isomer could be reached. According to Izawa and Stahl, high valent triflate salts perform better than low valent triflate salts.<sup>7</sup>



However, when a heterogeneous system consisting of special pyridine ligands (isonicotinate or 2-fluoro-3-pyridine carboxylic acid (<sup>2F3C</sup>pyr)) attached to the solid support is used, only one ligand can coordinate to each palladium center. Hence, only 1:1 ligand to Pd ratios were explored homogenously, in contrast to the 2:1 ratio used by Izawa and Stahl. A system with 0.05 mol% Pd(OAc)<sub>2</sub>, 0.5:1 Bi(OTf)<sub>3</sub>, 1:1 <sup>2F</sup>pyr and 50 equivalents weak acid was generally used and the reactions were performed at 95 °C with 16 bar O<sub>2</sub> during 17 hours. The replacement of acetic acid by another weak acid such as pivalic acid (PivOH), benzoic acid or phenylacetic acid gave rise to higher isomer selectivities and TONs. When chiral acids were used, such as R-(-)-mandelic acid or S-(+)-oxo-tetrahydrofuran carboxylic acid, a strong decrease in TON and isomer selectivity was observed. PivOH shows the best performance of all weak acids, achieving an isomer selectivity of 84 % and TON of 211, and was therefore used in the following reactions with triflate salts (Table 3.1).

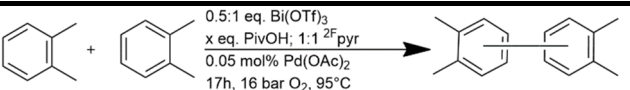
**Table 3.1:** TON for biaryl formation and isomer selectivity (%) towards 3,3',4,4'-tetramethylbiphenyl in the homocoupling of *o*-xylene upon varying the weak acid. Reaction conditions: 0.05 mol% Pd(OAc)<sub>2</sub>, 0.5:1 Bi(OTf)<sub>3</sub>, 1:1 <sup>2F</sup>pyr, *o*-xylene (2 mL), 95 °C, 16 bar O<sub>2</sub>, 17 hours.

Entry	Weak acid	Pk <sub>a</sub>	Isomer selectivity	TON
1	AA	4.75	72	134
2	PivOH	5.03	84	211
3	Benzoic acid	4.20	80	172
4	Phenylacetic acid	4.28	80	199
5	R-(-)-mandelic acid	3.41	62	13
6	S-(+)-oxo-2-tetrahydrofuran carboxylic acid	/	65	10



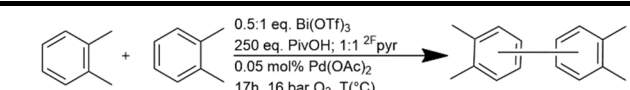
The concentration of PivOH was varied from 2 equivalents to 250 equivalents under identical conditions (Table 3.2). It was found that the isomer selectivity increases with the concentration of PivOH. However, the TON reached a maximum of 211 at 50 equivalents of PivOH. Higher isomer selectivities (e.g. 88%) were reached at high PivOH concentrations (e.g. 250 equivalents).

**Table 3.2:** TON biaryl formation and isomer selectivity (%) towards 3,3',4,4'-tetramethylbiphenyl in the homocoupling of o-xylene upon varying the concentration PivOH. Reaction conditions: Pd(OAc)<sub>2</sub> (0.05 mol%), 0.5:1 Bi(OTf)<sub>3</sub>, x eq. PivOH, 1:1 <sup>2F</sup>pyr, 95 °C, 16 bar O<sub>2</sub>, 17 hours.

			
Entry	PivOH (eq.)	Isomer selectivity	TON
1	0	77	74
2	2	81	113
3	10	84	177
4	50	84	211
5	100	86	183
6	250	88	195

The temperature of the reaction with 250 equivalents of PivOH was also increased from 95 °C to 110 °C (Table 3.3). Higher temperatures resulted in higher TONs, but a strong decrease in isomer selectivity could also be observed.

**Table 3.3:** TON for biaryl formation and isomer selectivity (%) towards 3,3',4,4'-tetramethylbiphenyl in the homocoupling of o-xylene upon varying the temperature. Reaction conditions: Pd(OAc)<sub>2</sub> (0.05 mol%), 0.5:1 Bi(OTf)<sub>3</sub>, 250 eq. pivOH, 1:1 <sup>2F</sup>pyr, 16 bar O<sub>2</sub>, 17 hours.

			
Entry	T (°C)	Isomer selectivity	TON
1	95	88	195
2	110	77	317

The effect of the triflate salt was studied by the addition of several different triflate salts under the previously applied reaction conditions using 50 equivalents PivOH as weak acid at 95 °C (Table 3.4). The importance of the triflate salt was highlighted by performing a reaction without any triflate salt, resulting in a TON of only 11. The triflate salts of Bi<sup>(III)</sup> and Sc<sup>(III)</sup> resulted in high TONs and acceptable isomer selectivities (i.e. above 80 %), while triflate salts of the lanthanides (La<sup>(III)</sup> and Yb<sup>(III)</sup>) resulted in both lower TONs and isomer selectivities. Finally, acceptable isomer selectivities, but lower TONs were obtained with the triflate salts of Fe<sup>(III)</sup> and Mg<sup>(II)</sup>.

**Table 3.4:** TON for biaryl formation and isomer selectivity (%) towards 3,3',4,4'-tetramethylbiphenyl in the homocoupling of *o*-xylene upon varying the triflate salt. Reaction conditions: Pd(OAc)<sub>2</sub> (0.05 mol%), 0.5:1 M(OTf)<sub>n</sub>, 50 eq. pivOH, 1:1 2<sup>F</sup>pyr, 95 °C, 16 bar O<sub>2</sub>, 17 hours.

<chem>Cc1ccccc1.Cc1ccccc1&gt;&gt;Cc1ccc(cc1)-c2cc(C)cc(C)c2</chem> 0.5:1 eq. M(OTf) <sub>n</sub> 50 eq. PivOH; 1:1 2 <sup>F</sup> pyr 0.05 mol% Pd(OAc) <sub>2</sub> 17h, 16 bar O <sub>2</sub> , 95°C			
Entry	Triflate salt	Isomer selectivity	TON
1	none	78	11
2	Bi(OTf) <sub>3</sub>	84	211
3	Fe(OTf) <sub>3</sub>	85	84
4	Sc(OTf) <sub>3</sub>	82	188
5	Yb(OTf) <sub>3</sub>	75	126
6	La(OTf) <sub>3</sub>	77	96
7	Al(OTf) <sub>3</sub>	78	132
8	Mg(OTf) <sub>2</sub>	88	77

The optimal amount of triflate salt was investigated for Bi<sup>(III)</sup>, Fe<sup>(III)</sup>, Sc<sup>(III)</sup> and Mg<sup>(II)</sup>. Bi<sup>(III)</sup> shows the highest TON of all triflate salts at 0.33:1 ratio (i.e. one <sup>-</sup>OTf is available per Pd atom), which is in accordance to the literature.<sup>7</sup> When higher amounts of Bi(OTf)<sub>3</sub> are added (> 0.333:1) the TON as well as the isomer selectivity drops significantly (Figure 3.2 and 3.3). Systems with Sc<sup>(III)</sup> triflate exhibited slightly lower TONs compared to Bi(OTf)<sub>3</sub>. For Fe(OTf)<sub>3</sub>, the highest isomer selectivity was achieved when a 0.5:1 ratio was used. However, the TON of the system with Fe(OTf)<sub>3</sub> was three times lower compared to the systems using Sc<sup>(III)</sup> or Bi<sup>(III)</sup> triflate, which does not correspond to the results described by the group of Stahl.<sup>7</sup> The isomer selectivity of Fe<sup>(III)</sup>, Sc<sup>(III)</sup> and Mg<sup>(II)</sup> seems to be less influenced by the amount of triflate salt added compared to Bi<sup>(III)</sup> (Figure 3.2). This might be explained by the fact that Fe<sup>(III)</sup>, Sc<sup>(III)</sup> and Mg<sup>(II)</sup> are rather hard cations while Bi<sup>(III)</sup> is intermediate hard-soft.

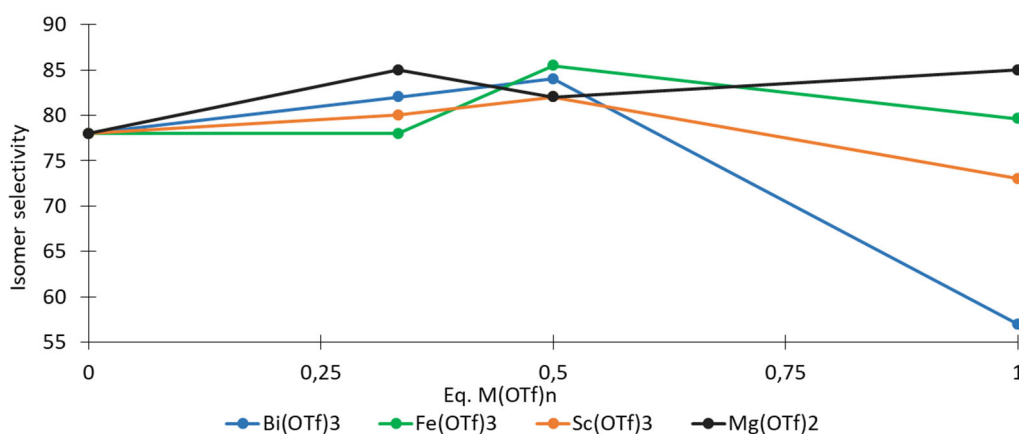


**Figure 3.2:** The isomer selectivity (%) towards 3,3',4,4'-tetramethylbiphenyl in the homocoupling of *o*-xylene upon varying the amount of triflate salt (for Bi<sup>(III)</sup>, Sc<sup>(III)</sup>, Fe<sup>(III)</sup> and Mg<sup>(II)</sup>). Reaction conditions: Pd(OAc)<sub>2</sub> (0.05 mol%), 50 eq. PivOH, 1:1 2<sup>F</sup>pyr, 95 °C, 16 bar O<sub>2</sub>, 17 hours.

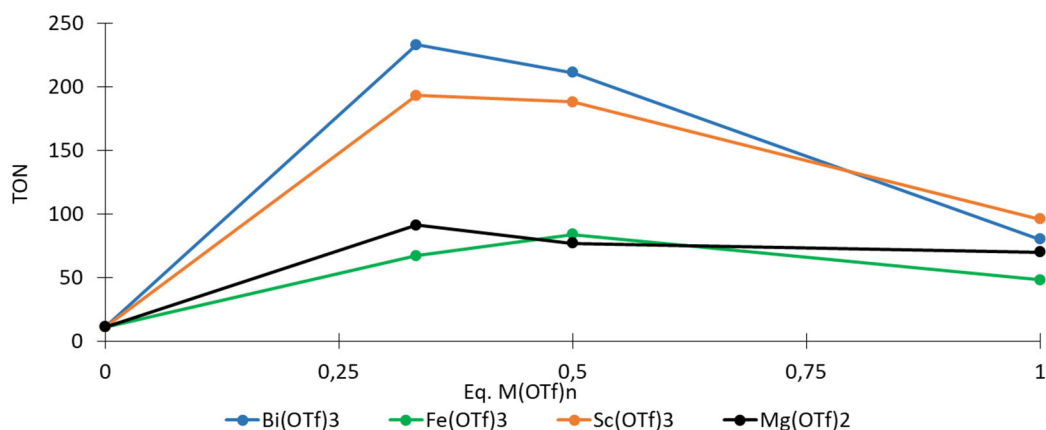


**Figure 3.3:** TON for biaryl formation in the homocoupling of *o*-xylene upon varying the amount of triflate salt used (for Bi(III), Sc(III), Fe(III) and Mg(II)). Reaction conditions: Pd(OAc)<sub>2</sub> (0.05 mol%), 50 eq. PivOH, 1:1 <sup>2F</sup>pyr, 95 °C, 16 bar O<sub>2</sub>, 17 hours.

Different type of pyridine ligands were screened in systems with 0.05 mol% Pd(OAc)<sub>2</sub>, 0.5 equivalents of triflate salt (Bi<sup>(III)</sup>, Sc<sup>(III)</sup>, Fe<sup>(III)</sup> and Mg<sup>(III)</sup>) and 50 equivalents of PivOH. The reactions were performed using <sup>2F</sup>pyr (L1), pyridine (L2) and 2-hydroxy-6-trifluoromethyl pyridine (L3) as ligands, but also a reaction in absence of ligands was performed. Additionally, ligands with a secondary functionality (e.g. carboxylic acid), which will be attached to the Zr<sub>6</sub>-cluster of MOF-808 (e.g. <sup>2F3C</sup>pyr (L4), 2-fluoropyridine 4-carboxylic acid (<sup>2F4C</sup>pyr, L5), isonicotinic acid (L6), nicotinic acid (L7) and picolinic acid (L8)), were tested under the homogeneous conditions (Figure 3.4). The blue line at regio ratio (RR) 4.00 points at an isomer selectivity of 80 %. The goal is to achieve isomer selectivities under heterogeneous conditions which are higher than 80 %. The RR and isomer selectivity (S) are linked to each other *via* the following formula:

$$RR = \frac{S}{1 - S} \text{ or } S = \frac{RR}{1 + RR}$$

The addition of L1 resulted in the highest TON and isomer selectivity of all ligands, while the addition of L2 resulted in a decrease in both TON and isomer selectivity. This is in contrast with the observations of Stahl and Fernández-Ibáñez, who both observed a higher isomer selectivity using pyridine compared to <sup>2F</sup>pyr.<sup>8,9</sup> The importance of the ligand was shown by the reaction without any ligand, which resulted in very low isomer selectivity. Furthermore, the addition of L3 had almost no influence on the isomer selectivity compared to the system without ligand. However, the addition of this ligand resulted in an increase (in case of Bi<sup>(III)</sup> as triflate salt) or decrease (Sc<sup>(III)</sup>, Fe<sup>(III)</sup> and Mg<sup>(III)</sup>) in TON.

When pyridine or <sup>2F</sup>pyr ligands with a secondary carboxylate group (L4-L8) were used, both isomer selectivity and TON decreased for all ligands. This can be explained by interaction of the carboxylate group with palladium, which does not give rise to the required steric effect.

In order to discriminate between the electronic effect of the secondary carboxylate group and the ligating effect of this group, the methyl esters of isonicotinic acid (L9), nicotinic acid (L10) and picolinic acid (L11) were also tested as ligands. The isomer selectivity is fortunately retained when L9 and L10 were used. However, when L11 was added, low isomer selectivities were observed, probably due to steric hindrance of the methyl ester in *ortho* position. Similar experiments were performed for 4-fluoro-3-pyridine diethyl phosphonate (L12), which exhibits similar features to 4-fluoro-3-pyridine phosphonic acid. This ligand was tested, since phosphonate ligands can be attached to TiO<sub>2</sub> NPs. Compared to the systems without ligands or with carboxylate-ligands, L12 performs well in terms of isomer selectivity, but not enough to reach isomer selectivities above 80 %.

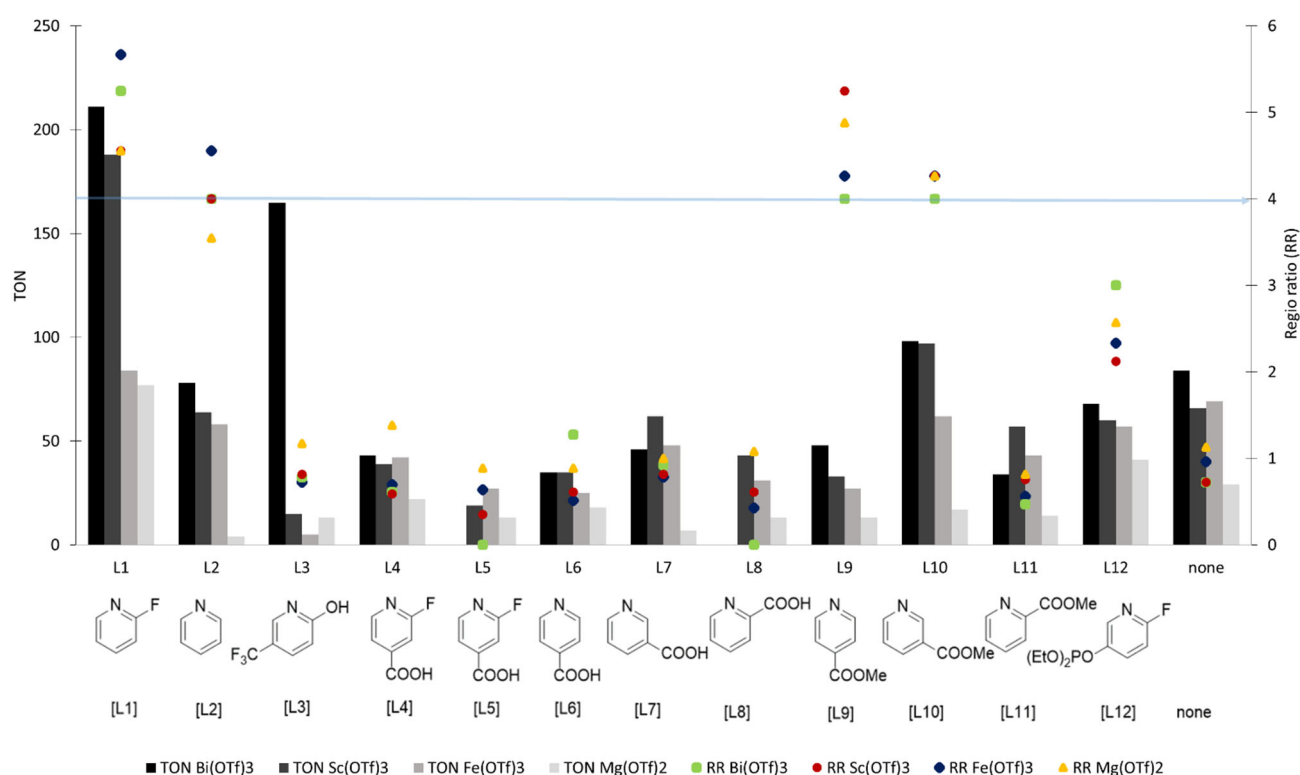


**Figure 3.4:** TON for biaryl formation and isomer selectivity (%) towards 3,3',4,4'-tetramethylbiphenyl in the homocoupling of *o*-xylene upon varying the ligand. Reaction conditions: Pd(OAc)<sub>2</sub> (0.05 mol%), 0.5:1 M(OTf)<sub>n</sub> with M = Bi<sup>(III)</sup>, Sc<sup>(III)</sup>, Fe<sup>(III)</sup> and Mg<sup>(III)</sup>; 50 eq. PivOH, 1:1 ligand (L1-L12) and no ligand, 95 °C, 16 bar O<sub>2</sub>, 17 hours.

The influence of the amount of ligand was explored for pyridine,  $^{2F}$ pyr and methyl nicotinate in a system with 0.5:1 Bi(OTf)<sub>3</sub> and 50 equivalents of PivOH (Figure 3.5). Low isomer selectivities could be observed at low ligand concentrations (0 or 0.5 equivalents) of pyridine,  $^{2F}$ pyr and methyl nicotinate. When the amount of ligand was increased to 2 eq., the isomer selectivity increased gradually for all ligands. However, when the amount of ligand was doubled to 4 eq., a drop in isomer selectivity could be observed for pyridine and methyl nicotinate, while a selectivity of 88 % was obtained with 4 eq. of  $^{2F}$ pyr. The TON and isomer selectivity of pyridine and methyl nicotinate followed a similar trend. The maximum TON for methyl nicotinate and pyridine was reached when 0.5 eq. of ligand was added, while for  $^{2F}$ pyr, the maximum TON was reached after addition of 1 eq. of ligand.

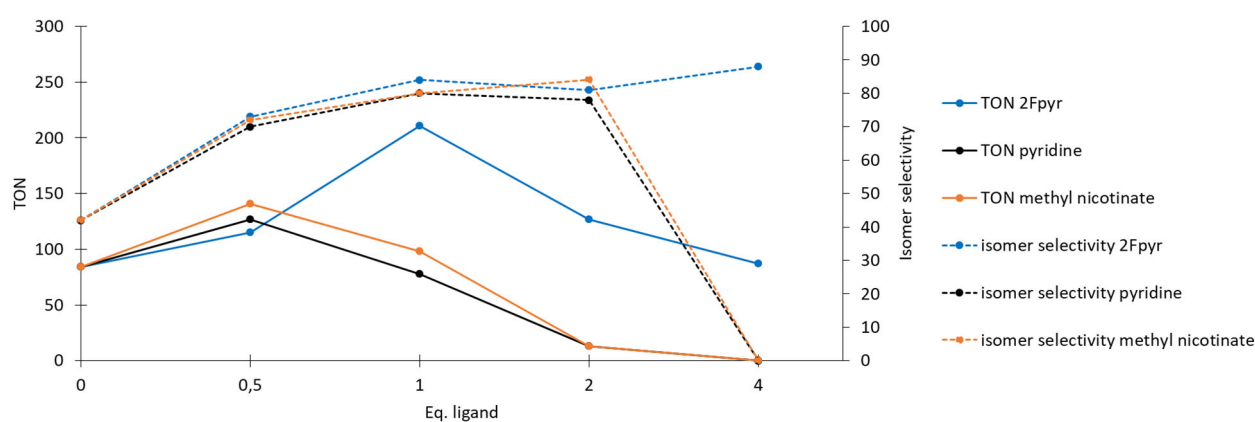
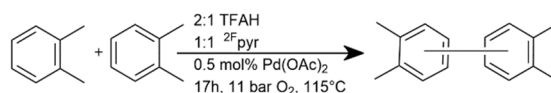


**Figure 3.5:** TON for the formation of a biaryl and isomer selectivity (%) towards 3,3',4,4'-tetramethylbiphenyl in the homocoupling of o-xylene upon varying the amount ligand (for  $^{2F}$ pyr, pyridine and methyl nicotinate). Reaction conditions: Pd(OAc)<sub>2</sub> (0.05 mol%), 50 eq. PivOH, 0.5:1 Bi(OTf)<sub>3</sub>, 1:1  $^{2F}$ pyr or pyridine, 95 °C, 16 bar O<sub>2</sub>, 17 hours.

## 1.2. Trifluoroacetate

Other active systems exist, in addition to the systems which make use of triflate salts. Fernández-Ibáñez and coworkers made use of a system consisting of 0.5 mol% Pd(OAc)<sub>2</sub>, 0.5 mol% or 1 mol% ligand and 1 mol% TFAH, at 115 °C and 11 bar O<sub>2</sub> during 17 hours. Several ligands were screened and the system with 0.5 mol% <sup>2</sup>Fpyr resulted in an optimal TON of 40 and an isomer selectivity of 83 %.<sup>55</sup>



Conditions analogue to the optimal system of Fernández-Ibáñez and coworkers were screened, beginning with varying the amount of TFAH in a system with 0.05 mol% Pd(OAc)<sub>2</sub> and one equivalent of <sup>2</sup>Fpyr as ligand. The reactions were conducted at 95 °C and 16 bar O<sub>2</sub> during 17 hours (Table 3.5). At low TFAH concentrations (e.g. 1 equivalent), a high isomer selectivity (88 %) could be reached, but the TON of 62 was rather low. At 2 equivalents of TFAH, the isomer selectivity reached an acceptable value of 84 % in combination with a high TON of 116. Higher amounts of TFAH resulted in both a decrease in isomer selectivity and TON.

**Table 3.5:** TON for biaryl formation and isomer selectivity (%) towards the 3,3',4,4'-tetramethylbiphenyl in the homocoupling of *o*-xylene upon varying the amount of trifluoroacetic acid. Reaction conditions: Pd(OAc)<sub>2</sub> (0.05 mol%), 1:1 <sup>2</sup>Fpyr, 95 °C, 16 bar O<sub>2</sub>, 17 hours.

Entry	Eq TFAH	Isomer selectivity	TON
1	1	88	62
2	2	84	116
3	4	72	122
4	6	64	106

Since TFAH performed quite well as additive, other, non-Brønsted acid sources of TFAH (e.g. Pd(TFA)<sub>2</sub> or Cu(TFA)<sub>2</sub>) were tested under similar homogeneous conditions. (Table 3.6). Interestingly, the use of Pd(TFA)<sub>2</sub> resulted in a highly active system with a TON of 99 and a good isomer selectivity of 81 %.

**Table 3.6:** TON for biaryl formation and isomer selectivity (%) towards the 3,3',4,4'-tetramethylbiphenyl in the homocoupling of *o*-xylene upon using other sources of TFAH. Reaction conditions: Pd-catalyst (0.05 mol%), 1:1 <sup>2</sup>Fpyr, co-cat, 95 °C, 16 bar O<sub>2</sub>, 17 hours.

Entry	Catalyst	Co-cat	Eq. co-cat	Isomer selectivity	TON
1	Pd(TFA) <sub>2</sub>	none	0	81	99
2	Pd(OAc) <sub>2</sub>	Cu(TFA) <sub>2</sub>	1	76	58

The impact of the temperature on the reaction with 2 equivalents of TFAH was also tested (Table 3.7). The TON increased with an increase in temperature, while the isomer selectivity decreased, which is in accordance to the reactions with triflate salts.

**Table 3.7:** TON for biaryl formation and isomer selectivity (%) towards the 3,3',4,4'-tetramethylbiphenyl in the homocoupling of *o*-xylene upon varying the temperature. Reaction conditions: Pd(OAc)<sub>2</sub> (0.05 mol%), 2:1 TFAH, 1:1 <sup>2F</sup>pyr, T(°C), 16 bar O<sub>2</sub>, 17 hours.

Entry	T (°C)	Isomer selectivity	TON
1	95	84	116
2	110	78	196

These reaction conditions using TFA-sources perform well, but differ strongly from the reactions with triflate salts. Hence, the same ligands with (L1-L3) and without secondary functionality (L4-L8) were also screened in the systems consisting of TFAH (2:1 and 4:1) and 0.05 mol% Pd(OAc)<sub>2</sub> or other TFA-sources (e.g. 0.05 mol% Pd(TFA)<sub>2</sub>), under the same reaction conditions as before (Figure 3.6). The absolute need for a ligand is shown by the reaction without any ligand, which resulted in very low isomer selectivities. The reaction with Pd(OAc)<sub>2</sub> and 4:1 TFAH was not sufficiently selective, since the isomer selectivity was for all ligands lower than 80 % (below the blue line in Figure 3.6).

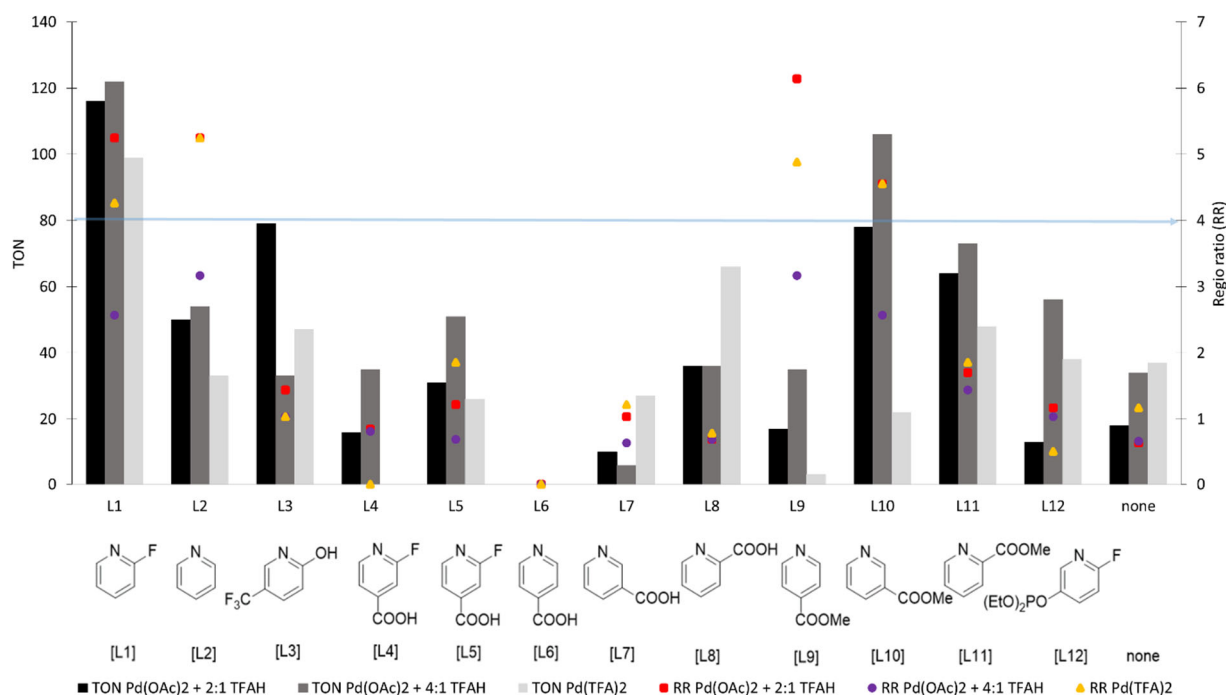


**Figure 3.6:** TON for biaryl formation and isomer selectivity (%) towards 3,3',4,4'-tetramethylbiphenyl in the homocoupling of *o*-xylene upon varying the ligand (L1-L12) and no ligand. . Reaction conditions: Pd-catalyst (0.05 mol%), 1:1 ligand, 95 °C, 16 bar O<sub>2</sub>, 17 hours, A) Pd(OAc)<sub>2</sub> + 2:1 TFAH, B) Pd(OAc)<sub>2</sub> + 4:1 TFAH and C) Pd(TFA)<sub>2</sub>.

The addition of L1 gave rise to the most active systems, in combination with high isomer selectivity. However, when L2 was added, the TON dropped, but the isomer selectivity increased. This is in accordance with the results of Fernández-Ibáñez and coworkers.<sup>9</sup> When L3 was used, the isomer selectivity strongly decreased for all reactions.

The effect of the ligands with a secondary carboxylic acid group (L4-L8) was similar as in the systems with triflate salts (see Figure 3.4). However, when the methyl esters of isonicotinic, nicotinic and picolinic acid were added (L9-L11) an increase in isomer selectivity was observed for L9 and L10, but not for L11. When 4-fluoro-3-pyridine diethyl phosphonate (L12) was used, a strong decrease in performance was observed, which is in contrast to the reaction with triflate salts (in which isomer selectivities around 70 % were reached) (see Figure 3.4).

The amount of ligands was screened for pyridine, <sup>2F</sup>pyr and methyl nicotinate in the system with 0.05 mol% Pd(TFA)<sub>2</sub> (Figure 3.7). Similar trends in isomer selectivity and TON were observed for methyl nicotinate and pyridine, which was also the case in previous system using triflate salts (see Figure 3.5). When the amount of pyridine or methyl nicotinate was increased, the TON reached a maximum of 72 at 0.25 equivalents pyridine or methyl nicotinate and decreased rapidly to zero at 2 equivalents of ligand. The isomer selectivity increased with increasing amounts of pyridine or methyl nicotinate, but decreased quickly when more than 1.5 equivalents were added. When <sup>2F</sup>pyr was used as ligand, the TON reached a maximum at 1 equivalent of ligand and remained quite high when more ligand was used. The isomer selectivity was slightly lower compared to the same conditions with pyridine, but remained at a high level at increased concentrations of <sup>2F</sup>pyr.

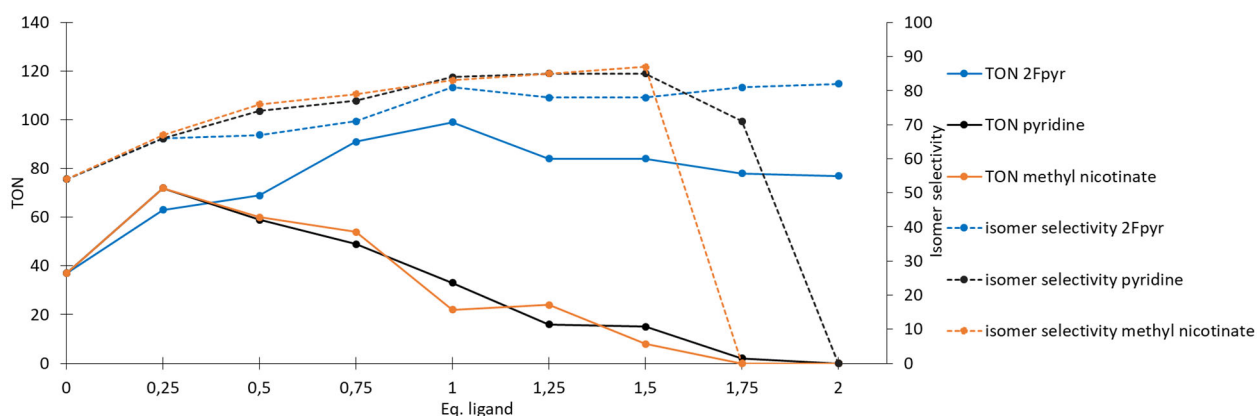


**Figure 3.7:** TON for biaryl formation and isomer selectivity (%) towards 3,3',4,4'-tetramethylbiphenyl in the homocoupling of o-xylene upon varying the amount of ligand. Reaction conditions: Pd(TFA)<sub>2</sub> (0.05 mol%), x:1 ligand (<sup>2F</sup>pyr, pyridine and methyl nicotinate), 95 °C, 16 bar O<sub>2</sub>, 17 hours.



### 1.3. Conclusion

The screening of the homogeneous reaction conditions is very relevant for the development of heterogeneous supports with immobilized pyridine-type ligands. Homogeneous systems with triflate salts resulted in high TONs and isomer selectivities, when the right triflate salt (e.g. triflate salts of Bi<sup>(III)</sup> or Sc<sup>(III)</sup>) are preferred over Fe<sup>(III)</sup> and Mg<sup>(II)</sup>) was used in the right quantity (e.g. 0.333 or 0.5 eq. are preferred over 1 eq.) in combination with a good weak acid (e.g. PivOH). Since the isomer selectivities of systems with Bi(OTf)<sub>3</sub> were found to be rather sensitive to slight changes in the amount of triflate salt, it could be interesting to use Sc(OTf)<sub>3</sub> rather than Bi(OTf)<sub>3</sub> under heterogeneous conditions (i.e. with immobilized pyridine-type ligands). Although higher isomer selectivities were reached at higher concentrations weak acid (e.g. 250 eq. PivOH), these conditions should be avoided in heterogeneous reaction conditions, since high acid concentrations can give rise to more leaching of the immobilized ligands (e.g. at the Zr<sub>6</sub>-cluster of MOF-808) and of Pd. Moreover, systems which make use of strong acids (e.g. TFAH) as additive should also be avoided. It was found that the palladium salt of this strong acid (i.e. Pd(TFA)<sub>2</sub>) was a good alternative, resulting in active and selective systems (e.g. TON is 99 and isomer selectivity of 81% for <sup>2</sup>Fpyr).

Additionally, the screening of the different pyridine-type of ligands in homogeneous systems, resulted in very useful information, since it was shown that some ligands have the potential to induce high isomer selectivities (e.g. <sup>2</sup>Fpyr, pyridine, methyl nicotinate and methyl isonicotinate), while others are unable to achieve this (e.g. methyl picolinate). The addition of ligands containing a secondary functionality (e.g. carboxylate) underlined the importance of strong attachment of the ligand at the heterogeneous support (e.g. MOF-808). If this attachment is not guaranteed, the ligand will be released, resulting in a decreased reaction performance. Furthermore, the screening of the amount of ligands was very relevant, since the use of too much strong coordinating ligands (e.g. pyridine or methyl nicotinate) could also give rise to a decrease in TON and isomer selectivity. Finally, it was shown that careful selection of the temperature is important due to the trade-of between TON and isomer selectivity. Higher temperatures (e.g. 110 °C) resulted in higher TONs, while lower temperatures (e.g. 95°C) resulted in higher isomer selectivities.

## II. *O*-xylene coupling – Heterogeneous reactions

### 1. Metal-organic frameworks as support – MOF-808

The best performing homogeneous reaction condition was 0.05 mol% Pd(OAc)<sub>2</sub>, 0.5:1 Bi(OTf)<sub>3</sub>, 1:1 <sup>2</sup>Fpyr and 50 equivalents of PivOH at 95 °C and 16 bar O<sub>2</sub> during 17 hours, resulting in a TON of 211 and isomer selectivity of 84 %. When small amounts (e.g. 10 mg) of MOF-808 (washed with DMF and ethanol, but no additional washing steps) were added to this homogeneous reaction, a TON of only 10 and isomer selectivity of 67 % was observed (Figure 3.8). Different types of zirconium sources (e.g. 10 mg of zirconia (ZrO<sub>2</sub>), ZrOCl<sub>2</sub>·8H<sub>2</sub>O (0.00825 mmol) (2:1 Cl/Pd ratio), ZrCl<sub>4</sub> (0.00825 mmol), Zr(OAc)<sub>x</sub>-solution (0.00825 mmol) and ZrO(NO<sub>3</sub>)<sub>2</sub>·xH<sub>2</sub>O (0.00825 mmol)), were added to the same homogeneous reaction to gain insight in the source of deactivation. In addition, the impact of H<sub>2</sub>O was examined (8 x 0.00825 mmol), since water is also present in ZrOCl<sub>2</sub>·8H<sub>2</sub>O and ZrO(NO<sub>3</sub>)<sub>2</sub>·xH<sub>2</sub>O.

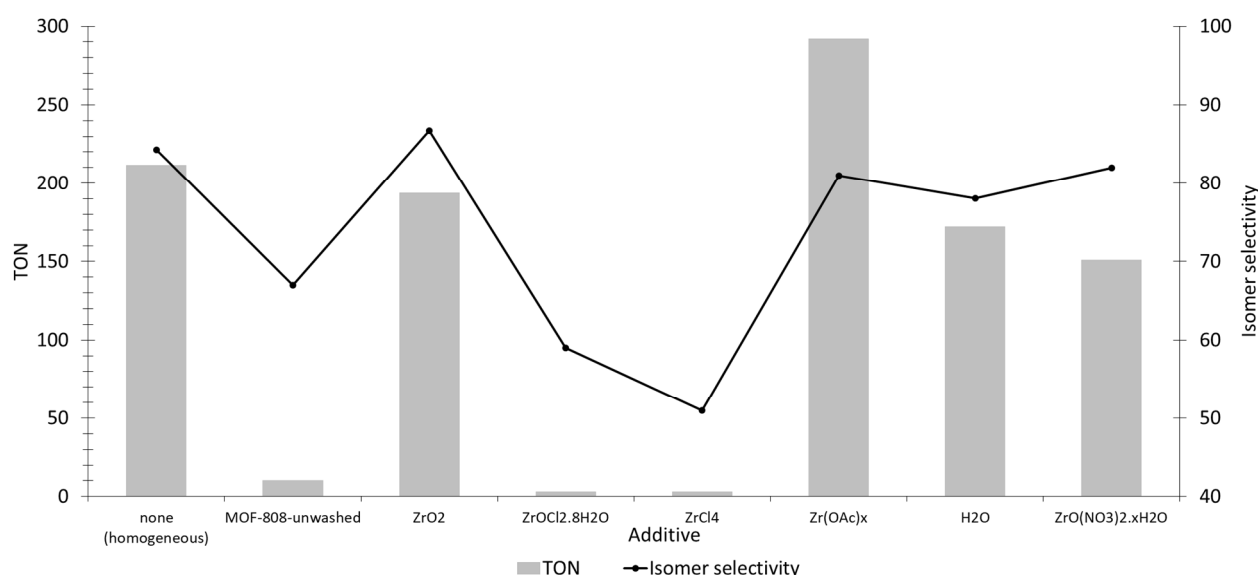


**Figure 3.8:** TON for biaryl formation and isomer selectivity (%) towards 3,3',4,4'-tetramethylbiphenyl in the homocoupling of *o*-xylene upon addition of an additive. Reaction conditions: 0.05 mol% Pd(OAc)<sub>2</sub>, 1:1 <sup>2</sup>Fpyr, 0.5:1 Bi(OTf)<sub>3</sub>, 50 eq. PivOH, additive, 95 °C, 16 bar O<sub>2</sub>, 17 hours.

It can be noticed that small amounts of chlorides present in the reaction medium, for example coming from ZrOCl<sub>2</sub>·8H<sub>2</sub>O or ZrCl<sub>4</sub> which are the commonly used Zr-salts for MOF-808 synthesis, have a severe impact on the activity and selectivity of the Pd-catalyst (Figure 3.8). The inhibition does not originate from zirconium itself, since addition of ZrO<sub>2</sub> or a Zr(OAc)<sub>x</sub>-solution did not result decrease in TON or isomer selectivity. Hence, the decrease in performance of the reaction after the addition of 10 mg unwashed MOF-808 was assumed to originate from the presence of small amounts of chlorides, coordinated to the Zr<sub>6</sub>-cluster after synthesis. In order to get rid of the chlorides, the development of an appropriate washing procedure which eliminates the chlorides or a synthesis procedure which avoids zirconium salts with chloride impurities is necessary.

## 1.1. Chloride removal MOF-808 from the $\text{ZrOCl}_2 \cdot 8\text{H}_2\text{O}$ salt to eliminate reaction inhibition

### 1.1.1. *Washing and synthesis procedure MOF-808*

The washing procedure for MOF-808 seems to be very important since chlorides can induce reaction inhibition. The washing procedure of MOF-808 consists of two steps: (i) removal of excess unreacted organic linker and Zr-salt from the pores by washing MOF-808 three times with DMF. Afterwards, MOF-808 is washed three times with ethanol to remove the DMF from the pores. (ii) Removal of the chlorides from the  $\text{Zr}_6$ -cluster and replacement of the chlorides by  $\text{OH}^-/\text{H}_2\text{O}$  sites (OCSs) or by weakly coordinating ligands at the  $\text{Zr}_6$ -cluster which can be used in a next step for 'ligand incorporation' or 'metalation'. Washing step (i) is performed after all MOF syntheses, while washing step (ii) is necessary when chlorides are present in the Zr-salt used for the MOF synthesis.

In the first washing procedure, several salts were used to remove the chlorides. A solvent was selected in which the salt dissolves (e.g. sodium acetate trihydrate in methanol or milliQ), resulting in salt dissociation (e.g.  $\text{NaOAc} \leftrightarrow \text{Na}^+ + \text{OAc}^-$ ). The anionic acetate group can take part in an equilibrium exchange with the anionic chloride, coordinated to the  $\text{Zr}_6$ -cluster. By using an excess of salt and/or multiple washing steps, the equilibrium can shift towards chloride ions in solution, which can be removed in a next step. In addition, a second type of washing procedure was developed, which makes use of strong acids to remove the chlorides. The strong acid dissociates and gives his proton to  $\text{Cl}^-$  to form hydrogen chloride (HCl), which can dissolve in the solvent (polar, protic solvents) and/or escape in the gas phase (non-polar, aprotic solvent). When hydrogen chloride escapes to the gas phase, the equilibrium is shifted and chloride at the  $\text{Zr}_6$ -cluster is replaced by the deprotonated strong acid.

In parallel, a new synthesis procedure for MOF-808, which makes use of chloride-free zirconium salts, was optimized.<sup>48,96</sup> In this way, the problem of chlorides inhibiting the reaction is bypassed. This was done by making use of  $\text{ZrO}(\text{NO}_3)_2 \cdot x\text{H}_2\text{O}$  as zirconium salt, since this salt does not induce strong inhibition (see Figure 3.8).

### 1.1.2. *Reaction inhibition tests*

After the washing procedures, 10 mg of washed MOF-808 was used as additive in the same homogeneous reaction as before (0.05 mol%  $\text{Pd}(\text{OAc})_2$ , 0.5:1  $\text{Bi}(\text{OTf})_3$ , 50 eq.  $\text{PivOH}$ , 1:1  $^{2\text{F}}\text{pyr}$ , 16 bar  $\text{O}_2$ , 95 °C, 17 hours) to see if the reaction was still inhibited (see Figure 3.8). The results are rather indicative since there was not always 10 mg washed MOF-808 available for every reaction, since significant amounts of MOF-808 were lost during the washing procedures. In the first washing procedure, MOF-808 was washed twice with a 0.1M solution of several salts (potassium acetate, sodium acetate trihydrate and calcium acetate monohydrate) in different solvents (milliQ and MeOH).

The use of monovalent salts (e.g. potassium acetate or sodium acetate trihydrate) resulted in a slight increase in TON and isomer selectivity, while divalent salts (e.g. calcium acetate monohydrate) resulted in a much higher increase in TON and selectivity. Nevertheless, the TON under homogeneous conditions was still higher (Table 3.8).

**Table 3.8:** Impact of MOF-808 as additive in the reaction after a washing procedure with salts on the TON for biaryl formation and isomer selectivity (%) towards 3,3',4,4'-tetramethylbiphenyl in the homocoupling of *o*-xylene. Reaction conditions: 0.05 mol% Pd(OAc)<sub>2</sub>, 0.5 eq. Bi(OTf)<sub>3</sub>, 50 eq. PivOH, 1:1 <sup>2F</sup>pyr, 95 °C, 16 bar O<sub>2</sub>, 17 hours. \*Washing procedure results in loss of MOF-808, less than 10 mg available for reaction.

Entry	Washing procedure	Isomer selectivity	TON
1	Homogeneous	84	211
2	Unwashed MOF-808	67	10
3	2x 0.1M NaOAc.3H <sub>2</sub> O (MilliQ)	80	64
4	2x 0.1M NaOAc.3H <sub>2</sub> O (MeOH)	72*	19
5	2x 0.1M Ca(OAc) <sub>2</sub> .H <sub>2</sub> O (MilliQ)	<b>87*</b>	<b>164</b>
6	2x 0.1M K(OAc) (MeOH)	63*	14
7	2 x 0.1M K(OAc) (MilliQ)	72	41

The second washing procedure makes use of propanesulfonic acid and sulfuric acid in different concentrations (0.13M, 0.063M and 0.032M) in different solvents (methanol as polar protic solvent and *o*-xylene as non-polar aprotic solvent). Again, higher TONs and isomer selectivities were obtained after washing MOF-808 with strong acids, but these values were still lower than in the homogeneous reaction without additive (Table 3.9).

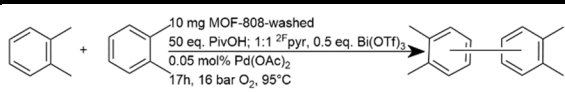
**Table 3.9:** Impact of MOF-808, washed with strong acids, on the TON for biaryl formation and isomer selectivity (%) towards 3,3',4,4'-tetramethylbiphenyl in the homocoupling of *o*-xylene. Reaction conditions: 0.05 mol% Pd(OAc)<sub>2</sub>, 0.5 eq. Bi(OTf)<sub>3</sub>, 50 eq. PivOH, 1:1 <sup>2F</sup>pyr, 95 °C, 16 bar O<sub>2</sub>, 17 hours. \*Washing procedure results in loss of MOF 808, less than 10 mg available for reaction.

		A) Propanesulfonic acid		B) Sulfuric acid	
Entry	Washing procedure	Isomer selectivity	TON	Isomer selectivity	TON
1	Homogeneous	84	211	84	211
2	Unwashed MOF-808	67	10	67	10
3	0.13M (MeOH)	<b>77</b>	<b>107</b>	75*	84
4	0.063M (MeOH)	78	88	77	65
5	0.032M (MeOH)	81	61	75	43
6	0.13M ( <i>o</i> -xylene)	77	91	69	39
7	0.063M ( <i>o</i> -xylene)	79	78	75	101
8	0.032M ( <i>o</i> -xylene)	80	84	<b>79</b>	<b>98</b>

Overall, the best performing washing procedures were washing twice with a 0.1M solution of calcium acetate monohydrate in milliQ (TON 164 and isomer selectivity 87 %) or washing once with a 0.13M solution of propanesulfonic acid in methanol (TON 107 and isomer selectivity 77 %) or washing once with a 0.032M solution of sulfuric acid in *o*-xylene (TON is 98 and isomer selectivity 79 %).

These washing procedures, as well as the synthesis procedure starting from  $\text{ZrO}(\text{NO}_3)_2 \cdot x\text{H}_2\text{O}$ , were performed on a larger scale and 10 mg MOF-808 was added to the same homogeneous reaction conditions as before (Table 3.10). Notably, a decrease in performance was observed for MOF-808 washed with calcium acetate monohydrate and with sulfuric acid compared to previous results. Surprisingly, when MOF-808 synthesized from  $\text{ZrO}(\text{NO}_3)_2 \cdot x\text{H}_2\text{O}$  was added to the reaction, a very strong inhibition was observed, which indicates that chlorides are not the only cause of inhibition. It might be possible that weakly coordinating species at the  $\text{Zr}_6$ -cluster are replaced by additives of the reaction mixture such as PivOH, triflate salts or Pd itself. Moreover, the homogeneous ligands (e.g.  $^{2\text{F}}\text{pyr}$  or pyridine) can be partially depleted in solution by interacting as a Lewis base with the Lewis acidic OCSs (homogeneous reaction of 0.05 mol%  $\text{Pd}(\text{OAc})_2$ , 0.5 eq.  $\text{Bi}(\text{OTf})_3$ , 50 eq. PivOH and no ligand has a TON of 84 and isomer selectivity of only 42 %). If several additives are depleted in solution, a less active and selective system might be the result.

**Table 3.10:** Scale up of washing procedures and synthesis procedure of MOF-808 and impact of 10 mg MOF-808 on the TON for biaryl formation and isomer selectivity (%) towards 3,3',4,4'-tetramethylbiphenyl in the homocoupling of *o*-xylene. Reaction conditions: 0.05 mol%  $\text{Pd}(\text{OAc})_2$ , 0.5 eq.  $\text{Bi}(\text{OTf})_3$ , 50 eq. PivOH, 1:1  $^{2\text{F}}\text{pyr}$ , 95 °C, 16 bar  $\text{O}_2$ , 17 hours.

			
Entry	Wash/Synthesis procedure	Isomer selectivity	TON
1	Homogeneous	84	211
2	Unwashed MOF-808	67	10
3	2x 0.1M $\text{Ca}(\text{OAc})_2 \cdot \text{H}_2\text{O}$ (MilliQ)	57	9
4	1x 0.13M propanesulfonic acid (MeOH)	81	93
5	1x 0.63M sulfuric acid ( <i>o</i> -xylene)	79	44
6	Synthesis with $\text{ZrO}(\text{NO}_3)_2 \cdot x\text{H}_2\text{O}$	63	13

### 1.1.3. Ligand incorporation and impact on cluster composition

After these washing or synthesis procedures, ligand incorporation is the next step. Six  $^{2\text{F}^{3\text{C}}}\text{pyr}$  ligands were added per  $\text{Zr}_6$ -cluster in methanol and stirred during 24 hours, this was followed by six washing steps with ethanol to remove the remaining  $^{2\text{F}^{3\text{C}}}\text{pyr}$  ligands, which were not properly attached to the  $\text{Zr}_6$ -cluster. The cluster composition was analyzed by  $^1\text{H}$ -NMR after the washing or synthesis procedures and after ligand incorporation to get insight into ligand incorporation and the functional groups that get replaced during the washing procedure (Table 3.11). In case of washing with strong acids (e.g. propanesulfonic acid), strong coordination was observed after the washing procedure, since approximately 4.4 propanesulfonates attached to the  $\text{Zr}_6$ -cluster. However, this has implications on the ligand incorporation step, since less space is available for these ligands. Only 0.6 of the 6 added  $^{2\text{F}^{3\text{C}}}\text{pyr}$  ligands per cluster attached to the  $\text{Zr}_6$ -cluster. When calcium acetate monohydrate was used in the washing step, quite a lot of acetate groups (4.2) were present at the  $\text{Zr}_6$ -cluster, which could efficiently be displaced by the  $^{2\text{F}^{3\text{C}}}\text{pyr}$  ligand (2.8  $^{2\text{F}^{3\text{C}}}\text{pyr}$  ligands and 0.7 remaining acetates). The

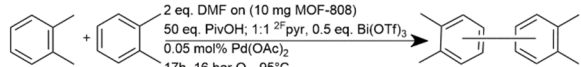
synthesis procedure from  $\text{ZrO}(\text{NO}_3)_2 \cdot x\text{H}_2\text{O}$  resulted mainly in formate ions on the  $\text{Zr}_6$ -cluster after synthesis (3.1 per  $\text{Zr}_6$ -cluster) and OCSs (1.4 per  $\text{Zr}_6$ -cluster), which could easily be displaced by the  $^{2\text{F}^{3\text{C}}}\text{pyr}$  ligand (3.2 per  $\text{Zr}_6$ -cluster).

**Table 3.11:** Cluster composition determined by  $^1\text{H}$ -NMR after the different washing procedures ( $\text{Ca}(\text{OAc})_2 \cdot \text{H}_2\text{O}$ , propanesulfonic acid, sulfuric acid) or synthesis procedure from  $\text{ZrO}(\text{NO}_3)_2 \cdot x\text{H}_2\text{O}$  and after ligand incorporation with  $^{2\text{F}^{3\text{C}}}\text{pyr}$ .

cluster composition after several washing/synthesis procedures						
Washing/synthesis procedure	acetate	$^{2\text{F}^{3\text{C}}}\text{pyr}$	OCSs	DMF	$\text{PrSO}_3^-$	formate
$\text{Ca}(\text{OAc})_2 \cdot \text{H}_2\text{O}$	4.2	0.0	1.2	0.6	0.0	0.0
$\text{PrSO}_3\text{H}$	0.5	0.0	0.2	0.8	4.4	0.0
$\text{H}_2\text{SO}_4$	0.8	0.0	1.2	4.0	0.0	0.0
$\text{ZrO}(\text{NO}_3)_2 \cdot x\text{H}_2\text{O}$ (DMF+EtOH)	0.0	0.0	1.4	1.5	0.0	3.1
cluster composition after ligand incorporation						
washing/synthesis procedure	acetate	$^{2\text{F}^{3\text{C}}}\text{pyr}$	OCSs	DMF	$\text{PrSO}_3^-$	formate
$\text{Ca}(\text{OAc})_2 \cdot \text{H}_2\text{O}$	0.7	2.8	0.3	2.2	0.0	0.0
$\text{PrSO}_3\text{H}$	0.3	0.6	0.1	2.3	2.8	0.0
$\text{H}_2\text{SO}_4$	0.5	0.5	2.4	2.6	0.0	0.0
$\text{ZrO}(\text{NO}_3)_2 \cdot x\text{H}_2\text{O}$ (DMF+EtOH)	0.0	3.2	-0.2	2.7	0.0	0.3

In each case, two or more DMF molecules resulting from the MOF synthesis solution were still coordinated to the  $\text{Zr}_6$ -cluster after ligand incorporation. To test the influence of these DMF molecules, a similar amount of DMF (as on 10 mg MOF-808) was added to the homogeneous reaction using 0.05 mol%  $\text{Pd}(\text{OAc})_2$ , 0.5:1  $\text{Bi}(\text{OTf})_3$ , 50 eq. pivOH and 1:1  $^{2\text{F}}\text{pyr}$ . This resulted in only a slight decrease in TON, while the isomer selectivity remained similar (Table 3.12).

**Table 3.12:** Influence of DMF on the TON for biaryl formation and isomer selectivity (%) towards 3,3',4,4'-tetramethylbiphenyl in the homocoupling of *o*-xylene. Reaction conditions:  $\text{Pd}(\text{OAc})_2$  (0.05 mol%), 1:1  $^{2\text{F}}\text{pyr}$ , 50 eq. PivOH, 0.5:1  $\text{Bi}(\text{OTf})_3$ , 95 °C, 16 bar  $\text{O}_2$ , 17 hours.

			
Entry	Reaction	Isomer selectivity	TON
1	Homogeneous	84	211
2	+DMF (2/cluster (10 mg MOF))	82	183

#### 1.1.4. Catalytic reactions

In the catalytic reactions, immobilized ligands on MOF-808 were added to the reaction solution instead of the homogeneous ligands. However, no catalytic reactions were performed with MOF-808 from  $\text{ZrOCl}_2 \cdot 8\text{H}_2\text{O}$  after ligand incorporation. All previously applied washing procedures (e.g. calcium acetate monohydrate, etc.) were omitted, since the presence of different molecules at the  $\text{Zr}_6$ -cluster (which could be released) and reagents in solution during the reaction can result in quite complex systems, which makes it difficult to decide which parameters result in inhibition. Moreover, the washing procedures with strong acids limit the amount of ligands attached to the  $\text{Zr}_6$ -cluster due to strong attachment. Furthermore, if no washing procedures are used, it is not guaranteed that chlorides are eliminated. MOF-808 from  $\text{ZrO}(\text{NO}_3)_2 \cdot x\text{H}_2\text{O}$  needs to be tuned further before use in catalytic reactions.

## 1.2. Tuning MOF-808 from the $\text{ZrO}(\text{NO}_3)_2 \cdot x\text{H}_2\text{O}$ salt

The use of MOF-808 from  $\text{ZrO}(\text{NO}_3)_2 \cdot x\text{H}_2\text{O}$ , omits the problem with chlorides, but several considerations need to be taken into account to obtain a performant system. Palladium requires a special type of pyridine ligand to reach high TONs and isomer selectivities. When MOF-808 is added in too low amounts (e.g. < 1:1 ligand/Pd), not every palladium atom can coordinate with a ligand, resulting in decreased isomer selectivities (see homogeneous conditions: amount of ligand). Not only the amount of ligand needs to be accurate, also the ratios of other reactants (e.g. TFAH,  $\text{M}(\text{OTf})_n$ ,  $\text{Pd}(\text{OAc})_2$ , etc.) need to be perfectly adjusted, since slight changes in composition of the reaction mixture can give rise to large changes in isomer selectivity and TON (see homogeneous reaction: screening of amount of TFAH, screening of the triflate salts and their amounts). Finally, removal of coordinating species at the  $\text{Zr}_6$ -cluster is required to eliminate interference with the catalytic system.

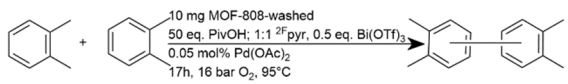
### 1.2.1. Washing procedure

In order to eliminate interference with the catalytic system, removal of as many coordinating species from the  $\text{Zr}_6$ -cluster as possible is required. This was done by washing MOF-808 from the  $\text{ZrO}(\text{NO}_3)_2 \cdot x\text{H}_2\text{O}$  salt during several days in methanol. In this way OCSs were generated on the  $\text{Zr}_6$ -cluster, which are also more susceptible for ligand incorporation.

### 1.2.2. Reaction inhibition test

After the washing procedure with methanol, 10 mg of washed MOF-808 was used as additive in the same homogeneous reaction as before (0.05 mol%  $\text{Pd}(\text{OAc})_2$ , 0.5:1.  $\text{Bi}(\text{OTf})_3$ , 50 eq. PivOH, 1:1  $^{2\text{F}}$ pyr, 16 bar  $\text{O}_2$ , 95 °C, 17 hours) to check if the reaction was still inhibited when the  $\text{Zr}_6$ -cluster is free of interfering species (see Figure 3.8). A TON of only 16 and isomer selectivity of 64 % was observed, which is not very different from the reaction with 10 mg of unwashed MOF-808 (Table 3.13). Hence, the presence of interfering species on the  $\text{Zr}_6$ -cluster is not the only reason for the decrease in reaction performance. It is hypothesized that the interaction of the additives (e.g. pyridine-type ligands, triflate salt, Pd itself, etc.) with the  $\text{Zr}_6$ -cluster is also a major source of deactivation.

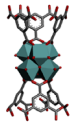
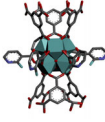
**Table 3.13:** Scale up of washing procedure and synthesis procedures of MOF-808 and impact of 10 mg MOF-808 on the TON for biaryl formation and isomer selectivity (%) towards 3,3',4,4'-tetramethylbiphenyl in the homocoupling of *o*-xylene. Reaction conditions: 0.05 mol%  $\text{Pd}(\text{OAc})_2$ , 0.5:1  $\text{Bi}(\text{OTf})_3$ , 50 equivalent PivOH, 1:1  $^{2\text{F}}$ pyr, 95 °C, 16 bar  $\text{O}_2$ , 17 hours.

			
Entry	Wash/Synthesis procedure	Isomer selectivity	TON
1	Homogeneous	84	211
2	Unwashed MOF-808	67	10
3	MOF-808-MeOH	64	16

### 1.2.3. Ligand incorporation and impact on cluster composition

After the washing procedure with methanol, six equivalents of  $^{2F3C}$ pyr were added per  $Zr_6$ -cluster in a methanol solution and stirred during 24 hours. Afterwards, MOF-808 was washed six times with ethanol to remove the weakly coordinating  $^{2F3C}$ pyr ligands. The cluster composition was analyzed by  $^1H$ -NMR after the washing procedure and after ligand incorporation (Table 3.14). After the washing procedure with methanol, a lot of OCSs were created (5.0 per  $Zr_6$ -cluster) and the remaining spaces were occupied by formates and methanol, which all can be quite easily displaced during ligand incorporation. After ligand incorporation, a lot of  $^{2F3C}$ pyr ligands were attached to the  $Zr_6$ -cluster (4.9 of the 6 available places were occupied by the ligands).

**Table 3.14:** Cluster composition determined by  $^1H$ -NMR after washing procedure with MeOH of MOF-808 synthesized from  $ZrO(NO_3)_2 \cdot xH_2O$  and after ligand incorporation with six  $^{2F3C}$ pyr ligands per  $Zr_6$ -cluster.

	Cluster composition after washing procedure MeOH					
	$^{2F3C}$ pyr	Formic acid	MeOH	OCSs	$M_w$ (g/mol)	$^{2F3C}$ pyr/Pd (5 mg MOF-808)
	0	0.7	0.3	5.0	1299	0
	Cluster composition after ligand incorporation					
	$^{2F3C}$ pyr	Formic acid	MeOH	OCSs	$M_w$ (g/mol)	$^{2F3C}$ pyr/Pd (5 mg MOF-808)
	4.9	0.1	0	1.0	1821	1.63

XRD patterns were measured of MOF-808 after the washing procedure with methanol and after the ligand incorporation with  $^{2F3C}$ pyr to ensure that the structure of MOF-808 was preserved (Figure 3.9). These powder diffractograms resembled the simulated powder diffractogram of MOF-808 and showed that the structure was not destroyed.

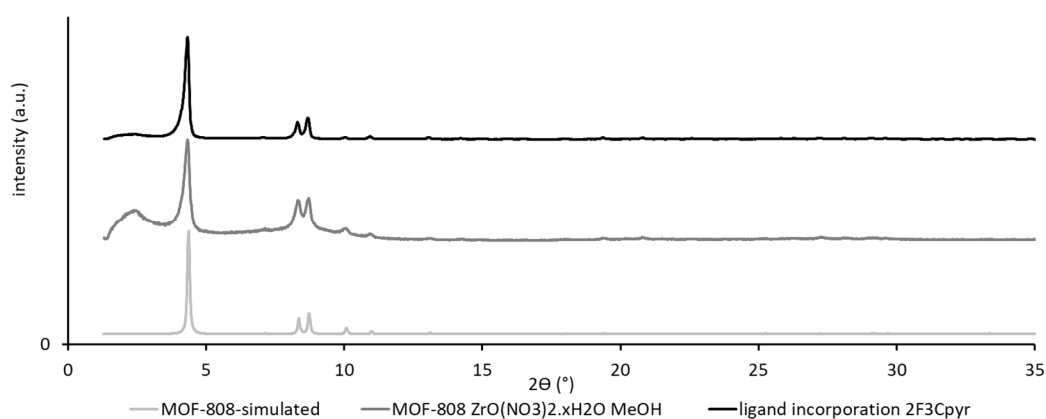


**Figure 3.9:** Powder diffractograms of MOF-808: simulated, after synthesis from  $ZrO(NO_3)_2 \cdot xH_2O$  and washing procedure with methanol and after ligand incorporation with  $^{2F3C}$ pyr.



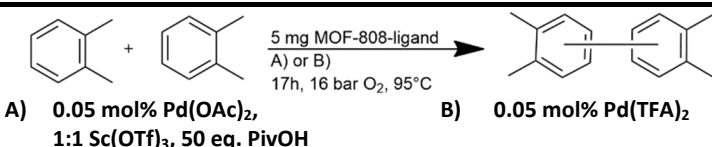
### 1.2.4. Catalytic reactions

Reaction conditions were selected based on the best performing homogeneous conditions (e.g. 0.05 mol% Pd(OAc)<sub>2</sub>, 1:1 Sc(OTf)<sub>3</sub>, 50 eq. PivOH and 0.05 mol% Pd(TFA)<sub>2</sub> with each 1:1 <sup>2F</sup>pyr at 95 °C, during 17 hours and 16 bar O<sub>2</sub>). However, in catalytic reactions with MOF-808, the homogeneous ligand (<sup>2F</sup>pyr) is replaced by immobilized ligand (<sup>2F3C</sup>pyr) on MOF-808. Reactions were performed with 5 mg of MOF-808 from ZrO(NO<sub>3</sub>)<sub>2</sub>·xH<sub>2</sub>O after washing procedure with methanol (i.e. absence of coordinating species in the system) and also after ligand incorporation with <sup>2F3C</sup>pyr. The cluster composition after ligand incorporation was [Zr<sub>6</sub>O<sub>4</sub>(OH)<sub>4</sub>(btc)<sub>2</sub>(H<sub>2</sub>O/OH)<sub>1.0</sub>(HCOO)<sub>0.1</sub>(<sup>2F3C</sup>pyr)<sub>4.9</sub>], which corresponds to a molecular weight of 1821 g/mol. When 5 mg of this MOF-808 was added in the reaction, 0.0135 mmol <sup>2F3C</sup>pyr ligands were present, which is equivalent to a 1.63:1 <sup>2F3C</sup>pyr/Pd ratio (see Table 3.14).

Reactions with 5 mg MOF-808 after the washing procedure with methanol (i.e. no coordinating species) resulted in isomer selectivities of 37 % for the reaction with 0.05 mol% Pd(OAc)<sub>2</sub>, 1:1 Sc(OTf)<sub>3</sub> and 50 eq. PivOH, and 48 % for the reaction with 0.05 mol% Pd(TFA)<sub>2</sub>. These isomer selectivities are very similar to the isomer selectivities obtained under homogeneous reaction conditions in absence of ligand (respectively 40 % and 54 %), while the TON was higher (62 vs. 45 in the system with triflate salts) or lower (25 vs. 37 in the system with Pd(TFA)<sub>2</sub>) compared to the homogeneous reaction without ligands (Table 3.15).

Reactions with 5 mg MOF-808 after ligand incorporation resulted in isomer selectivities of 39 % for the reaction with 0.05 mol% Pd(OAc)<sub>2</sub>, 1:1 Sc(OTf)<sub>3</sub> and 50 eq. PivOH, and 50 % for the reaction with 0.05 mol% Pd(TFA)<sub>2</sub>. Surprisingly, these isomer selectivities are also very similar compared to the homogeneous reaction in absence of ligands (respectively 40 % and 54 %), although ligands are present in this case. However, higher isomer selectivities were expected (respectively 73 % and 81 %), since one ligand can coordinate one palladium center (1:1 ratio <sup>2F</sup>pyr/Pd) (Table 3.15).

**Table 3.15:** TON for biaryl formation and isomer selectivity (%) towards 3,3',4,4'-tetramethylbiphenyl in the homocoupling of *o*-xylene. Introduction of 5 mg MOF-808 after washing procedure with methanol or after ligand incorporation with <sup>2F3C</sup>pyr. Reaction conditions: 5 mg MOF-808, A) or B), 95 °C, 16 bar O<sub>2</sub>, 17 hours.

					
Entry	5 mg MOF-808	Isomer selectivity	TON	Isomer selectivity	TON
1	MOF-808-MeOH	37	62	48	25
2	MOF-808- <sup>2F3C</sup> pyr <sub>4.9</sub>	39	63	50	10
3	Homogeneous (no <sup>2F</sup> pyr)	40	45	54	37
4	Homogeneous (1:1 <sup>2F</sup> pyr)	73	96	81	99

The discrepancy between the obtained isomer selectivities under heterogeneous conditions with MOF-808- $^{2F3C}$ pyr<sub>4.9</sub> (39 % in the system with triflate salts and 50 % in the system with Pd(TFA)<sub>2</sub>) and the expected isomer selectivities under homogeneous conditions (73 % for the system with triflate salts and 81 % for the system with Pd(TFA)<sub>2</sub>), might be due to the conformation of the attached ligands. Nitrogen occupies the *meta* position in  $^{2F3C}$ pyr, while it might need to be in the *para* position, such as in  $^{2F4C}$ pyr, to execute the right steric effect on palladium. Moreover, MOF-808 with too many ligands per Zr<sub>6</sub>-cluster might give rise to steric hindrance inside the pore, which implies that these ligands cannot take part in the reaction (Figure 3.10).

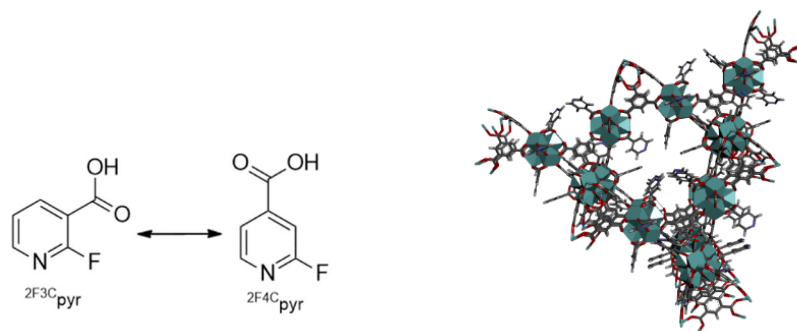


**Figure 3.10:** The difference in conformation of  $^{2F3C}$ pyr and  $^{2F4C}$ pyr (left) and MOF-808 with on average three  $^{2F3C}$ pyr ligands per Zr<sub>6</sub>-cluster (right).

### 1.3.Conclusion

During the reaction inhibition tests, washed MOF-808 was tested as additive in a homogeneous reaction in the presence of 1:1  $^{2F}$ pyr ligand (with 0.05 mol% Pd(OAc)<sub>2</sub>, 0.5:1 Bi(OTf)<sub>3</sub> and 50 eq. PivOH). Strong inhibition of the system was observed by introduction of 10 mg MOF-808 (independently of the washing procedure) compared to the homogeneous reaction (TON decreased from 211 to 16 and isomer selectivity from 84 % to 64 % after addition of 10 mg MOF-808 washed with methanol). However, when the same MOF-808 washed with methanol was used as additive in a homogeneous reaction in the absence of ligands (e.g. 0.05 mol% Pd(OAc)<sub>2</sub>, 1:1 Sc(OTf)<sub>3</sub> and 50 eq. PivOH), no significant change in reaction performance was observed (TON changed from 45 to 62 and isomer selectivity from 40 % to 37 % by the introduction of MOF-808). This indicates that inhibition is mainly caused by depletion of the pyridine-type ligand in solution. This is not necessarily a problem, since there is no need for homogeneous pyridine ligands during the catalytic reaction, when the ligand is immobilized on MOF-808.

Similar isomer selectivities were obtained in the reactions with MOF-808 after washing procedure with methanol and after ligand incorporation with  $^{2F3C}$ pyr as in the homogeneous reaction in absence of ligands, independently on the presence or absence of  $^{2F3C}$ pyr ligands at the  $Zr_6$ -cluster. These unexpected results might be due to the conformation of the ligand ( $^{2F3C}$ pyr vs  $^{2F4C}$ pyr) or due to sterical hindrance in the pore, which might impede the interaction between palladium and the attached ligands. Furthermore, it can be noted that these ligands stay properly attached to the  $Zr_6$ -clusters, since the release of pyridine-type ligands should result in a decrease in TON and isomer selectivity (see homogeneous conditions: screening of the ligands with secondary functionality). In order to exclude the effect of steric hindrance in the pores, easier systems without pores need to be considered, such as functionalized  $TiO_2$  NPs or poly(4-vinylpyridine).

## 2. Other heterogeneous supports as alternatives for MOFs

### 2.1. TiO<sub>2</sub> nanoparticles

Besides MOFs, TiO<sub>2</sub> NPs can also serve as support for pyridine-type ligands. A ligand with a carboxylic acid group can bind to the surface of a TiO<sub>2</sub> particle in several ways (electrostatic interaction, hydrogen bonding and chemical adsorption (e.g. ester linkage, bridging and chelating)).<sup>94</sup> Isonicotinic acid and <sup>2</sup>F<sup>3</sup>Cpyr were attached to the TiO<sub>2</sub> NPs *via* an immersion method developed by Brumbach *et al.*<sup>93</sup> However, TGA measurements showed that these materials contain almost no ligands on the TiO<sub>2</sub> surface. Hence, the pH of the immersion solution was measured to elucidate why the ligands did not attach to the surface. The pH of the immersion solution was 9, which is well above the pK<sub>a</sub> of the acid (e.g. pK<sub>a</sub> of isonicotinic acid is 4.96) and above the point of zero charge of TiO<sub>2</sub> (e.g. PZC of TiO<sub>2</sub> (P25) NPs is 6.2).<sup>97,98</sup> This means that both the ligand and the TiO<sub>2</sub> surface were negatively charged and repelled each other.

Catalytic reactions were performed using 5 mg of these NPs (without ligands) under different reaction conditions (0.05 mol% Pd(OAc)<sub>2</sub>, 1:1 Sc(OTf)<sub>3</sub> and 50 eq. PivOH and with 0.05 mol% Pd(TFA)<sub>2</sub>) (Table 3.16). The isomer selectivity was similar to the homogeneous conditions without ligands, which was expected since almost no ligands were present. However, higher TONs were observed compared to the homogeneous system without ligands. Isolation of the palladium atoms on the surface of the TiO<sub>2</sub> NPs may impede Pd<sup>(0)</sup> aggregation and thus catalyst deactivation, resulting in higher TONs compared to the homogeneous system.<sup>88</sup>

**Table 3.16:** TON for biaryl formation and isomer selectivity (%) towards the 3,3',4,4'-tetramethylbiphenyl in the homocoupling of *o*-xylene upon varying the amount of ligand. Reaction conditions: A) 0.05 mol% Pd(OAc)<sub>2</sub>, 1:1 Sc(OTf)<sub>3</sub>, 50 eq. PivOH or B) Pd(TFA)<sub>2</sub> (0.05 mol%), 5 mg TiO<sub>2</sub>-ligand, 95 °C, 16 bar O<sub>2</sub>, 17 hours.

Entry	TiO <sub>2</sub> -ligand	Amount	Isomer selectivity	TON	Isomer selectivity	TON
1	<sup>2</sup> F <sup>3</sup> Cpyr	5 mg	40	121	54	56
2	Isonicotinic acid	5 mg	41	86	53	46
3	Homogeneous (no ligand)	-	40	45	54	37
4	Homogeneous ( <sup>2</sup> Fpyr)	-	73	96	81	99
5	Homogeneous (pyridine)	-	70	87	84	33

Since the immersion method developed by Brumbach *et al.* resulted in high a pH of the immersion solution, a set of different pH values was explored (4-6). Isonicotinic acid was used as ligand, which has a pK<sub>a</sub> of 4.96. The immersion method was performed in milliQ water as solvent and tri-ethylamine was used to adjust the pH (see Chapter 2 Materials and Methods Section I.1.2).

The coverage degree was determined by TGA and confirmed to decrease with increasing pH. At low pH (e.g. pH 4), the surface of TiO<sub>2</sub> is positively charged and isonicotinic acid is partially deprotonated. Hence, it is anticipated that isonicotinate will interact electrostatically with the positively charged TiO<sub>2</sub> surface. Indeed, TGA revealed a coverage degree of 7.26 mmol ligands per g TiO<sub>2</sub> (see Chapter 2 Material and Methods Section III.3) (Figure 3.11). At higher pH (e.g. pH 6), the surface of TiO<sub>2</sub> gets negatively charged and repels isonicotinate, resulting in a non-functionalized surface.

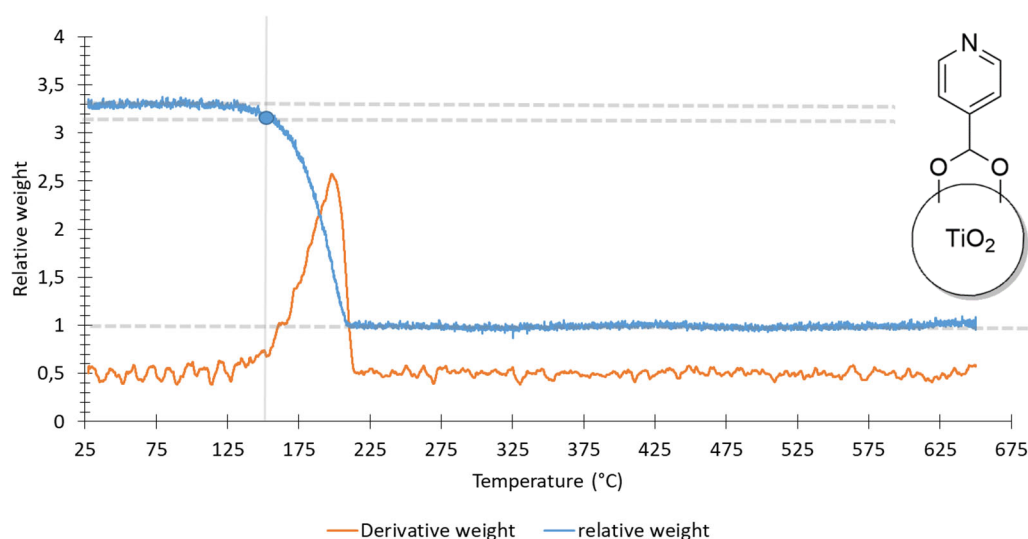


**Figure 3.11:** TGA of sample TiO<sub>2</sub> functionalized with isonicotinic acid with an immersing solution of pH 4 before reaction. The TGA shows that ligands are present on the surface at low pH.

Reactions were performed with 5 mg of isonicotinate-functionalized TiO<sub>2</sub> NPs with high amounts of ligands on the surface (pH 4 of the immersion solution; corresponding to an isonicotinate/Pd ratio of 4.40:1) and low amounts of ligands (pH 6 of the immersion solution; almost no ligands). Notably, TiO<sub>2</sub>-isonicotinate NPs with many ligands on the surface are not active in contrast to NPs with almost no ligands (Table 3.17).

**Table 3.17:** TON for biaryl formation and isomer selectivity (%) towards the 3,3',4,4'-tetramethylbiphenyl in the homocoupling of *o*-xylene upon varying the amount of ligand. Reaction conditions: Pd(TFA)<sub>2</sub> (0.05 mol%), 5 mg TiO<sub>2</sub>-ligand, 95 °C, 16 bar O<sub>2</sub>, 17 hours.

<div style="text-align: center;"> </div>						
			A) 0.05 mol% Pd(OAc) <sub>2</sub> , 1:1 Sc(OTf) <sub>3</sub> , 50 eq. PivOH		B) 0.05 mol% Pd(TFA) <sub>2</sub>	
Entry	pH immersion solution	Amount	Isomer selectivity	TON	Isomer selectivity	TON
1	4 (TiO <sub>2</sub> -isonicotinate)	5 mg	0	0	0	0
2	6 (TiO <sub>2</sub> -no ligand)	5 mg	43	85	52	50
3	Homogeneous (no ligand)	-	40	45	54	37
4	Homogeneous (pyridine)	-	70	87	84	33

This can be explained by the fact that the carboxylate groups of the ligands are not strongly attached to the  $\text{TiO}_2$  support. Release of excess of ligands from the support results in reaction inhibition (e.g. see homogeneous conditions: when  $> 1.5$  eq. of pyridine was used in a system with  $\text{Pd}(\text{TFA})_2$ , the reaction was completely inhibited; TON is 0). Moreover, if carboxylate ligands are used, low isomer selectivities as well low TONs are observed, due to interaction of the carboxylate group with palladium, instead of the pyridine functionality. This was confirmed under homogeneous conditions (see Chapter 3 Section I.1.1 and I.1.2). When for example 1:1 isonicotinic acid/Pd was used in a system with 0.05 mol%  $\text{Pd}(\text{TFA})_2$ , complete inhibition was observed, while low TONs and isomer selectivities were observed in a system with 0.05 mol%  $\text{Pd}(\text{OAc})_2$ , 0.5:1  $\text{Sc}(\text{OTf})_3$  and 50 eq. PivOH. The release of the ligands from the  $\text{TiO}_2$  support, prepared *via* the immersion method at pH 4, was also confirmed by a second TGA measurement after reaction (Figure 3.12). The relative weight of the  $\text{TiO}_2$  functionalized NPs at low temperatures (e.g. 25 °C) is lower after reaction (2.7) compared to before reaction (3.3), this means that mass is lost compared to the situation before reaction (Figure 3.11). However, some *o*-xylene (boiling point 144.4 °C) and other reaction products (e.g. bixylyls) were still present on the NPs, which were also burned away and also resulted in weight loss, which makes it complicated to calculate the exact amounts of ligands at the surface of the NPs after reaction.

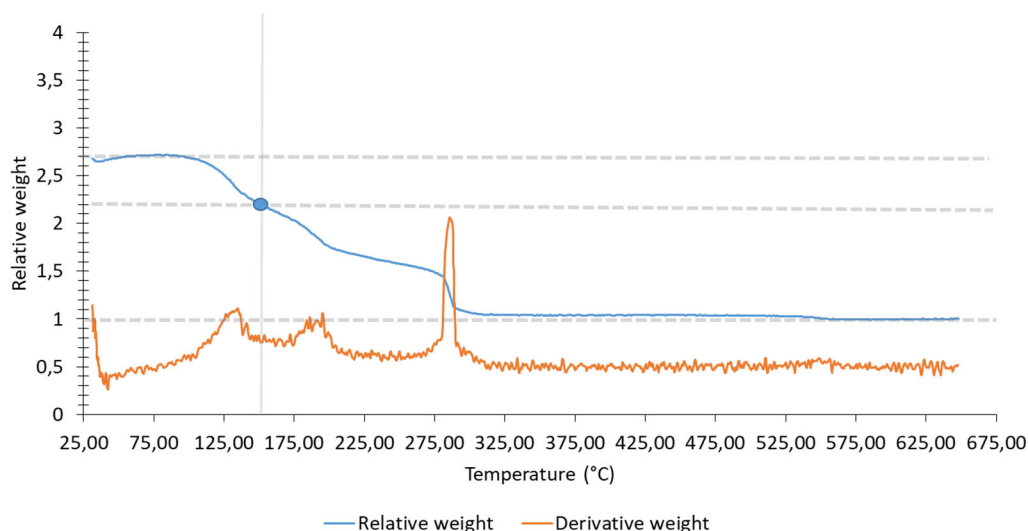


**Figure 3.12:** TGA of sample  $\text{TiO}_2$  functionalized with isonicotinic acid with an immersing solution of pH 4 after reaction. The TGA shows that part of the ligands are released from the support.

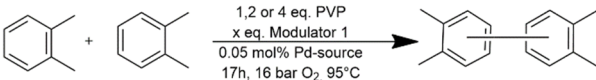
## 2.2. Poly(4-vinylpyridine)

Poly(4-vinylpyridine) is an interesting material with immobilized pyridine-type ligands, which is easy to study, since no pores are present. However, this system is not tunable, since the type of ligand cannot be changed. Several catalytic reactions were carried out with different amounts of poly(4-vinylpyridine) (1, 2 and 4 eq.) with 0.05 mol% Pd(TFA)<sub>2</sub> and with 0.05 mol% Pd(OAc)<sub>2</sub> and TFAH (in 2:1 and 4:1 ratio) (Table 3.18). The amount of poly(4-vinylpyridine) added to the reaction was calculated by:

$$1 \text{ eq.} = 0.00825 \text{ mmol} \times \text{Mw}_{1 \text{ unit vinylpyridine}} = 0.00825 \text{ mmol} \times 105 \text{ g/mol} = 0.87 \text{ mg}$$

In all reactions, the isomer selectivity of the reaction with poly(4-vinylpyridine) resembled the isomer selectivity under the same homogeneous conditions without the pyridine ligand, although pyridine-type ligands were undeniably present in the poly(4-vinylpyridine) material. This is in accordance to the reactions with MOF-808-<sup>2F3C</sup>pyr<sub>4.9</sub> (see Chapter 3 Section II.1.2).

**Table 3.18:** TON for biaryl formation and isomer selectivity (%) towards the 3,3',4,4'-tetramethylbiphenyl in the homocoupling of *o*-xylene upon varying the amount of ligand. Reaction conditions: Poly(4-vinylpyridine) (1,2 or 4 eq.), A) 0,05 mol % Pd(TFA)<sub>2</sub>, B) 0,05 mol% Pd(OAc)<sub>2</sub> and 2:1 TFAH, C) 0,05 mol% Pd(OAc)<sub>2</sub> and 4:1 TFAH, 95°C, 16 bar O<sub>2</sub>, 17 hours.

						
Entry	Pd-source	Eq. poly(4-vinylpyridine)	Modulator 1	Eq. modulator 1	Isomer selectivity	TON
1	Pd(TFA) <sub>2</sub>	1	-	-	60	62
2	Pd(TFA) <sub>2</sub>	2	-	-	60	51
3	Pd(TFA) <sub>2</sub>	4	-	-	61	35
4	Pd(OAc) <sub>2</sub>	1	TFAH	2	41	11
5	Pd(OAc) <sub>2</sub>	1	TFAH	4	39	19
6	Pd(TFA) <sub>2</sub>	Homogeneous (no ligand)	-	-	54	37
7	Pd(OAc) <sub>2</sub>	Homogeneous (no ligand)	TFAH	2	39	18
8	Pd(OAc) <sub>2</sub>	Homogeneous (no ligand)	TFAH	4	40	34
9	Pd(TFA) <sub>2</sub>	Homogeneous (pyridine)	-	-	84	33
10	Pd(OAc) <sub>2</sub>	Homogeneous (pyridine)	TFAH	2	84	50
11	Pd(OAc) <sub>2</sub>	Homogeneous (pyridine)	TFAH	4	76	54

## 2.3. Conclusion

The carboxylate groups of the pyridine-type ligands did not coordinate strongly enough to the surface of the TiO<sub>2</sub> NPs, resulting in a release of the ligands from the support. As a consequence, the reaction was inhibited completely. Hence, NPs with strongly coordinating ligands are required (e.g. with phosphonate groups) to obtain performing systems. For poly(4-vinylpyridine), the isomer selectivity was found to be similar as the isomer selectivity of the homogeneous reaction in absence of ligands. Although, ligands were clearly present and no steric hindrance is expected, since this material is pore-free, no influence of the pyridine-type ligands could be observed.

### 3. Mechanistical insights

The low isomer selectivities obtained in the systems with the immobilized ligands might arise from a bimetallic transmetalation mechanism (see Chapter 1 Literature study section I.3.2). This implies that each Pd center requires at least one pyridine ligand during the transmetalation step to obtain the desired product in high selectivities. In a system with immobilized ligands, this is impossible since at least one Pd center has to detach from its immobilized ligand to perform the transmetalation with an immobilized or also 'free' Pd center. Hence, it is hypothesized that high isomer selectivity is only possible with the addition of extra 'mobile' ligands (Figure 3.13).

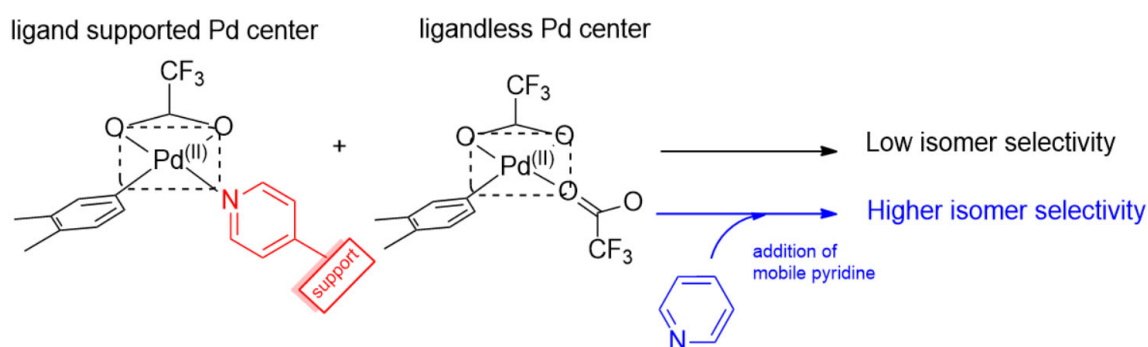


**Figure 3.13:** Addition homogeneous 'mobile' pyridine is required in order to obtain high isomer selectivity when a bimetallic mechanism takes place in a system with immobilized ligands.

It is thus of great importance to check first if there is indeed a bimetallic step in the reaction mechanism. This can be done by varying the Pd concentration while keeping other reaction conditions and ratios constant and measuring the initial rates (0-4 hours), as was demonstrated by the group of Stahl.<sup>5,6</sup> At low Pd concentrations, the transmetalation is rate-limiting and the rate has a second order dependence due to the bimetallic nature of the transmetalation step. However, at higher Pd concentrations, the C-H activation is rate-limiting and a first order rate dependence is expected (see Chapter 1 Literature study section I.3.2).<sup>5,6</sup> The least complex system with Pd(TFA)<sub>2</sub> and 1:1 pyridine was selected to test this hypothesis and, indeed, a bimetallic step in the reaction mechanism was confirmed (Figure 3.14).

Moreover, the substrate KIE effect was measured under these reaction conditions (0.05 mol% Pd(TFA)<sub>2</sub> and 1:1 pyridine) to determine the rate-limiting step. A value of  $k_H/k_D = 1.32$  was obtained, which, according to Fernández-Ibáñez, might imply rate-limiting dissociation of the dimeric Pd species.<sup>9</sup> However, these conditions correspond to the red arrow in Figure 3.14, pointing at a rate-limiting transmetalation.



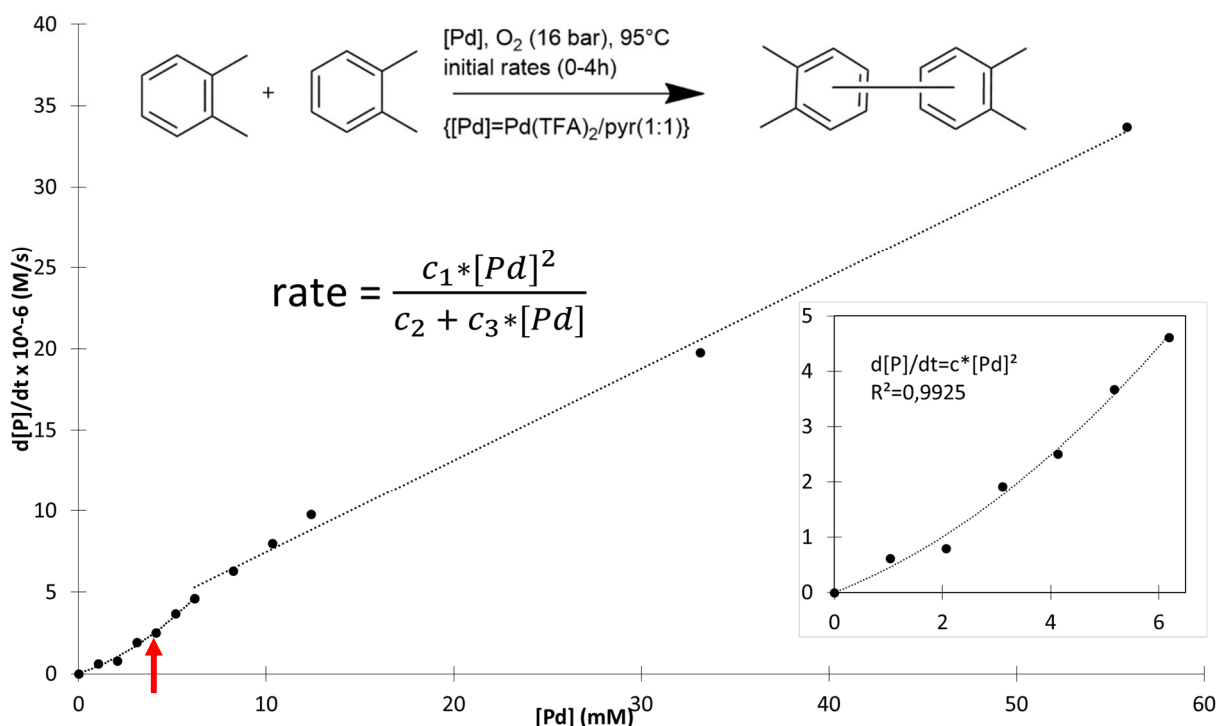


**Figure 3.14:** Kinetic dependence of the rate of Pd-catalyzed CDC of *o*-xylene on [Pd]. Reaction conditions: 16.6 mmol *o*-xylene, [Pd]: 1-60 mM, 1:1 pyridine, 16 bar O<sub>2</sub>, 95 °C, 0-4 hours.

Furthermore, it needs to be tested if the increase in isomer selectivity due to the presence of pyridine-type ligands is determined in the bimetallic transmetalation step. Addition of extra, subequivalent amounts, 'mobile' (homogeneous) ligands to a system with immobilized ligands, should result in an increase in isomer selectivity compared to the system with only immobilized ligands (so in absence of 'mobile' ligands). Furthermore, an increase in isomer selectivity is expected compared to the purely homogeneous reaction (only 'mobile' ligands present), since the addition of a material with immobilized ligands is useless otherwise.

### 3.1. Poly(4-vinylpyridine)

The poly(4-vinylpyridine) system was studied first, since this material with immobilized pyridine-type ligands is the easiest to study. Reactions were performed with 0.05 mol% Pd(TFA)<sub>2</sub>, poly(4-vinylpyridine) (1 eq. and 4 eq.) and the addition of 'mobile' (homogeneous) ligands (e.g. <sup>2F</sup>pyr and pyridine) in subequivalent amounts at 95°C during 17 hours with 16 bar O<sub>2</sub>.

#### 3.1.1. <sup>2F</sup>pyr as 'mobile' ligand

The first reactions were performed with extra homogeneous <sup>2F</sup>pyr (0.25, 0.50, 0.75 and 1 eq.). The isomer selectivity was higher when poly(4-vinylpyridine) (1 and 4 eq.) in combination with subequivalent amounts of 'mobile' <sup>2F</sup>pyr (< 1 eq.) was used compared to the homogeneous reaction with only subequivalent amounts of <sup>2F</sup>pyr (Figure 3.15). This indicates that the presence of the immobilized ligands has a positive influence on the isomer selectivity for a range of (subequivalent) 'mobile' ligand concentrations. However, the isomer selectivity of the systems with immobilized and

subequivalent amounts of 'mobile'  $^{2F}$ pyr ligands is still rather low (maximum of 76 %) compared to the homogeneous conditions (only 'mobile' ligands), where isomer selectivities above 80 % could be reached (1:1  $^{2F}$ pyr with 0.05 mol% Pd(TFA)<sub>2</sub> resulted in an isomer selectivity of 81 %) (Figure 3.15). The TON was similar compared to the homogeneous conditions with only the 'mobile' ligands, when 1 eq. of poly(4-vinylpyridine) was used. However, when higher amounts of poly(4-vinylpyridine) were used (e.g. 4 eq.), the TON decreased (Figure 3.16).

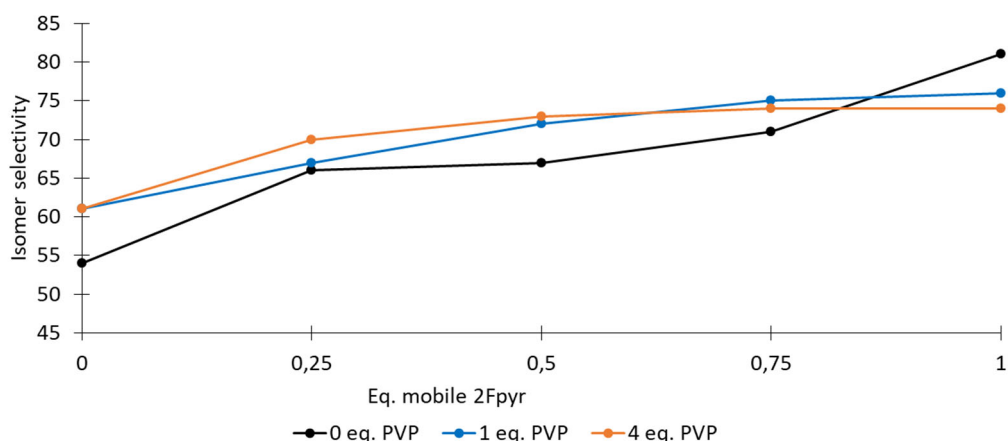


**Figure 3.15:** Isomer selectivity (%) towards 3,3',4,4'-tetramethylbiphenyl in the homocoupling of *o*-xylene upon addition of 'mobile'  $^{2F}$ pyr (0, 0.25, 0.50, 0.75 and 1 eq.). Reaction conditions: 0.05 mol% Pd(TFA)<sub>2</sub>, poly(4-vinylpyridine) (0, 1 or 4 eq.), 95 °C, 16 bar O<sub>2</sub>, 17 hours.

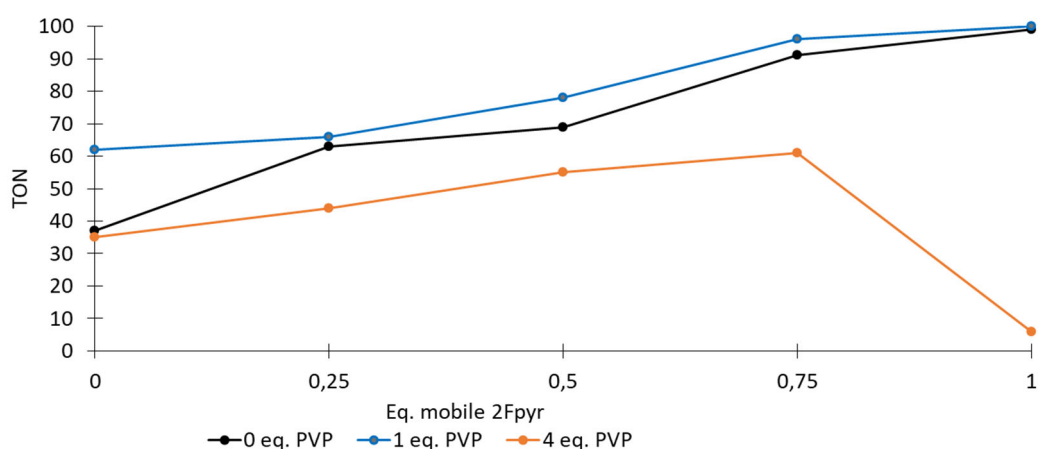


**Figure 3.16:** TON for biaryl formation in the homocoupling of *o*-xylene upon addition of 'mobile'  $^{2F}$ pyr (0, 0.25, 0.50, 0.75 and 1 eq.). Reaction conditions: 0.05 mol% Pd(TFA)<sub>2</sub>, poly(4-vinylpyridine) (0, 1 or 4 eq.), 95 °C, 16 bar O<sub>2</sub>, 17 hours.

The combination of subequivalent amounts of  $^{2F}$ pyr as 'mobile' ligand and poly(4-vinylpyridine) as immobilized ligand, resembles a mixed ligand system of  $^{2F}$ pyr and pyridine. Hence, homogeneous tests were performed with different ratios of  $^{2F}$ pyr and pyridine (Table 3.19). Surprisingly, the isomer selectivity of the 'mobile' mixed ligand systems was always lower than 80 %, while the addition of a single 'mobile' ligand resulted in isomer selectivities above 80 % (e.g. 1:1  $^{2F}$ pyr or 1:1 pyridine with 0.05 mol% Pd(TFA)<sub>2</sub> result in respectively isomer selectivities of 81 % and 84 %).

**Table 3.19:** TON for biaryl formation and isomer selectivity (%) towards 3,3',4,4'-tetramethylbiphenyl in the homocoupling of *o*-xylene upon varying the ratio of mixed ligand systems. Reaction conditions: 0.05 mol% Pd(TFA)<sub>2</sub>, *x* eq. pyridine + *y* eq. <sup>2F</sup>pyr (*x*+*y*=1), 95 °C, 16 bar O<sub>2</sub>, 17 hours.

<chem>Cc1ccccc1</chem> + <chem>Cc1ccccc1</chem> $\xrightarrow[\substack{0.05 \text{ mol\% Pd(TFA)}_2 \\ 17 \text{ h, 16 bar O}_2, 95^\circ\text{C}}]{\substack{x \text{ eq. pyr} + y \text{ eq. } ^{2F}\text{pyr} \\ x+y=1}}$ <chem>Cc1ccc(cc1)-c2cc(C)cc(C)c2</chem>				
Entry	Amount pyridine (Eq.)	Amount <sup>2F</sup> pyr (Eq.)	Isomer selectivity	TON
1	0	1	81	99
2	0,25	0,75	75	72
3	0,5	0,5	76	65
4	0,75	0,25	79	45
5	1	0	84	33

### 3.1.2. Pyridine as 'mobile' ligand

The same reactions were performed for 1 and 4 eq. poly(4-vinylpyridine) and 0.05 mol% Pd(TFA)<sub>2</sub>, but subequivalent amounts of 'mobile' pyridine instead of <sup>2F</sup>pyr were added. An isomer selectivity of 82 % and TON of 35 was obtained for the reaction with 4 eq. poly(4-vinylpyridine) and 0.5 eq. of 'mobile' pyridine. For even higher amounts of pyridine (0.75 eq.), an isomer selectivity of 82 % and a TON of 33 was obtained (Figure 3.17 and 3.18). The isomer selectivities under these conditions are very similar compared to the homogeneous reaction with 0.05 mol% Pd(TFA)<sub>2</sub> and 1:1 pyridine, which resulted in an isomer selectivity of 84 % and a TON of 33. It is important to point-out that not too much 'mobile' ligands should be added to the reaction mixture (i.e. 0.5 eq. pyridine is preferred over 0.75 eq.), since these ligands can attract palladium to the solution, resulting in more leaching. Reactions with 4 eq. poly(4-vinylpyridine) are preferred, even though they result in lower TONs, since the use of more immobilized ligands increases the probability that palladium remains in the support.

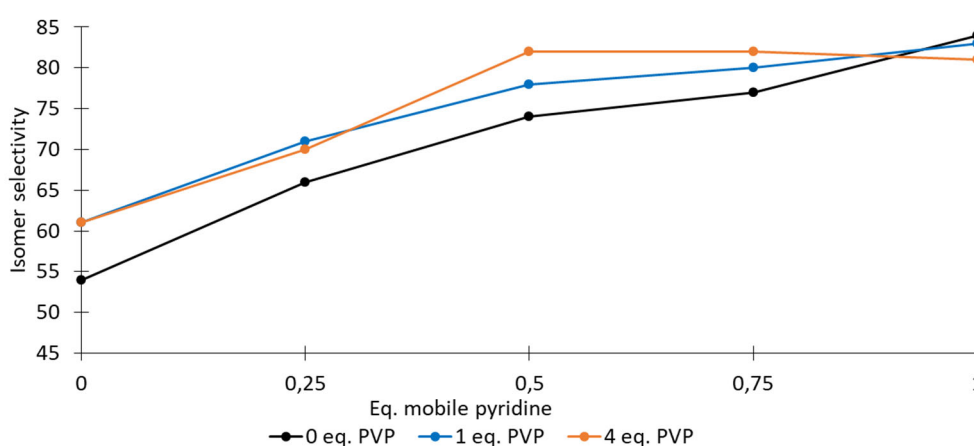


**Figure 3.17:** Isomer selectivity (%) towards 3,3',4,4'-tetramethylbiphenyl in the homocoupling of *o*-xylene upon addition of 'mobile' pyridine (0, 0.25, 0.50, 0.75 and 1 eq.). Reaction conditions: 0.05 mol% Pd(TFA)<sub>2</sub>, poly(4-vinylpyridine) (0, 1 or 4 eq.), 95 °C, 16 bar O<sub>2</sub>, 17 hours.

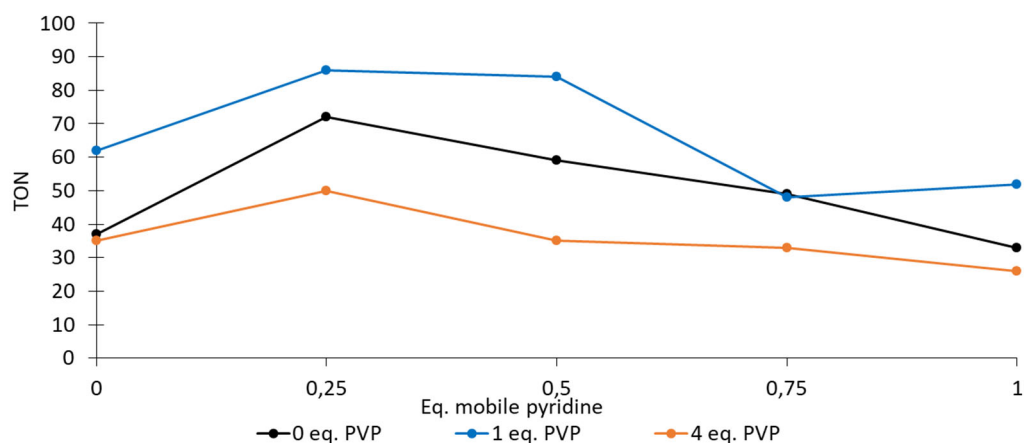


**Figure 3.18:** TON for biaryl formation in the homocoupling of *o*-xylene upon addition of 'mobile' pyridine (0, 0.25, 0.50, 0.75 and 1 eq.). Reaction conditions: 0.05 mol% Pd(TFA)<sub>2</sub>, poly(4-vinylpyridine) (0, 1 or 4 eq.), 95 °C, 16 bar O<sub>2</sub>, 17 hours.

Since it was shown that the isomer selectivity increases in the system with 0.05 mol% Pd(TFA)<sub>2</sub>, 4 eq. of poly(4-vinylpyridine) and 0.5 eq. of pyridine, these conditions were repeated for reactions with Pd(OAc)<sub>2</sub> and TFAH (2:1 and 4:1) to check if this also applies to other reaction conditions. In this case, strong acids such as TFAH can be used, since the pyridine-type ligands are covalently bound to the polymer backbone in poly(4-vinylpyridine). Again, an increase in isomer selectivity was observed with 4 eq. of poly(4-vinylpyridine) and 0.5 eq. of 'mobile' pyridine compared to the homogeneous reaction with only 0.5 eq. of 'mobile' pyridine. Moreover, the obtained isomer selectivity resembles the isomer selectivity of the homogeneous reaction with 0.05 mol% Pd(OAc)<sub>2</sub>, 2:1 or 4:1 TFAH and 1:1 pyridine (Table 3.20).

**Table 3.20:** TON for biaryl formation and isomer selectivity (%) towards 3,3',4,4'-tetramethylbiphenyl in the homocoupling of *o*-xylene upon varying the amount of ligand. Reaction conditions: 4 eq. poly(4-vinylpyridine) and 0.5 eq. pyridine, A) 0.05 mol% Pd(TFA)<sub>2</sub>, B) 0.05 mol% Pd(OAc)<sub>2</sub> and 2:1 TFAH, C) 0.05 mol% Pd(OAc)<sub>2</sub> and 4:1 TFAH, 95 °C, 16 bar O<sub>2</sub>, 17 hours.

<chem>Cc1ccccc1</chem> + <chem>Cc1ccccc1</chem> $\xrightarrow[17\text{h, 16 bar O}_2, 95^\circ\text{C}]{\text{4 eq. PVP + 0.5 eq. pyridine (A, B, C)}}$ <chem>Cc1ccc(cc1)-c2ccccc2C</chem>						
Entry	Reaction	Pd-source	Modulator 1	Eq. Modulator 1	Isomer selectivity	TON
1	A) 4 eq. PVP + 0.5 eq. pyridine	Pd(TFA) <sub>2</sub>			82	35
2	B) 4 eq. PVP + 0.5 eq. pyridine	Pd(OAc) <sub>2</sub>	TFAH	2	80	28
3	C) 4 eq. PVP + 0.5 eq. pyridine	Pd(OAc) <sub>2</sub>	TFAH	4	73	19
4	homogeneous (0.5 eq. pyridine)	Pd(TFA) <sub>2</sub>			74	59
5	homogeneous (0.5 eq. pyridine)	Pd(OAc) <sub>2</sub>	TFAH	2	67	55
6	homogeneous (0.5 eq. pyridine)	Pd(OAc) <sub>2</sub>	TFAH	4	61	41
7	homogeneous (1 eq. pyridine)	Pd(TFA) <sub>2</sub>			84	33
8	homogeneous (1 eq. pyridine)	Pd(OAc) <sub>2</sub>	TFAH	2	84	50
9	homogeneous (1 eq. pyridine)	Pd(OAc) <sub>2</sub>	TFAH	4	76	54

### 3.2. TiO<sub>2</sub> and CeO<sub>2</sub> NPs

The same experiments were conducted with the systems consisting of functionalized TiO<sub>2</sub> and CeO<sub>2</sub> NPs. The NPs were functionalized with pyridine-type phosphonate ligands by “Le Centre National de la Recherche Scientifique” (CNRS) in Montpellier. TiO<sub>2</sub>-2-pyridine-phosphonate NPs were prepared either *via* one-pot reaction ( $S_{\text{BET}}$  of 106 m<sup>2</sup>/g, 0.99 mmol ligand/g TiO<sub>2</sub>) or *via* surface modification (SM) ( $S_{\text{BET}}$  of 106 m<sup>2</sup>/g, 0.26 mmol ligand/g TiO<sub>2</sub>), while CeO<sub>2</sub>-2-pyridine-phosphonate NPs were only prepared *via* SM ( $S_{\text{BET}}$  of 250 m<sup>2</sup>/g, 0.12 mmol ligand/g CeO<sub>2</sub>) (Figure 3.19).

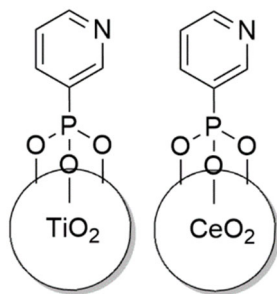


**Figure 3.19:** TiO<sub>2</sub> and CeO<sub>2</sub> NPs functionalized with 2-pyridine-phosphonate, either by one-pot reaction or SM

#### 3.2.1. TiO<sub>2</sub> NPs one-pot – amount of immobilized ligands

The TiO<sub>2</sub> NPs prepared *via* one-pot reaction were used to test the effect of the amount of immobilized ligands on the performance of the reaction. Reactions were performed with 0.05 mol% Pd(TFA)<sub>2</sub> and an amount of TiO<sub>2</sub> NPs which provides 0.5, 1 and 2 eq. of 2-pyridine-phosphonate ligands, with the addition of subequivalent amounts of ‘mobile’ pyridine (0, 0.25, 0.50 and 0.75 eq.) at 95 °C, during 17 hours with 16 bar O<sub>2</sub>. In contrast to the system with poly(4-vinylpyridine), the isomer selectivity with the use of TiO<sub>2</sub>-2-pyridine-phosphonate NPs in combination with ‘mobile’ pyridine is lower compared to the homogeneous reaction with only subequivalent ‘mobile’ pyridine (Figure 3.20). Moreover, the more ligands present on the TiO<sub>2</sub> NPs, the lower the isomer selectivity, which is also in contrast to the system with poly(4-vinylpyridine). The nitrogen atom in *meta* position might exert the wrong steric and/or the electronic effect or the phosphonate group might have a bad influence on the isomer selectivity. In order to discriminate between the electronic effect of the secondary phosphonate group and the ligating effect of this group, a homogeneous reaction was performed with the ethyl ester of a phosphonate ligand. The homogeneous reaction with 0.05 mol% Pd(TFA)<sub>2</sub> and 1:1 4-fluoro-3-pyridine diethyl phosphonate resulted in a TON of 41 and an isomer selectivity of only 61 %. This indicates that that the phosphonate groups exerts the wrong electronic effect. The TONs of reactions with TiO<sub>2</sub> NPs, providing 0.5 eq. of 2-pyridine-phosphonate ligands, in combination with ‘mobile’ pyridine ligands are very similar to the TONs of the homogeneous reaction with ‘mobile’ pyridine. When larger amounts of TiO<sub>2</sub> NPs are added (e.g. representing 1 or 2 eq. 2-pyridine-phosphonates) a strong decrease in TON is observed (Figure 3.21).

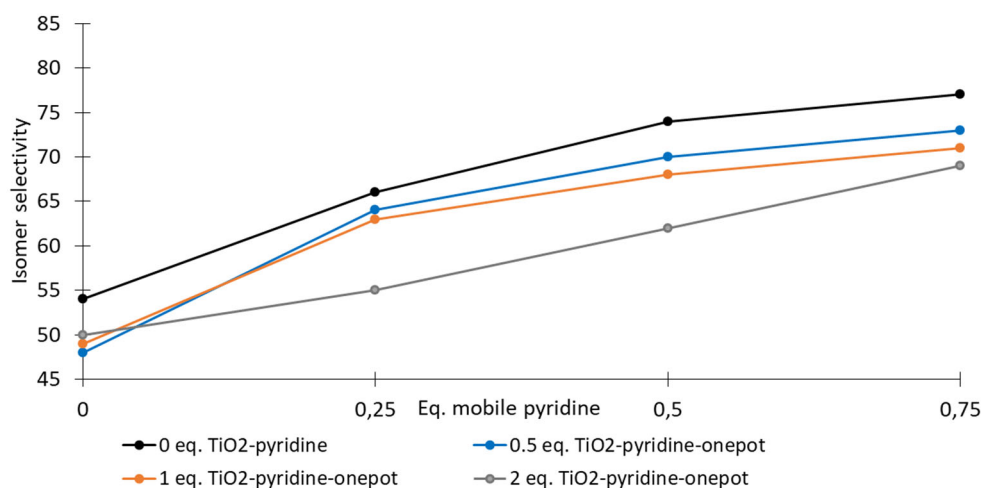


**Figure 3.20:** Isomer selectivity (%) towards 3,3',4,4'-tetramethylbiphenyl in the homocoupling of *o*-xylene upon addition of 'mobile' pyridine (0, 0.25, 0.50 and 0.75 eq.). Reaction conditions: 0.05 mol% Pd(TFA)<sub>2</sub>, TiO<sub>2</sub>-pyridine-onepot (0, 0.5, 1 and 2 eq.), 95 °C, 16 bar O<sub>2</sub>, 17 hours.

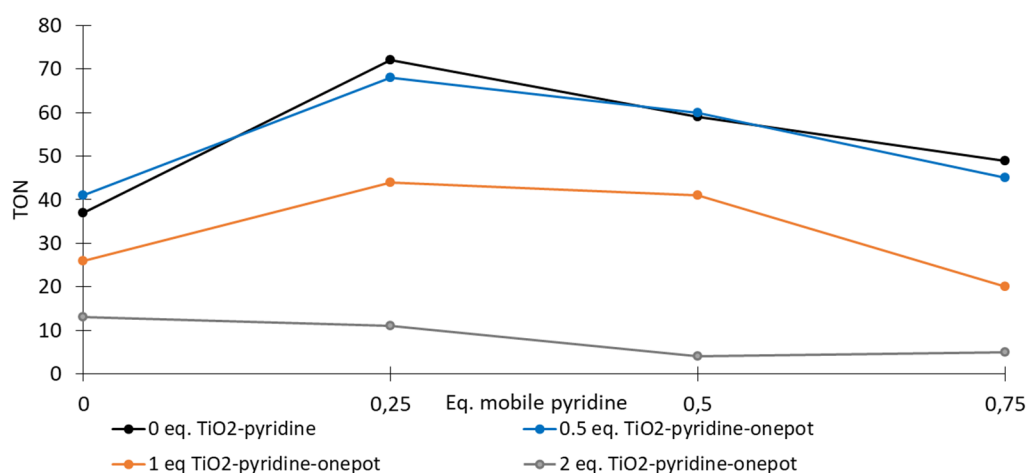


**Figure 3.21:** TON for biaryl formation in the homocoupling of *o*-xylene upon addition of 'mobile' pyridine (0, 0.25, 0.50 and 0.75 eq.). Reaction conditions: 0.05 mol% Pd(TFA)<sub>2</sub>, TiO<sub>2</sub>-pyridine-onepot (0, 0.5, 1 and 2 eq.), 95 °C, 16 bar O<sub>2</sub>, 17 hours.

### 3.2.2. TiO<sub>2</sub> and CeO<sub>2</sub> NPs – one-pot and surface modification

TiO<sub>2</sub> and CeO<sub>2</sub> NPs prepared *via* SM were also tested under the same reaction conditions as above (0.05 mol% Pd(TFA)<sub>2</sub> and varying subequivalent amounts of 'mobile' pyridine) by adding an amount of TiO<sub>2</sub> NPs which provides 0.5 eq. of 2-pyridine-phosphonate ligands at the surface of TiO<sub>2</sub> and CeO<sub>2</sub> NPs. Again, the isomer selectivity for all NPs in combination with 'mobile' pyridine was lower compared to the homogeneous reaction with only subequivalent 'mobile' pyridine. Furthermore, the isomer selectivity was very similar for all types of NPs (Figure 3.22). However, the TON was the lowest for CeO<sub>2</sub> NPs ( $4.8 \times 10^{-7}$  mmol ligand/m<sup>2</sup>), followed by TiO<sub>2</sub> NPs prepared *via* SM ( $2.5 \times 10^{-6}$  mmol ligand/m<sup>2</sup>) and TiO<sub>2</sub> NPs prepared *via* one-pot reaction ( $9.3 \times 10^{-6}$  mmol ligand/m<sup>2</sup>). Hence, the higher the degree

of ligand coverage, the fewer NPs needed to be added to the reaction and the higher the resulting TON (Figure 3.23). Moreover, the more ligands on the surface of the NP, the less remaining space on the surface of the NP on which additives or Pd can interact. This implies that the total amount of ligands in the system determines the isomer selectivity, rather than the degree of ligand coverage on the NP, which has more implication on the TON. This might be indirectly caused by an impurity on the NPs, which has a higher impact on the performance of the system when the NPs are added in higher amounts in case of lower coverage degrees.

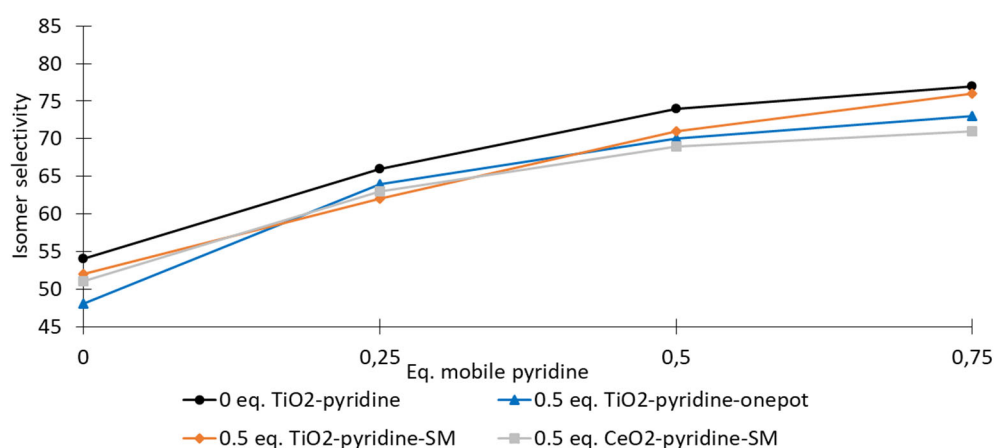


**Figure 3.22:** Isomer selectivity (%) towards 3,3',4,4'-tetramethylbiphenyl in the homocoupling of *o*-xylene upon addition of 'mobile' pyridine (0, 0.25, 0.50 and 0.75 eq.). Reaction conditions: 0.05 mol% Pd(TFA)<sub>2</sub>, 0 and 0.5 eq. TiO<sub>2</sub>-pyridine-onepot, TiO<sub>2</sub>-pyridine-SM and CeO<sub>2</sub>-pyridine SM, 95 °C, 16 bar O<sub>2</sub>, 17 hours.

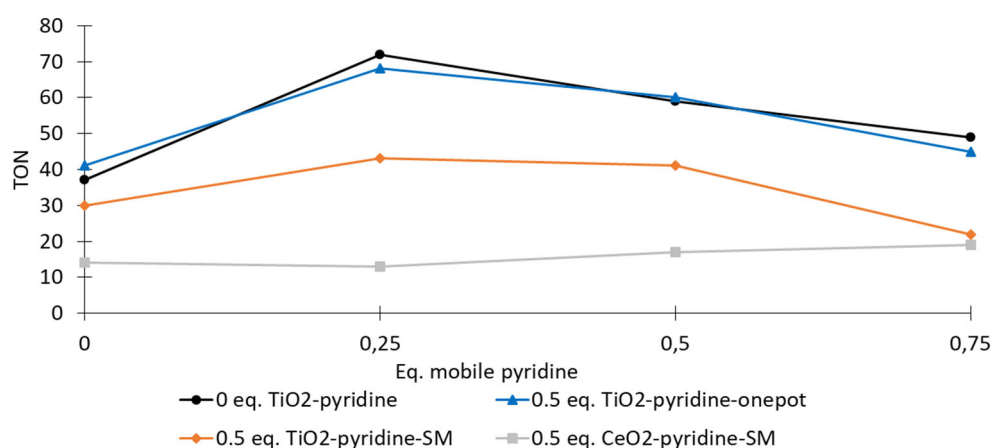


**Figure 3.23:** TON for biaryl formation in the homocoupling of *o*-xylene upon addition of 'mobile' pyridine (0, 0.25, 0.50 and 0.75 eq.). Reaction conditions: 0.05 mol% Pd(TFA)<sub>2</sub>, 0 and 0.5 eq. TiO<sub>2</sub>-pyridine-onepot, TiO<sub>2</sub>-pyridine-SM and CeO<sub>2</sub>-pyridine SM, 95 °C, 16 bar O<sub>2</sub>, 17 hours.

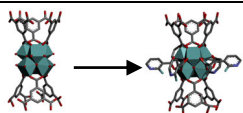
### 3.3.MOF-808

#### 3.3.1. Isonicotinic, nicotinic and picolinic acid – ‘mobile’ pyridine

MOF-808 is an ideal support to study the effect of the conformation of the nitrogen atom (*ortho*, *meta* or *para*), since a plethora of pyridine-type ligands with carboxylic acid groups are commercially available. This is in contrast to poly(4-vinylpyridine) and TiO<sub>2</sub> NPs with phosphonate ligands (rather than carboxylates), in which the pyridine-type ligands are mainly commercially available in the *meta* conformation. From Chapter 3 Section II.1.2, it is known that the washing procedure with methanol generates OCSs on the Zr<sub>6</sub>-cluster and subsequent ligand incorporation with carboxylate ligands is possible. Moreover, the homogeneous reactions with the methyl esters of isonicotinic acid and nicotinic acid (but not for picolinic acid) as pyridine-type ligands indicated that the isomer selectivity was retained when a carboxylate group is present on the ligand (see Chapter 3 section I.1.1 and I.1.2).

MOF-808 was functionalized with 2 eq. isonicotinic acid, nicotinic acid and picolinic acid following the previously described method (see Chapter 2 Materials and Methods section III.4) and the cluster composition was studied by <sup>1</sup>H-NMR. On average, the clusters contained approximately two ligands, but also formates and OCSs (Table 3.21).

**Table 3.21:** Cluster composition determined by <sup>1</sup>H-NMR after washing procedure with MeOH of MOF-808 synthesized from ZrO(NO<sub>3</sub>)<sub>2</sub>.xH<sub>2</sub>O and after ligand incorporation with isonicotinic, nicotinic and picolinic acid.

	Cluster composition after washing procedure MeOH					
	Ligand	Formic acid	MeOH	OCSs	M <sub>w</sub> (g/mol)	Ligand/Pd (5 mg MOF-808)
	0	0.7	0.3	5.0	1299	0
Amount	Cluster composition after ligand incorporation					
	Ligand	Formic acid	MeOH	OCSs	M <sub>w</sub> (g/mol)	Ligand/Pd (5 mg MOF-808)
	2 eq. isonicotinic acid	2.0	0.2	0	1473	0.82
	2 eq. nicotinic acid	2.1	0.7	0	1488	0.86
	2 eq. picolinic acid	1.9	0.2	0	1464	0.79

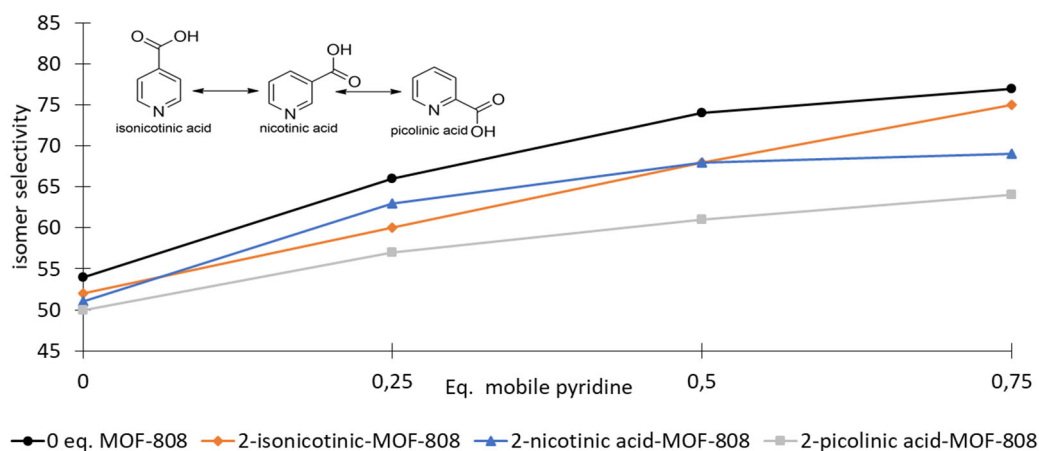
First, homogeneous reactions with 0.05 mol% Pd(TFA)<sub>2</sub> were carried out with mixed ligand systems of the methyl esters of isonicotinic, nicotinic and picolinic acid and with pyridine to predict the isomer selectivities which can be reached in a mixed ligand system (Table 3.22). The homogeneous mixed ligand systems display isomer selectivities well above 80 % for methyl isonicotinate and methyl nicotinate, but not for methyl picolinate. Hence, an increase in isomer selectivity is expected when MOF-808-ligand<sub>x</sub> (ligand = isonicotinic acid, nicotinic acid) is used in combination with subequivalent amounts of ‘mobile’ pyridine, unless the ligand connected with the Zr<sub>6</sub>-cluster exerts the wrong steric or electronic properties (e.g. picolinic acid) or steric hindrance in the pore inhibits the interaction between the Pd centers and the ligands (which is not expected when only two ligands are attached to the Zr<sub>6</sub>-cluster) or additives are depleted from solution and coordinate at the remaining OCSs.



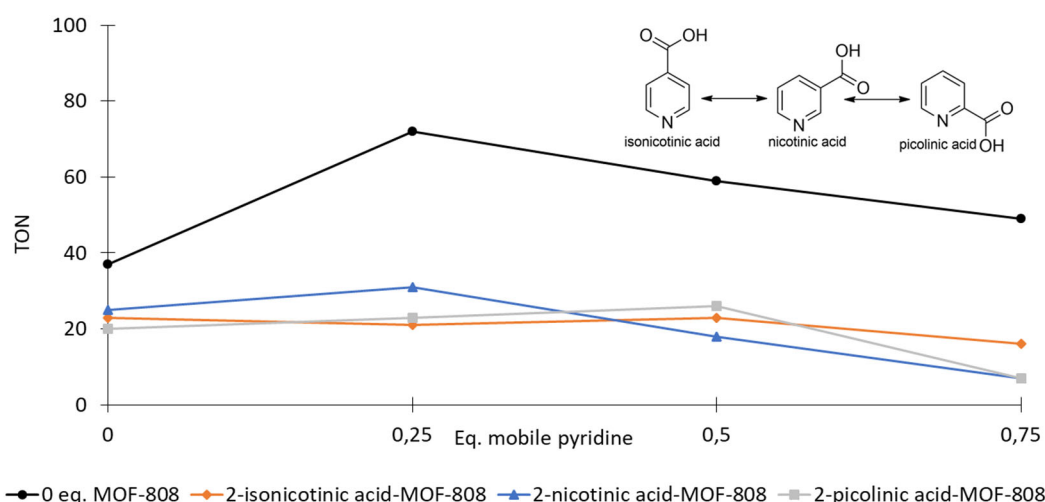
**Table 3.22:** TON for biaryl formation and isomer selectivity (%) towards 3,3',4,4'-tetramethylbiphenyl in the homocoupling of *o*-xylene upon using a mixed ligand system with pyridine. Reaction conditions: 0.05 mol% Pd(TFA)<sub>2</sub>, *x* eq. pyridine + *y* eq. (A, B or C), with *x* + *y* = 1, 95 °C, 16 bar O<sub>2</sub>, 17 hours.

Entry	Ratio ligand/pyridine	A) Methyl isonicotinate		B) Methyl nicotinate		C) Methyl picolinate	
		Isomer selectivity	TON	Isomer selectivity	TON	Isomer selectivity	TON
1	0/1	84	33	84	33	84	33
2	0.25/0.75	82	33	83	28	79	32
3	0.50/0.50	84	27	84	38	76	46
4	0.75/0.25	86	27	82	17	72	55
5	1/0	85	13	83	22	65	48

Catalytic reactions were performed with 0.05 mol% Pd(TFA)<sub>2</sub> and 5 mg MOF-808 functionalized with 2 eq. of ligand (isonicotinic, nicotinic and picolinic acid corresponding to a ligand/Pd ratio of respectively 0.82:1, 0.86:1 and 0.79:1) (see Table 3.21). This was followed by a screening of the optimal subequivalent amount of 'mobile' pyridine (0, 0.25, 0.5 and 0.75 eq.). If these immobilized ligands would exert a positive effect (which is the case homogeneously, except for picolinic acid), an increase in isomer selectivity is expected compared to the homogeneous reaction with only subequivalent amounts of 'mobile' pyridine, since each palladium atom requires a ligand in the bimetallic mechanism. However, the isomer selectivity with MOF-808, functionalized with 2 eq. of ligands, in combination with 'mobile' pyridine is surprisingly lower compared to the homogeneous reaction in presence of only the 'mobile' pyridine. This result was independent on the conformation of the ligand on MOF-808 (isonicotinic, nicotinic vs. picolinic acid) (Figure 3.24). Furthermore, when functionalized MOF-808 was added, the TONs were quite low compared to the homogeneous reaction (Figure 3.25). When even higher amounts of functionalized MOF-808 were added (e.g. 10 mg MOF-808 with isonicotinic acid, which corresponds to ~1.64 eq. ligand/Pd), complete inhibition of the system was observed (TON is 0).



**Figure 3.24:** Isomer selectivity (%) towards 3,3',4,4'-tetramethylbiphenyl in the homocoupling of *o*-xylene upon addition of 'mobile' pyridine (0, 0.25, 0.50 and 0.75 eq.). Reaction conditions: 0.05 mol% Pd(TFA)<sub>2</sub>, 0 or 5 mg MOF-808 functionalized with 2 eq. of ligands (ligand = isonicotinic acid, nicotinic acid or picolinic acid), 95 °C, 16 bar O<sub>2</sub>, 17 hours.

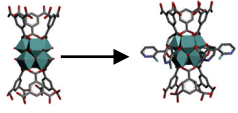


**Figure 3.25:** TON for biaryl formation in the homocoupling of *o*-xylene upon addition of 'mobile' pyridine (0, 0.25, 0.50 and 0.75 eq.). Reaction conditions: 0.05 mol% Pd(TFA)<sub>2</sub>, 0 and 5 mg MOF-808 functionalized with 2 eq. ligands (ligand = isonicotinic acid, nicotinic acid or picolinic acid), 95 °C, 16 bar O<sub>2</sub>, 17 hours.

### 3.3.2. <sup>2F3C</sup>pyr and <sup>2F4C</sup>pyr – 'mobile' <sup>2F</sup>pyr

MOF-808 was also functionalized with 2 or 6 eq. of <sup>2F3C</sup>pyr and <sup>2F4C</sup>pyr following the previously described method (see Chapter 2 Materials and Methods Section III.4). In this way, both the effect of the conformation of the nitrogen group (*meta* versus *para*) and the impact of the amount of ligands at the Zr<sub>6</sub>-cluster (2 versus 6 eq.) could be studied. The cluster composition was studied by <sup>1</sup>H-NMR after the washing step with methanol and after ligand incorporation. Approximately two ligands were present on MOF-808 functionalized with 2 eq. of ligands (<sup>2F3C</sup>pyr and <sup>2F4C</sup>pyr). However, this was not the case for MOF-808 functionalized with 6 eq. of ligands; only 4.9 <sup>2F3C</sup>pyr and 4.1 <sup>2F4C</sup>pyr were observed at the Zr<sub>6</sub>-cluster (Table 3.23).

**Table 3.23:** Cluster composition determined by <sup>1</sup>H-NMR after washing procedure with MeOH of MOF-808 synthesized from ZrO(NO<sub>3</sub>)<sub>2</sub>·xH<sub>2</sub>O and after ligand incorporation with <sup>2F3C</sup>pyr and <sup>2F4C</sup>pyr.

	Cluster composition after washing procedure MeOH					
	Ligand	Formic acid	MeOH	OCSs	M <sub>w</sub> (g/mol)	Ligand/Pd (5 mg MOF-808)
	0	0.7	0.3	5	1299	0
Cluster composition after ligand incorporation						
Amount	Ligand	Formic acid	MeOH	OCSs	M <sub>w</sub> (g/mol)	Ligand/Pd (5 mg MOF-808)
2 eq. <sup>2F3C</sup> pyr	2.0	0.2	0	3.8	1509	0.80
2 eq. <sup>2F4C</sup> pyr	1.8	0.1	0	4.1	1486	0.73
6 eq. <sup>2F3C</sup> pyr	4.9	0.1	0	1.0	1821	1.63
6 eq. <sup>2F4C</sup> pyr	4.1	1.1	0	0.8	1747	1.42

Reactions were performed with 0.05 mol% Pd(TFA)<sub>2</sub> and 5 mg of MOF-808 functionalized with, respectively, 2 eq. <sup>2F3C</sup>pyr and <sup>2F4C</sup>pyr (i.e. corresponding to ligand/Pd ratios of 0.80:1 and 0.73:1) and 6 eq. of <sup>2F3C</sup>pyr and <sup>2F4C</sup>pyr (i.e. corresponding to ligand/Pd ratios of 1.63:1 and 1.42:1) (see Table 3.23). Furthermore, subequivalent amounts of ‘mobile’ <sup>2F</sup>pyr were varied (0, 0.25, 0.50 and 0.75 eq.). The system with MOF-808 functionalized with 2 eq. of <sup>2F3C</sup>pyr or <sup>2F4C</sup>pyr displayed a lower isomer selectivity compared to the homogeneous reaction with only subequivalent amounts of ‘mobile’ <sup>2F</sup>pyr, while MOF-808 functionalized with 6 eq. of <sup>2F3C</sup>pyr or <sup>2F4C</sup>pyr showed a similar isomer selectivity (Figure 3.26). Furthermore, low TONs were observed for reactions with immobilized ligands on MOF-808, with the lowest TONs being observed for the MOFs which contained the highest amount of ligands (Figure 3.27). Again, when higher amounts of functionalized MOF-808 were added (e.g. 10 mg MOF-808-<sup>2F3C</sup>pyr<sub>2</sub>, corresponding to 1.60:1 ligand/Pd), the reaction was completely inhibited (TON=0).

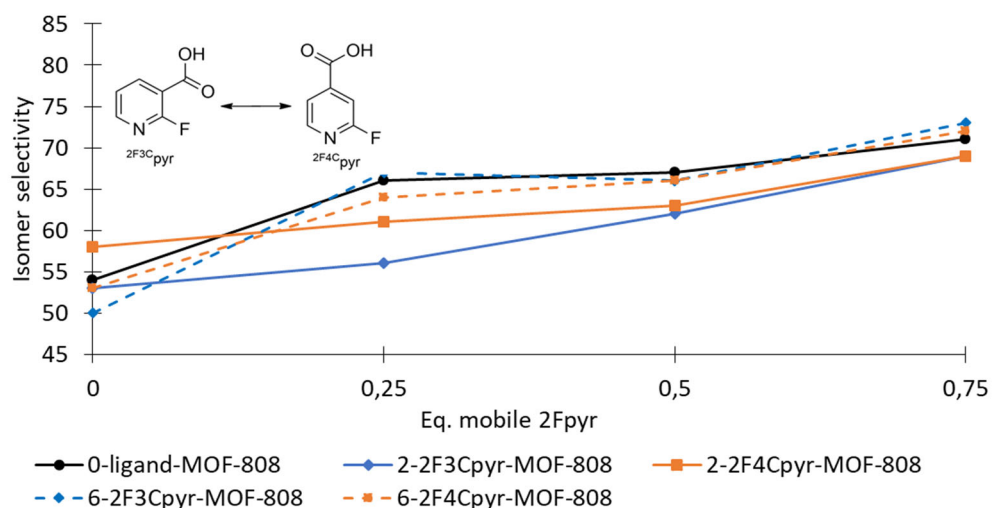


**Figure 3.26:** Isomer selectivity (%) towards 3,3',4,4'-tetramethylbiphenyl in the homocoupling of *o*-xylene upon addition of ‘mobile’ <sup>2F</sup>pyr (0, 0.25, 0.50 and 0.75 eq.). Reaction conditions: 0.05 mol% Pd(TFA)<sub>2</sub>, 0 and 5 mg of MOF-808 functionalized with x eq. of ligand (ligand = <sup>2F3C</sup>pyr or <sup>2F4C</sup>pyr, x=2 or 6 eq.), 95 °C, 16 bar O<sub>2</sub>, 17 hours.

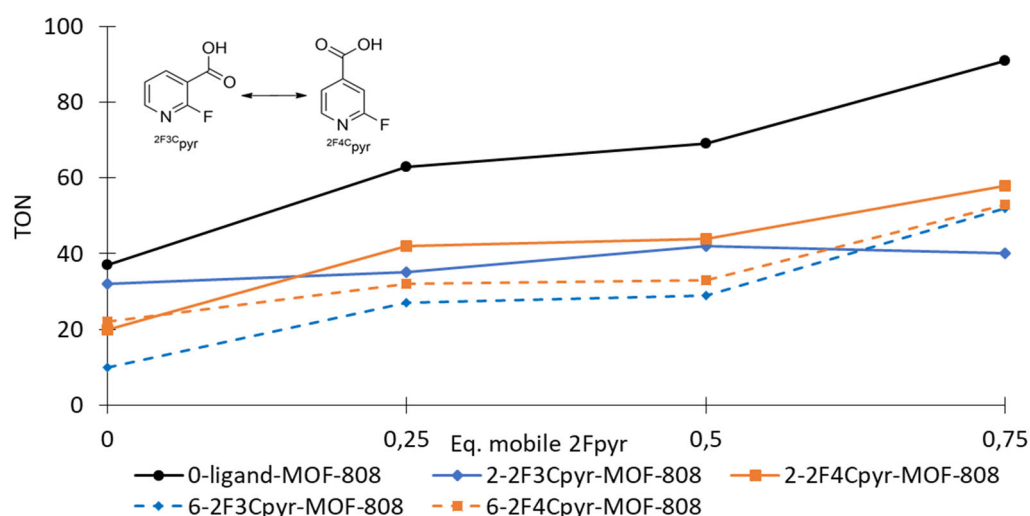


**Figure 3.27:** TON for biaryl formation in the homocoupling of *o*-xylene upon addition of ‘mobile’ <sup>2F</sup>pyr (0, 0.25, 0.50 and 0.75 eq.). Reaction conditions: 0.05 mol% Pd(TFA)<sub>2</sub>, 0 and 5 mg MOF-808 functionalized with x eq. ligand (ligand = <sup>2F3C</sup>pyr or <sup>2F4C</sup>pyr, x = 2 or 6 eq.), 95 °C, 16 bar O<sub>2</sub>, 17 hours.

### 3.4. Conclusion

In order to obtain higher isomer selectivities, 'mobile' ligands are required on top of the immobilized ligands as a consequence of the bimetallic transmetalation step in the reaction mechanism. Moreover, careful selection of the 'mobile' ligand was found to be critical, since some mixed ligand systems have more potential to perform better than others (e.g. methyl nicotinate and pyridine performs better than <sup>2F</sup>pyr and pyridine). Finally, the combination of subequivalent amounts of 'mobile' pyridine (0.5 eq.) and 4 eq. poly(4-vinylpyridine) resulted in a high isomer selectivity (82 %). However, such high isomer selectivities could not be reached in mixed-ligand systems with functionalized TiO<sub>2</sub> or CeO<sub>2</sub> NPs or with MOF-808-ligand<sub>x</sub>.

## 4. Heterogeneity of the system

### 4.1. Hot filtration tests

High isomer selectivities (82 %) were reached in a system with 0.05 mol% Pd(TFA)<sub>2</sub>, 4 eq. of poly(4-vinylpyridine) and 0.5 eq. of 'mobile' pyridine, which can compete with the homogeneous reaction with 1 eq. pyridine (isomer selectivity of 84 %). Recovery and re-use of the heterogeneous material with the immobilized ligands is required to surpass the homogeneous system in performance. Hence, it is important to know if all palladium centers stay attached to the immobilized ligands.

Therefore, hot filtration tests were performed on the reactions with 0.05 mol% Pd(TFA)<sub>2</sub>, 4 eq. poly(4-vinylpyridine) and 0 or 0.5 eq. 'mobile' pyridine (95 °C, 16 bar O<sub>2</sub>). These hot filtration test were also performed on comparable preloaded samples to obtain even better contact between Pd and poly(4-vinylpyridine). 4 eq. poly(4-vinylpyridine) was preloaded with 0.05 mol% Pd(TFA)<sub>2</sub> in a dichloromethane (DCM) solution for 24 hours, followed by evaporation of the DCM. The reactions were stopped after 4 hours, the poly(4-vinylpyridine) support was removed and the filtrate was reused for further reaction (which ends at 17 hours). Moreover, the normal reaction profiles were measured (i.e. similar reactions without filtration step and in absence of poly(4-vinylpyridine)). The normal reaction profiles of 0.05 mol% Pd(TFA)<sub>2</sub>, 4 eq. poly(4-vinylpyridine) and 0 or 0.5 eq. 'mobile' pyridine are respectively 0.05 mol% Pd(TFA)<sub>2</sub> and 0.05 mol% Pd(TFA)<sub>2</sub> with 0.5 eq. 'mobile' pyridine at 95 °C, 16 bar O<sub>2</sub> and 17 hours.

First, hot filtration reactions with 0.05 mol% Pd(TFA)<sub>2</sub> and 4 eq. poly(4-vinylpyridine) without the addition of extra 'mobile' pyridine were performed (blue and green dashed line in Figure 3.28). If all Pd would remain strongly attached to the immobilized ligands, a horizontal dashed line is expected. This is clearly not the case, which means that (part of the) palladium leached and ended up in the reaction solution. Moreover, an isomer selectivity similar to the homogeneous reaction without any ligands is expected before and after filtration (since no 'mobile' or immobilized ligands are present and the addition of poly(4-vinylpyridine) alone does not result in an increase in selectivity due to the bimetallic mechanism). In both cases (before and after filtration) an isomer selectivity of 59 % was observed (see blue dashed line in Figure 3.28). If all palladium would have been leached in the reaction solution, a similar reaction rate before and after filtration is expected, indicated by the normal reaction profile with 0.05 mol% Pd(TFA)<sub>2</sub> (the blue full line in Figure 3.28). However, the reaction rate before filtration is higher than after filtration, which means that not all palladium ended up in the solution and thus a part of the palladium remained attached to the support. Since the slope of the blue full line (0.14), is almost double of the slope of the blue or green dashed line (≈0.07), it is estimated that approximately half of the palladium remained in the support.

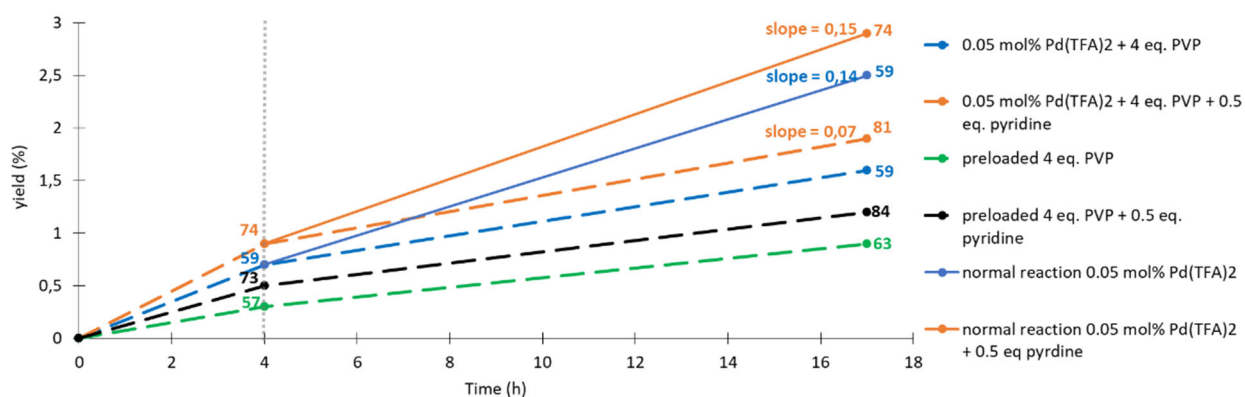


**Figure 3.28:** Yield for biaryl formation in the homocoupling of *o*-xylene at 4 hours reaction times and after filtration (dashed lines, end at 17 hours). In addition, normal kinetics are measured (full lines). Reaction conditions: 0.05 mol% Pd(TFA)<sub>2</sub> with 4 eq. poly(4-vinylpyridine) (or preloaded), with 0 or 0.5 eq. pyridine, 95 °C, 16 bar O<sub>2</sub>, 17 hours.

The hot filtration reactions with 0.05 mol% Pd(TFA)<sub>2</sub>, 4 eq. poly(4-vinylpyridine) and 0.5 eq. ‘mobile’ pyridine (black and orange dashed line in Figure 3.28) resulted in low isomer selectivities (73 % or 74 %) immediately after filtration (i.e. after 4 hours), which are, surprisingly, very similar to the isomer selectivity of the homogeneous reaction with 0.05 mol% Pd(TFA)<sub>2</sub> with 0.5 eq. ‘mobile’ pyridine (74 %) (i.e. in absence of poly(4-vinylpyridine) after 17 hours (orange full line in Figure 3.28). Moreover, after filtration and removal of poly(4-vinylpyridine) and complete reaction of 17 hours, high isomer selectivities (84 % and 81 %) were obtained, although the immobilized ligands were absent. This indicates that about half of the palladium remained attached to the support and the other half interacted with the 0.5 eq. ‘mobile’ pyridine in solution (i.e. 1:1 ligand/Pd ratio, which is accordance to the results described in Chapter 3 Section II.3.1.). This suggest that the poly(4-vinylpyridine) support acts as a reservoir for Pd.

The reaction with 0.05 mol% Pd(TFA)<sub>2</sub>, 4 eq. poly(4-vinylpyridine) and 0.5 eq. ‘mobile’ pyridine (orange dashed line in Figure 3.28) was studied in more detail, since low isomer selectivities were observed after 4 hours. Samples were taken at different reaction times (0, 4, 6, 8, 10, 15 and 17 hours) and the isomer selectivities were determined (Figure 3.29). The isomer selectivity and yield increased gradually up to 8 hours. After 8 hours, no increase in yield could be observed and only a small increase in isomer selectivity was noticed. This means that the Pd is already deactivated after 8 hours. Nevertheless, this is interesting since the reaction time can be shortened to 8 instead of 17 hours, although the isomer selectivity is slightly lower (80 % vs 82 %).

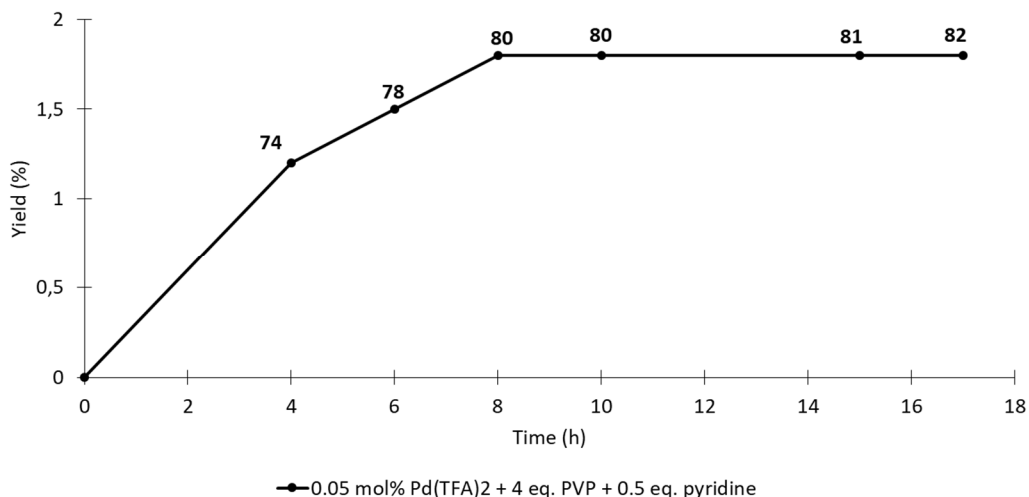


**Figure 3.29:** Yield for biaryl formation in the homocoupling of *o*-xylene upon varying the reaction time. Reaction conditions: 0.05 mol% Pd(TFA)<sub>2</sub> with 4 eq. poly(4-vinylpyridine), with 0 or 0.5 eq. pyridine, 95 °C, 16 bar O<sub>2</sub>, 4, 6, 8, 10, 15 and 17 hours.

It is hypothesized that the palladium centers attached to the poly(4-vinylpyridine) material are continuously interchanging with the palladium centers in solution, until all Pd is deactivated (Figure 3.30). This would explain why similar isomer selectivities and TONs were obtained in the system with 0.05 mol% Pd(TFA)<sub>2</sub>, 4 eq. poly(4-vinylpyridine) and 0.5 eq. ‘mobile’ pyridine compared to the homogeneous system with 0.05 mol% Pd(TFA)<sub>2</sub> and 1:1 pyridine/Pd. In fact, the transmetalation step can occur in two ways: transmetalation between two ligand-associated Pd complexes in solution, which results in high isomer selectivities if the ligand/Pd ratio is right, and transmetalation between a Pd center attached to poly(4-vinylpyridine) and a ligand-associated Pd center in solution, which can also result in high isomer selectivities if the immobilized ligand exerts the right steric and electronic properties and if the ligand/Pd ratio in solution is optimal.

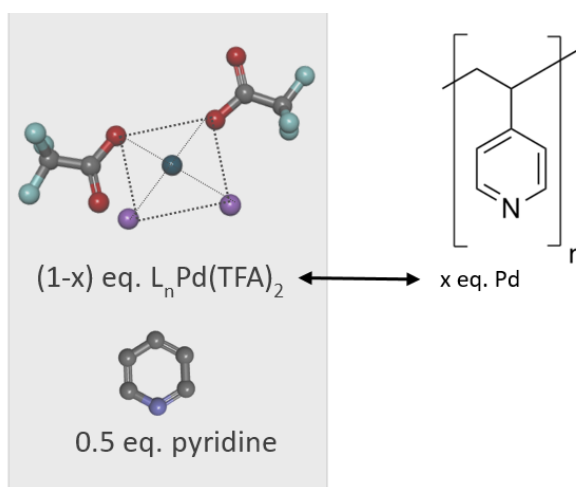


**Figure 3.30:** Possible locations of palladium: in solution (grey box), or at immobilized ligand (poly(4-vinylpyridine)). Pd is continuously interchanged between immobilized ligand and solution until all palladium is deactivated.

## 4.2. Recycling tests

There are two main strategies which can be used to recycle the Pd that remains in the support. The first strategy takes into account the amount of palladium that is lost in the solution after reaction (about 50%). A recycle can be performed by reusing the support (containing still approximately 0.5 eq. of the initial amount of Pd) and by adding 0.5 eq. of 'mobile' pyridine compared to the remaining amount of palladium in the support (which corresponds to  $0.5 \times 0.5^x$  eq. pyridine compared to the initial amount of palladium, with x the amount of recycles). More palladium is added for this approach (e.g. 0.5 mol% instead of 0.05 mol%), since approximately half of the amount of palladium will be released in the reaction solution in each recycle step.

A recycle experiment was conducted with 0.5 mol% Pd(TFA)<sub>2</sub>, 4 eq. of poly(4-vinylpyridine) and 0.5 eq. of 'mobile' pyridine (under the same conditions as before: 95 °C, 16 bar O<sub>2</sub> and 17 hours). The support was recycled only once and a cumulative TON of 15, yield of 7.6 % and average isomer selectivity of 81 % were obtained. Unfortunately, the system was not active anymore after the second recycle (TON=0). Hence, this system was not significantly better than the homogeneous system, in which a comparable amount of palladium is used (i.e. 0.5 mol% Pd(TFA)<sub>2</sub> and 1:1 pyridine, which resulted in a TON of 13, a yield of 6.3 % and isomer selectivity of 84 %) (Figure 3.31). This approach suffers from the disadvantage that a lot of Pd is lost and the pyridine/Pd ratios in solution are not necessarily balanced, since the poly(4-vinylpyridine) support is pulling stronger in the following recycle steps at the remaining palladium atoms which stay attached to the support and make the interchange with palladium in solution harder. Moreover, the palladium atoms which remained attached to the support could be largely inactivated after the first reaction (see Figure 3.29).

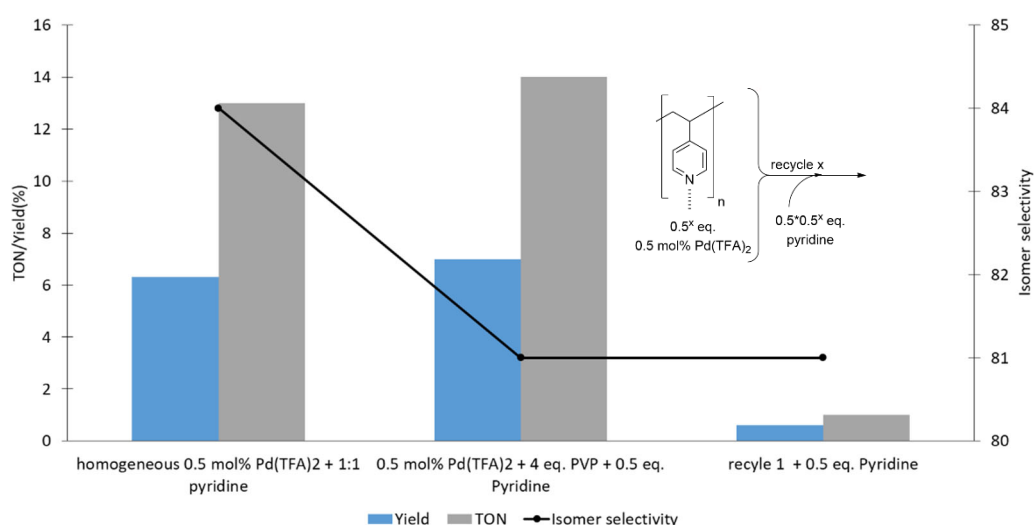


**Figure 3.31:** Yield (%) and TON for biaryl formation in the homocoupling of *o*-xylene upon catalyst recycle. Reaction conditions: Heterogeneous reaction: 0.5 mol% Pd(TFA)<sub>2</sub> with 4 eq. poly(4-vinylpyridine) with 0.5 eq. pyridine and recycle. Homogeneous reaction: 0.5 mol% Pd(TFA)<sub>2</sub> with 1 eq. pyridine, 95 °C, 16 bar O<sub>2</sub> and 17 hours.



The second approach also takes into account that half of the palladium is leached in the solution after the reaction. In this case, a recycle was performed by reusing the support (which still contains about half of the initial amount of Pd), and by the addition of the leached amount of Pd (to obtain the initial amount of Pd) and 0.5 eq. 'mobile' pyridine. In this way, the optimal pyridine/Pd ratios in solution are guaranteed. The amount of Pd used in "n" homogeneous reactions is equal to the amount of Pd used in the "2n-1" recycled reactions (i.e. the amount of Pd after three reactions with 0.05 mol% Pd(TFA)<sub>2</sub> and 1:1 pyridine is the same as the amount of Pd after five recycled reactions, starting from 0.05 mol% Pd(TFA)<sub>2</sub>, 4 eq. poly(4-vinylpyridine) and 0.5 eq. 'mobile' pyridine). Moreover, only 0.5 eq. of 'mobile' pyridine is required in each recycle step containing 4 eq. poly(4-vinylpyridine) as support, while the homogeneous reaction requires 1 eq. of 'mobile' pyridine to obtain high isomer selectivity. In this way, both the costs of Pd and pyridine are reduced.

Five recycle reactions were performed, starting from 0.05 mol% Pd(TFA)<sub>2</sub>, 4 eq. poly(4-vinylpyridine) and 0.5 eq. 'mobile' pyridine. A cumulative TON of 95 was obtained and an average isomer selectivity of 83.6 % (Figure 3.32). In this system, an equal amount of palladium was used as in three homogeneous reactions with 0.05 mol% Pd(TFA)<sub>2</sub> and 1:1 pyridine, which resulted in a cumulative TON of 99 and isomer selectivity of 84 %. Hence, most palladium atoms, which remain attached to the poly(4-vinylpyridine), were deactivated after reaction (see Figure 3.29). Only the newly added palladium centers are active. In this way, 1:1 ligand/Pd ratios were obtained in the solution, resulting in high isomer selectivities (around 84%). However, since only half of the palladium atoms are active, the TON is halved after the recycle (Figure 3.32).

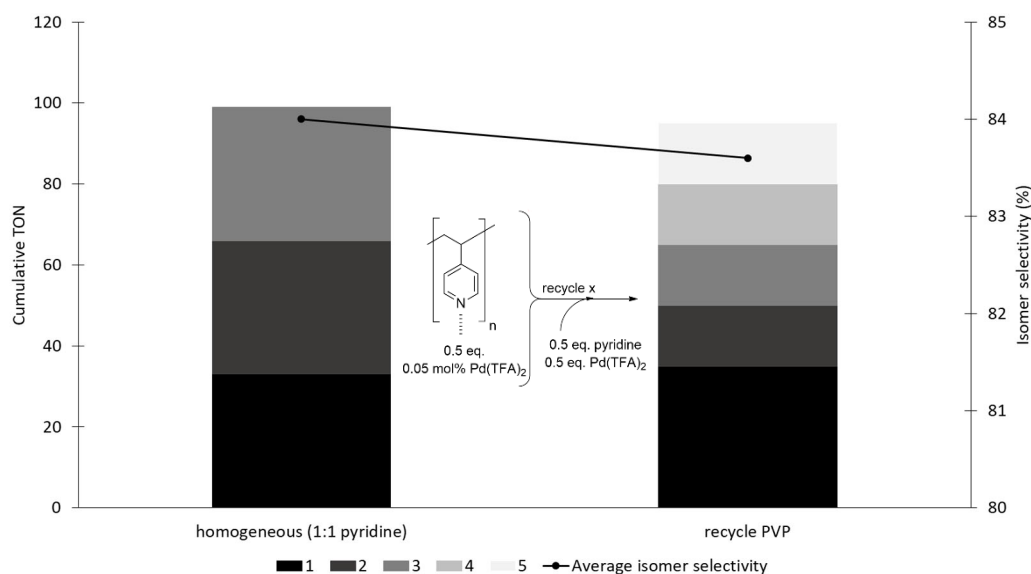


**Figure 3.32:** TON for biaryl formation and average isomer selectivity (%) towards 3,3',4,4'-tetramethylbiphenyl in the homocoupling of *o*-xylene upon catalyst recycle. Reaction conditions: Heterogeneous reaction: 0.05 mol% Pd(TFA)<sub>2</sub> with 4 eq. poly(4-vinylpyridine) with 0.5 eq. pyridine and recycle: add 1.38 mg Pd to obtain 0.05 mol% and 0.5 eq. pyridine. Homogeneous reaction: 0.05 mol% Pd(TFA)<sub>2</sub> with 1 eq. pyridine, 95 °C, 16 bar O<sub>2</sub> and 17 hours.

### 4.3. Conclusion

In conclusion, it was established that 4 eq. poly(4-vinylpyridine) acts as a reservoir to obtain optimal ligand/Pd ratios in solution (e.g. 1:1), when 0.5 eq. 'mobile' pyridine was added, resulting in high isomer selectivity. This might also explain why the addition of TiO<sub>2</sub> or CeO<sub>2</sub> functionalized NPs and MOF-808-ligand<sub>x</sub> did not result in high isomer selectivities. Palladium can interact in these cases with both the immobilized ligand, the 'mobile' ligand in solution and with the surface functional groups of the TiO<sub>2</sub> NPs and at the OCSs of the Zr<sub>6</sub>-cluster of MOF-808, respectively. At that moment, three possible interactions can occur. Firstly, one ligandless Pd at the support can interact with either ligand-associated Pd in solution or with ligandless Pd on the support, both resulting in low isomer selectivities after transmetalation, since a bimetallic mechanism (in which both Pd centers require a ligand to obtain high isomer selectivity) is supposed. A second possibility is the interaction of Pd attached to the immobilized ligand with a ligand-associated Pd center in solution. This can result in high isomer selectivity after the transmetalation event if the immobilized ligands exert the right steric and electronic effects (not the case for the phosphonate ligands on the TiO<sub>2</sub> NPs, but should be the case for functionalized MOF-808, except for picolinic acid) and if the ligand/Pd ratios in solution are optimal to give high isomer selectivity. The third pathway is a transmetalation between two ligand-associated palladium centers in solution, which results in high isomer selectivities when the ligand/Pd ratios are optimal. However, the ligand/Pd ratios in solution can be out of balance, due to interaction of Pd with the support and with the immobilized ligand (which has implication on the isomer selectivity due to the second and third possible interaction). (Figure 3.33). Hence, to obtain a system with MOF-808-ligand<sub>x</sub>, which performs analogously to poly(4-vinylpyridine), all remaining OCSs need to be displaced by ligands (e.g. isonicotinic acid) and the amount of MOF-808 added to the reaction mixture needs to be perfectly balanced to obtain the appropriate ligand/Pd ratios in the reaction solution.

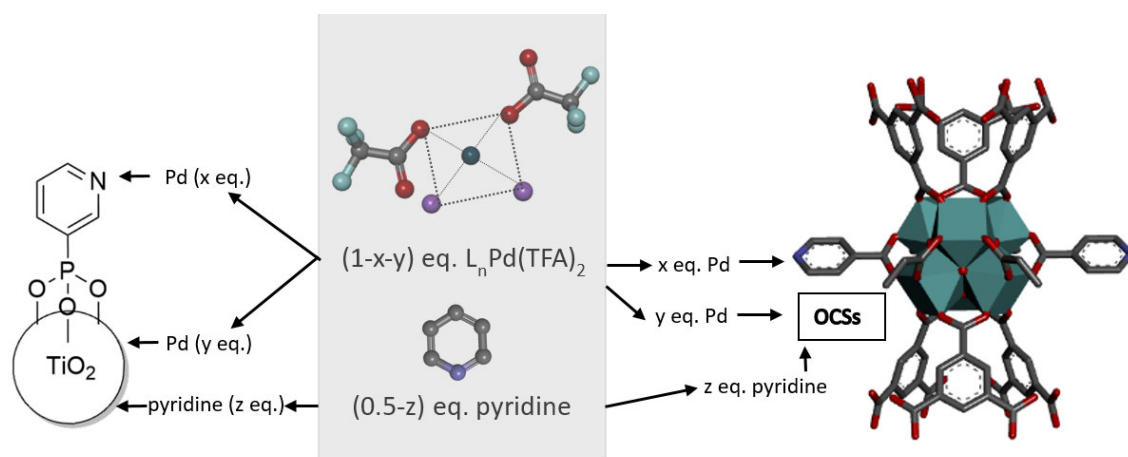


**Figure 3.33:** Possible locations of palladium and the 'mobile' pyridine ligand: in solution (grey box), at the immobilized ligands or at the open sites of the surface of a TiO<sub>2</sub> particle (left) or at the OCSs of MOF-808 (right).

### III. Side project Kiel – MOF synthesis with biphenylhexacarboxylic acid linker

The synthesis of new Zr-MOFs and other metal MOFs with special 2,2',4,4',6,6'-biphenylhexacarboxylic acid (BPHeC) linker was optimized in collaboration with the group of prof. Stock at the Christian Albrecht University of Kiel (Germany). In Kiel, a high throughput reactor system was used in which 24 synthesis conditions could be explored at the same time. Furthermore, the samples were directly washed *via* a high throughput filtration system. Afterwards, the well plate was placed in the HT PXRD (Figure 3.34).

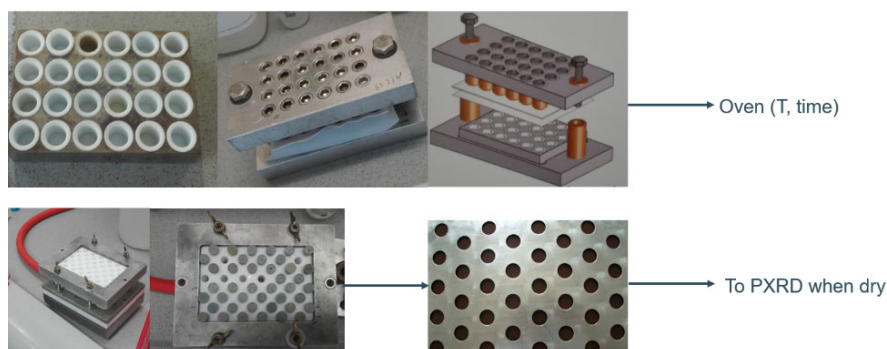


**Figure 3.34:** High throughput reactor system and high throughput filtration system, which can be immediately used in HT PXRD.

#### 1. Zirconium MOFs

First, several modulators such as formic acid, acetic acid, hydrogen chloride and methanol were tested in different modulator/DMF ratios in a total volume of 1 mL (e.g. 0:1, 0.2:0.8, 0.4:0.6, etc). A metal to linker ratio of 1:1 was applied with 0.02 mmol zirconyl chloride octahydrate and the solution was heated to 120 °C for 24 hours. After PXRD analysis, only one synthesis solution showed some clear reflections. In this system, formic acid was used as modulator in a 0.6:0.4 ratio. The powder pattern was compared with the powder pattern of zirconium formate and it was found to be quite similar. However, there were some different reflections. After upscaling this reaction, the powder pattern matched the pattern of zirconium formate completely (Figure 3.35).

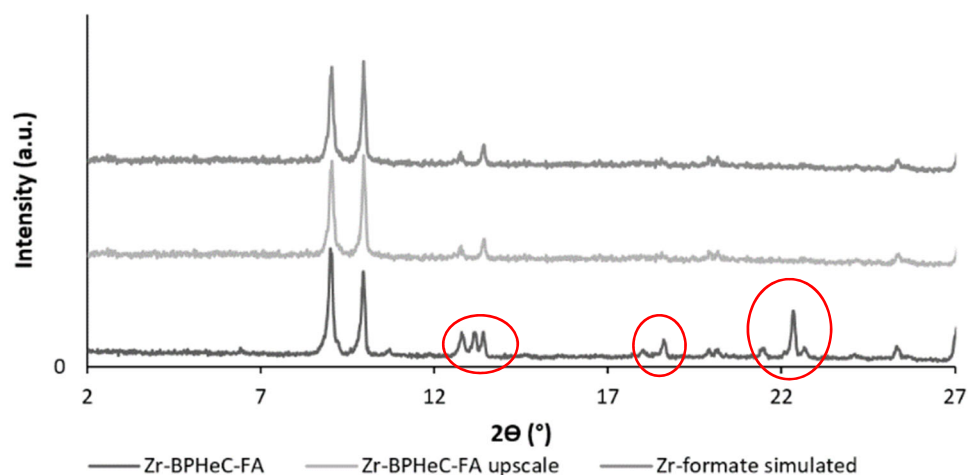


**Figure 3.35:** Succeeded powder diffractograms of first HT synthesis and simulated powder diffractogram of zirconium formate.

A second HT synthesis was performed based on a synthesis procedure of PCN-700.<sup>99</sup> Benzoic acid, acetic acid and TFAH were tested as modulators in different ratios compared to zirconium (e.g. benzoic acid: 45 and 91; acetic acid 13.5, 27 and 54; TFAH 7.5, 15 and 30 equivalents). These conditions were performed with and without methanol as extra additive (48  $\mu$ L or 0  $\mu$ L). DMF was used as solvent to fill the remaining volume of the Teflon liner to 1 mL and a 1:1 metal to linker ratio was applied with 0.04 mmol zirconyl chloride octahydrate. These synthesis solutions were heated to 120 °C during 24 hours. The use of benzoic acid as modulator resulted in two different powder patterns, depending on the presence of methanol. In absence of methanol, a similar powder pattern as PCN-700 was obtained, while in presence of methanol, the powder pattern resembled the pattern of UiO-67 (Figure 3.36 and 3.37).

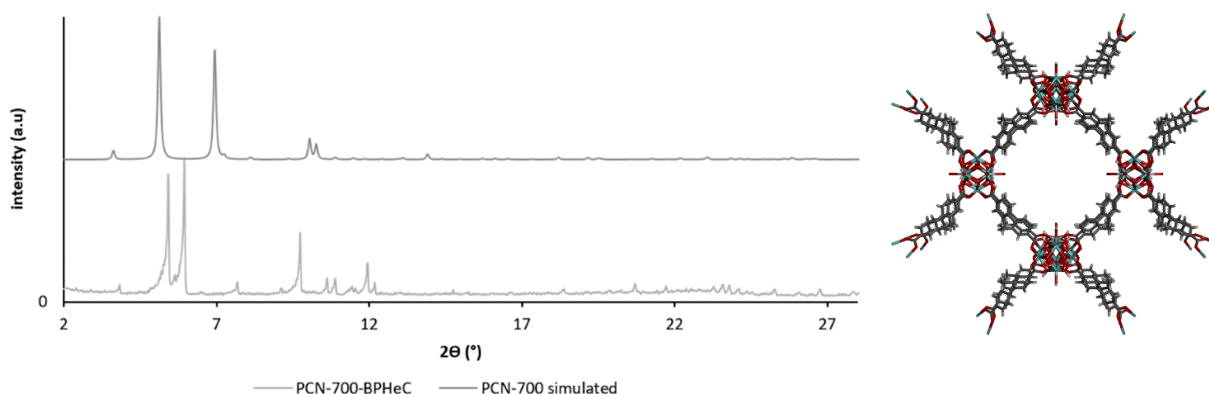


**Figure 3.36:** Succeeded powder diffractogram of second HT synthesis without methanol as additive and simulated powder diffractogram of PCN-700 (left) and the structure of PCN-700 (right).

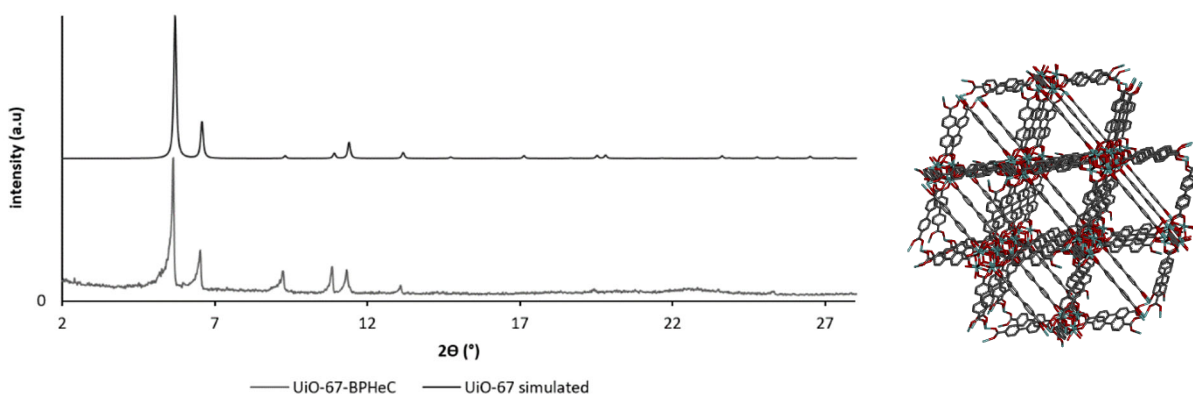


**Figure 3.37:** Succeeded powder diffractogram of second HT synthesis with methanol as additive and simulated powder diffractogram of UiO-67 (left) and the structure of UiO-67 (right).

The structural agreement of these patterns with PCN-700 and UiO-67 was confirmed by performing Le Bail Fits (Figure 3.38). The PCN-700 crystallizes in a tetragonal space group  $P4_2/mmc$  with unit cell parameters  $a = b = 23.07 \text{ \AA}$  and  $c = 14.16 \text{ \AA}$  with  $\alpha = \beta = \gamma = 90^\circ$ .<sup>100</sup> The cell parameters of PCN-700-BPHeC ( $a = b = 22.90 \text{ \AA}$  and  $c = 19.32 \text{ \AA}$ ) were slightly shifted compared to 'normal' PCN-700 with  $\text{Me}_2\text{-bpd}^{2-}$  linkers ( $a = b = 23.07 \text{ \AA}$  and  $c = 14.16 \text{ \AA}$ ). Analogously, the UiO-67 crystallizes in a cubic space group  $Fm\bar{3}m$ . However, the cell parameters of UiO-67-BPHeC ( $a = b = c = 26.89 \text{ \AA}$ ) were similar as the ones of UiO-67 with  $\text{bpd}^{2-}$  linkers ( $a = b = c = 26.88 \text{ \AA}$ ).<sup>10,101,102</sup>

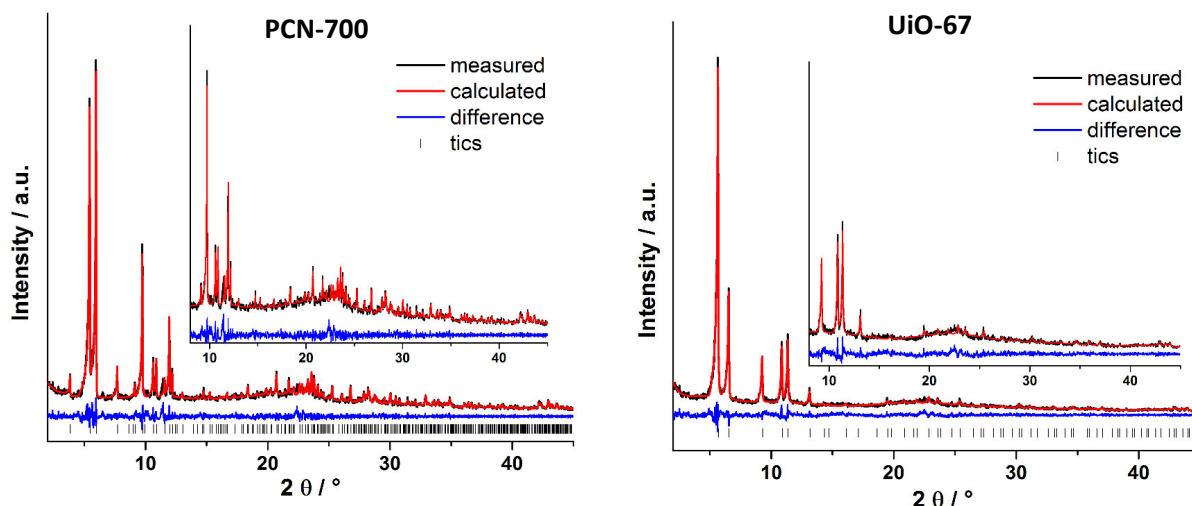


**Figure 3.38:** Le Bail fits of PCN-700-BPHeC (left) and UiO-67-BPHeC (right) show structural agreement with PCN-700 and UiO-67. The black lines indicate the experimental data, while red lines represent the calculated data and vertical lines mark the allowed Bragg positions. The blue curves indicate the difference between the measured and the calculated pattern.

Longer XRD measurements of these samples were performed three days later to solve the structure. However, the reflections were not as sharp as before and some of the reflections were merged due to peak broadening (Figure 3.39 and 3.40).

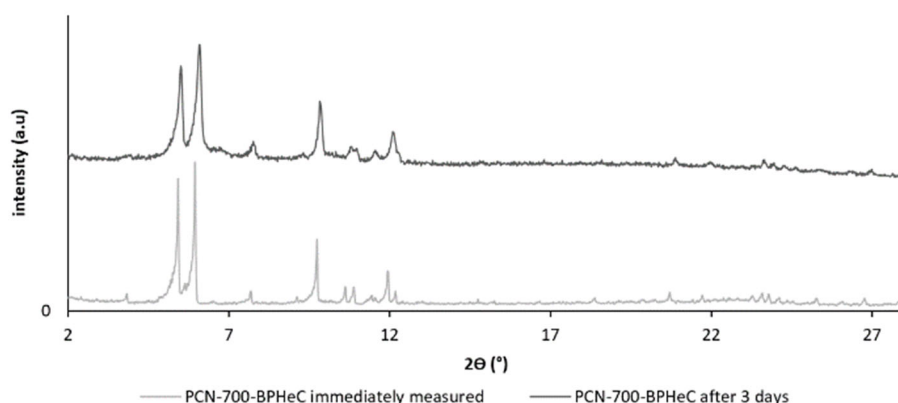


**Figure 3.39:** The powder diffractograms of PCN-700-BPHeC immediately after synthesis and three days later.

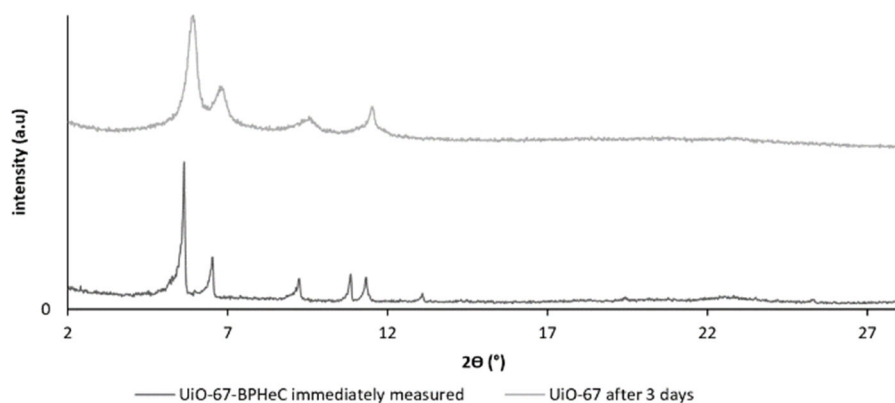


**Figure 3.40:** The powder diffractograms of UiO-67-BPHeC immediately after synthesis and three days later.

## 2. Other metals MOFs

Combinations of the BPHeC linker with other metals than zirconium (e.g. iron, chromium, aluminium and titanium) were also screened *via* the HT synthesis procedure. Iron(III) chloride hexahydrate, chromium(III) nitrate nonahydrate, aluminium(III) nitrate nonahydrate and a Ti-cluster were used as metal precursor salts. Hydrogen chloride (300  $\mu$ L or 0  $\mu$ L) was tested as additive and the syntheses were performed in DMF as solvent. Both a 1:1 and 2:1 metal to linker ratio with 0.01 mmol of BPHeC was tested. The synthesis solutions were heated to 120  $^{\circ}$ C during 24 hours. Only with iron, a powder pattern with sharp reflections was obtained. This was valid in case of both 1:1 and 2:1 metal to linker ratios in absence of hydrogen chloride.

A second HT-synthesis screening was conducted with iron(III) chloride hexahydrate and 1 mL DMF as solvent in the presence of modulators such as methanol (48  $\mu$ L) and acetic acid (48  $\mu$ L). Both 1:1 and 2:1 metal to linker ratios were tested. All these conditions resulted in the formation of the Fe-BPHeC material, although a 1:1 metal to linker ratio and acetic acid as modulator yielded the most crystalline pattern. Again, peak broadening could be observed after 3 days (Figure 3.41).

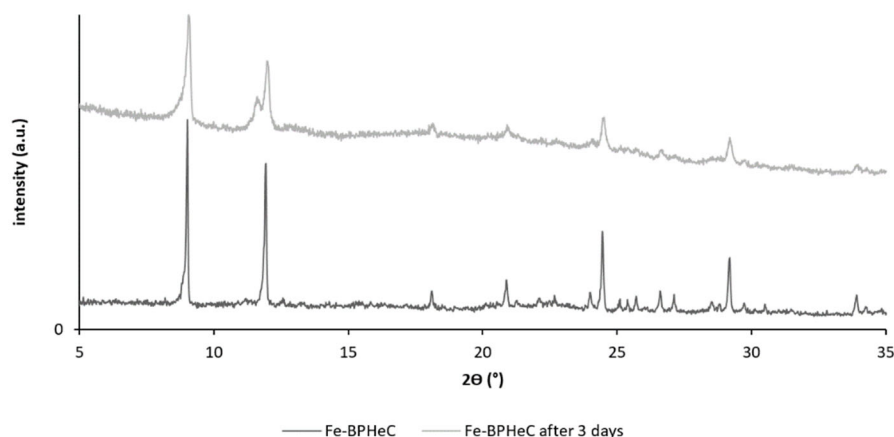


**Figure 3.41:** The powder diffractogram of Fe-BPHeC, with acetic acid as modulator and 1:1 metal to linker ratio immediately measured and three days later.

Finally, it was tested if new cerium MOFs could be synthesized with the BPhEC linker. A batch synthesis in a 8 mL glass vial was performed with 200  $\mu$ L of a 0.533 M cerium(IV) ammoniumhexantrate solution and a 2:1 metal to linker ratio in 600  $\mu$ L of DMF as solvent. The use of modulators such as formic acid or acetic acid (50 eq.) was also tested. The mixture was stirred during a short reaction time of 15 minutes at 100 °C. Notably, only the synthesis solution without modulator resulted in a powder pattern with sharp reflections. Surprisingly, no peak broadening could be observed after a second measurement, which was performed three days later (Figure 3.42). The first reflection in the powder patterns of Ce-BPhEC and Fe-BPhEC occurs at much higher angles compared to PCN-700-BPhEC and UiO-67-BPhEC, which might indicate that the pores in Ce-BPhEC and Fe-BPhEC are smaller.

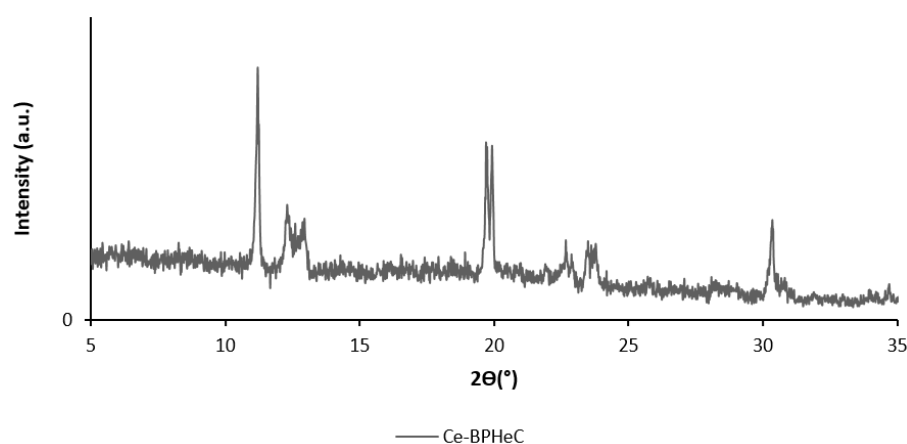


**Figure 3.42:** The powder diffractogram of Ce-BPhEC immediately measured. The pattern after three days was similar.

### 3. Conclusion

New MOFs were easily synthesized by screening different metal salts and synthesis conditions in combination with the BPhEC linker. HT synthesis screening resulted in two new Zr-MOFs, which showed structural analogies to UiO-67 and PCN-700. However, the powder patterns of these MOFs displayed peak broadening after a second HT PXRD measurement three days later. This has implications on the stability and, as a consequence, on the applicability of these MOFs in catalytic reactions. Finally, two other new MOFs were synthesized by making use of iron(III) chloride hexantrate and a cerium(IV) ammoniumhexantrate solution as metal precursors.

# General conclusion

Attempts were made to obtain a selective heterogeneous catalyst for the CDC of *o*-xylene. Firstly, homogeneous conditions were explored to find reaction conditions that are favorable for heterogenization. All these homogeneous conditions require a special type of pyridine ligand to obtain high isomer selectivities, which could be immobilized at different supports, such as MOF-808 (with isonicotinic acid, nicotinic acid and picolinic acid or  $^{2F3C}$ pyr and  $^{2F4C}$ pyr), TiO<sub>2</sub> NPs functionalized with pyridine-type phosphonate ligands and poly(4-vinylpyridine). Reaction conditions with strong acids, such as TFAH, were avoided since these acids can give rise to leaching of the ligand and the palladium centers. Therefore, reaction conditions with Pd(TFA)<sub>2</sub> (salt of the strong acid) were mainly used, since these conditions are least likely to cause leaching.

Unfortunately, reactions performed with the materials with immobilized ligands gave rise to low isomer selectivities, which were very similar to the isomer selectivities under comparable homogeneous conditions in absence of the pyridine ligand. This was investigated in more detail and a bimetallic transmetalation step was identified in the catalytic cycle. This means that two different palladium centers activate both a single *o*-xylene molecule, followed by transmetalation. Hence, to reach a high isomer selectivity, both Pd centers require a pyridine ligand. Consequently, high isomer selectivities with materials with immobilized ligands can only be reached by addition of extra 'mobile' ligands in solution. This was demonstrated by a system with 4 eq. poly(4-vinylpyridine) with the addition 0.5 eq. extra 'mobile' homogeneous pyridine (isomer selectivity of 82%). However, we did not manage to reach high isomer selectivities in the systems with MOF-808-ligand<sub>x</sub> or functionalized TiO<sub>2</sub> NPs. Hot filtration experiments with 4 eq. poly(4-vinylpyridine) with 0 and 0.5 eq. 'mobile' pyridine indicated that poly(4-vinylpyridine) acts merely as reservoir for palladium in solution. An absolute heterogeneous system could not be obtained, since about half of the Pd was lost in solution after reaction.

A side project in Kiel (Germany) focused on the synthesis of new MOFs with a special biphenylhexacarboxylic acid linker, containing many functional groups, which have the potential to retain noble metal centers. HT synthesis screening lead to of the discovery of two new Zr-MOFs, a UiO-67-BPHeC and a PCN-700-BPHeC. In addition, two other new MOFs structures were obtained by using a cerium(IV) ammoniumhexanitrate solution and iron(III) chloride hexahydrate as metal precursors.



# Bibliography

1. Khan, F., Dlugosch, M., Liu, X. & Banwell, M. G. The Palladium-Catalyzed Ullmann Cross-Coupling Reaction : A Modern Variant on a Time-Honored Process. (2018). doi:10.1021/acs.accounts.8b00169
2. Negishi, E. I. Magical power of transition metals: Past, present, and future (Nobel Lecture). *Angew. Chemie - Int. Ed.* **50**, 6738–6764 (2011).
3. Biffis, A., Centomo, P., Del Zotto, A. & Zecca, M. Pd Metal Catalysts for Cross-Couplings and Related Reactions in the 21st Century: A Critical Review. *Chem. Rev.* **118**, 2249–2295 (2018).
4. Wei, Y. & Su, W. Pd ( OAc )<sub>2</sub> -Catalyzed Oxidative C - H / C - H Cross-Coupling of Electron-Deficient Polyfluoroarenes with Simple Arenes. 16377–16379 (2010).
5. Wang, D., Izawa, Y. & Stahl, S. S. Pd-Catalyzed Aerobic Oxidative Coupling of Arenes: Evidence for Transmetalation between Two Pd(II)-Aryl Intermediates. (2014).
6. Wang, D., Izawa, Y. & Stahl, S. S. S2. 1–15
7. Wang, D. & Stahl, S. S. Pd-Catalyzed Aerobic Oxidative Biaryl Coupling: Non-Redox Cocatalysis by Cu(OTf)<sub>2</sub> and Discovery of Fe(OTf)<sub>3</sub> as a Highly Effective Cocatalyst. *J. Am. Chem. Soc.* **139**, 5704–5707 (2017).
8. Izawa, Y. & Stahl, S. S. Aerobic oxidative coupling of o-xylene: Discovery of 2-fluoropyridine as a ligand to support selective Pd-catalyzed C-H functionalization. *Adv. Synth. Catal.* **352**, 3223–3229 (2010).
9. Slagmoot, C. A. M. R. Van, Verzijl, G. K. M., Lefort, L., Alsters, P. L. & Fernandez-ibmchez, M. Palladium-Catalyzed Cross-Dehydrogenative Coupling of o -Xylene : Evidence of a New Rate-Limiting Step in the Search for Industrially Relevant Conditions. 1–8 (2018). doi:10.1002/cctc.201701973
10. Øien-Ødegaard, S. *et al.* UiO-67-type Metal-Organic Frameworks with Enhanced Water Stability and Methane Adsorption Capacity. *Inorg. Chem.* **55**, 1986–1991 (2016).
11. Torborg, C. & Beller, M. Recent applications of palladium-catalyzed coupling reactions in the pharmaceutical, agrochemical, and fine chemical industries. *Adv. Synth. Catal.* **351**, 3027–3043 (2009).
12. Huang, Z. & Dong, G. Catalytic CC bond forming transformations via direct β-CH functionalization of carbonyl compounds. *Tetrahedron Lett.* **55**, 5869–5889 (2014).
13. Pharmacopeia, U. S. Drug Design and Relationship Pharmacologic Activity AND J A M E S J . K N I T T E L. 29–37
14. Campbell, A. N. & Stahl, S. S. Overcoming the {\textquotedblleft}Oxidant Problem{\textquotedblright}: Strategies to Use O<sub>2</sub> as the Oxidant in Organometallic C{\textendash}H Oxidation Reactions Catalyzed by Pd (and Cu). *Acc. Chem. Res.* **45**, 851–863 (2012).
15. Yamaguchi, J., Yamaguchi, A. D. & Itami, K. C-H bond functionalization: Emerging synthetic tools for natural products and pharmaceuticals. *Angew. Chemie - Int. Ed.* **51**, 8960–9009 (2012).
16. Colacot, T. J. & Matthey, J. The 2010 Nobel Prize in Chemistry: Palladium-catalysed cross-

- coupling the importance of carbon-carbon coupling for real world applications. *Platin. Met. Rev.* **55**, 84–90 (2011).
17. Khan, M. U., Mesbah, M., Ferreira, L. & Williams, D. J. Development of road deterioration models incorporating flooding for optimum maintenance and rehabilitation strategies. *Road Transp. Res.* **23**, 3–24 (2014).
  18. Ram, C., Sivamani, S., Micha Premkumar, T. & Hariram, V. Computational study of leading edge jet impingement cooling with a conical converging hole for blade cooling. *ARPJ. Eng. Appl. Sci.* **12**, 6397–6406 (2017).
  19. Hassan, J., Sévignon, M., Gozzi, C., Schulz, E. & Lemaire, M. Aryl-aryl bond formation one century after the discovery of the Ullmann reaction. *Chem. Rev.* **102**, 1359–1469 (2002).
  20. Banwell, M. G., Jones, M. T. & Reekie, T. A. Article The Palladium-Catalysed Ullmann Cross-Coupling Reaction. (2014).
  21. Liu, Q. *et al.* A General Electrochemical Strategy for Sandmeyer Reaction. *Chem. Sci.* (2018). doi:10.1039/C8SC03346C
  22. Wilcox, T. & Hirshkowitz, A. NIH Public Access. **85**, 1–27 (2015).
  23. Andrada, D., Soria-Castro, S., Caminos, D., Argüello, J. & Peñéñory, A. Understanding the Heteroatom Effect on the Ullmann Copper-Catalyzed Cross-Coupling of X-Arylation (X = NH, O, S) Mechanism. *Catalysts* **7**, 388 (2017).
  24. Mondal, S. Recent advancement of Ullmann-type coupling reactions in the formation of C–C bond. *ChemTexts* **2**, 17 (2016).
  25. Chen, J. Pd/C-catalyzed Suzuki cross- and self-couplings & the development of a lab-scale hydrogenation system. 139 (2008).
  26. Melchor, M. G. *A Theoretical Study of Pd-Catalyzed C – C Cross-Coupling Reactions*. Springer Theses (2013). doi:10.1007/978-3-319-01490-6
  27. Kuhl, N., Hopkinson, M. N., Wencel-Delord, J. & Glorius, F. Beyond directing groups: Transition-metal-catalyzed C-H activation of simple arenes. *Angew. Chemie - Int. Ed.* **51**, 10236–10254 (2012).
  28. Johansson Seechurn, C. C. C., Kitching, M. O., Colacot, T. J. & Snieckus, V. Palladium-catalyzed cross-coupling: A historical contextual perspective to the 2010 nobel prize. *Angew. Chemie - Int. Ed.* **51**, 5062–5085 (2012).
  29. Li, H., Johansson Seechurn, C. C. C. & Colacot, T. J. Development of preformed Pd catalysts for cross-coupling reactions, beyond the 2010 nobel prize. *ACS Catal.* **2**, 1147–1164 (2012).
  30. Funes-Ardoiz, I. & Maseras, F. Oxidative Coupling Mechanisms: Current State of Understanding. *ACS Catal.* **8**, 1161–1172 (2018).
  31. Hunter, K. N. H. C. A., Lehn, M. J. K. J., Olivucci, S. V. L. M., Venturi, J. T. M. & Yamamoto, C. W. H. W. H. *Topics in Current Chemistry Topics in Current Chemistry*. (2001).
  32. Zafar, M. N., Mohsin, M. A., Danish, M., Nazar, M. F. & Murtaza, S. Palladium catalyzed Heck-Mizoroki and Suzuki-Miyaura coupling reactions (Review). *Russ. J. Coord. Chem.* **40**, 781–800 (2014).
  33. Macgregor, M. S., Etienne, M. M., Campagne, M. J. & Clot, M. E. Ligand electronic influence in Pd-catalyzed C-C coupling. (2016).

34. Tereniak, S. J., Landis, C. R. & Stahl, S. S. Are phosphines viable ligands for Pd-Catalyzed aerobic oxidation reactions? Contrasting insights from a survey of six reactions. *ACS Catal.* **8**, 3708–3714 (2018).
35. Kantchev, E. A. B., O'Brien, C. J. & Organ, M. G. *Palladium complexes of N-heterocyclic carbenes as catalysts for cross-coupling reactions - A synthetic chemist's perspective.* *Angewandte Chemie - International Edition* **46**, (2007).
36. Magano, J. & Dunetz, J. R. Large-scale applications of transition metal-catalyzed couplings for the synthesis of pharmaceuticals. *Chem. Rev.* **111**, 2177–2250 (2011).
37. Liljenberg, M., Stenlid, J. H. & Brinck, T. Theoretical Investigation into Rate-Determining Factors in Electrophilic Aromatic Halogenation. *J. Phys. Chem. A* **122**, 3270–3279 (2018).
38. Sheppard, T. D. Metal-catalysed halogen exchange reactions of aryl halides. *Org. Biomol. Chem.* **7**, 1043–1052 (2009).
39. Leas, D. A., Dong, Y., Vennerstrom, J. L. & Stack, D. E. One-Pot, Metal-Free Conversion of Anilines to Aryl Bromides and Iodides. *Org. Lett.* **19**, 2518–2521 (2017).
40. Ahl, T. H. K. & Ag, B. Anthraquinone. *IARC Monogr. Eval. Carcinog. Risks to Humans* **101**, (2012).
41. Zhang, L. & Jiao, L. Pyridine-catalyzed radical borylation of aryl halides. *J. Am. Chem. Soc.* **139**, 607–610 (2017).
42. Chen, K., Wang, L., Meng, G. & Li, P. Recent Advances in Transition-Metal-Free Aryl C-B Bond Formation. *Synth.* **49**, 4719–4730 (2017).
43. Kabalka, G. W., Sastry, U., Sastry, K. A. R., Knapp, F. F. & Srivastava, P. C. Synthesis of arylboronic acids via the reaction of borane with arylmagnesium halides. *J. Organomet. Chem.* **259**, 269–274 (1983).
44. Wedi, P. & van Gemmeren, M. Arene-Limited Nondirected C–H Activation of Arenes. *Angew. Chemie - Int. Ed.* **57**, 13016–13027 (2018).
45. McGlacken, G. P. & Bateman, L. M. Recent advances in aryl-aryl bond formation by direct arylation. *Chem. Soc. Rev.* **38**, 2447–2464 (2009).
46. Campeau, L. C. & Fagnou, K. Palladium-catalyzed direct arylation of simple arenes in synthesis of biaryl molecules. *Chem. Commun.* 1253–1264 (2006). doi:10.1039/b515481m
47. Mpungose, P. P., Vundla, Z. P., Maguire, G. E. M. & Friedrich, H. B. The current status of heterogeneous palladium catalysed Heck and Suzuki cross-coupling reactions. *Molecules* **23**, 1–24 (2018).
48. Lei, A., Shi, W., Liu, C. & Liu, W. *Related Titles Handbook of Reagents for Organic Synthesis - Catalyst Components for Coupling Catalysis in Asymmetric Synthesis 2e Modern Tools for the Synthesis of Complex Bioactive Cross-Coupling Reactions.*
49. Salih, K. S. M. & Thiel, W. R. Palladium-Catalyzed Coupling Reactions with Magnetically Separable Nanocatalysts. *Palladium-Catalyzed Coupling React. Pract. Asp. Futur. Dev.* 57–78 (2013).
50. Wang, D., Izawa, Y. & Stahl, S. S. Pd-Catalyzed Aerobic Oxidative Coupling of Arenes : Evidence for Transmetalation between Two Pd ( II ) -Aryl Intermediates Pd-Catalyzed Aerobic Oxidative Coupling of Arenes : Evidence for Transmetalation between Two Pd ( II ) -Aryl Intermediates. (2014). doi:10.1021/ja505405u

51. Liu, C. *et al.* Oxidative Coupling between Two Hydrocarbons: An Update of Recent C-H Functionalizations. *Chem. Rev.* **115**, 12138–12204 (2015).
52. Uri, D. & Porter, A. L. the Formation of Biaryl Bonds Via Cross-Dehydrogenative Coupling. (2013).
53. Wang, D., Weinstein, A. B., White, P. B. & Stahl, S. S. Ligand-Promoted Palladium-Catalyzed Aerobic Oxidation Reactions. *Chem. Rev.* **118**, 2636–2679 (2018).
54. Borja-Cacho, D. & Matthews, J. NIH Public Access. *Nano* **6**, 2166–2171 (2008).
55. Slagmaat, C. A. M. R. Van, Verzijl, G. K. M., Lefort, L., Alsters, P. L. & Fern, M. Palladium-Catalyzed Cross-Dehydrogenative Coupling of o -Xylene : Evidence of a New Rate-Limiting Step in the Search for Industrially Relevant Conditions. 2620–2626 (2018). doi:10.1002/cctc.201701973
56. Stahl, S. S. & Alsters, P. L. *www.ebook3000.com*.
57. Chen, L., Gao, Z. & Li, Y. Immobilization of Pd(II) on MOFs as a highly active heterogeneous catalyst for Suzuki-Miyaura and Ullmann-type coupling reactions. *Catal. Today* **245**, 122–128 (2015).
58. Parvulescu, V. I. & Kemnitz, E. New Materials for Catalytic Applications. *New Mater. Catal. Appl.* 1–373 (2016). doi:10.1016/C2014-0-02886-9
59. Carole, W. A. & Colacot, T. J. Understanding Palladium Acetate from a User Perspective. *Chem. - A Eur. J.* **22**, 7686–7695 (2016).
60. Balcells, D. & Nova, A. Designing Pd and Ni Catalysts for Cross-Coupling Reactions by Minimizing Off-Cycle Species. *ACS Catal.* **8**, 3499–3515 (2018).
61. Haines, B. E., Berry, J. F., Yu, J. Q. & Musaev, D. G. Factors Controlling Stability and Reactivity of Dimeric Pd(II) Complexes in C-H Functionalization Catalysis. *ACS Catal.* **6**, 829–839 (2016).
62. Carole, W. A. & Colacot, T. J. Understanding Palladium Acetate from a User Perspective. 7686–7695 (2016). doi:10.1002/chem.201601450
63. Wang, Y., Wang, Y., Zhang, W. & Lu, X. Supporting Information for : 1–56 (1999).
64. Liu, Y. *et al.* Direct aerobic oxidative homocoupling of benzene to biphenyl over functional porous organic polymer supported atomically dispersed palladium catalyst. *Appl. Catal. B Environ.* **209**, 679–688 (2017).
65. Ashenhurst, J. A. Intermolecular oxidative cross-coupling of arenes. *Chem. Soc. Rev.* **39**, 540–548 (2010).
66. Rong, Y., Li, R. & Lu, W. Palladium(II)-catalyzed coupling of p-xylene via regioselective C-H activation in TFA. *Organometallics* **26**, 4376–4378 (2007).
67. Yang, Y., Lan, J. & You, J. Oxidative C – H / C – H Coupling Reactions between Two ( Hetero ) arenes. (2017). doi:10.1021/acs.chemrev.6b00567
68. Fei, H. & Cohen, S. M. A robust, catalytic metal-organic framework with open 2,2'-bipyridine sites. *Chem. Commun.* **50**, 4810–4812 (2014).
69. Bai, Y. *et al.* Zr-based metal–organic frameworks: design, synthesis, structure, and applications. *Chem. Soc. Rev.* **45**, 2327–2367 (2016).
70. Marshall, R. J. & Forgan, R. S. Postsynthetic Modification of Zirconium Metal-Organic

- Frameworks. *Eur. J. Inorg. Chem.* **2016**, 4310–4331 (2016).
71. Yuan, S., Qin, J. S., Lollar, C. T. & Zhou, H. C. Stable Metal-Organic Frameworks with Group 4 Metals: Current Status and Trends. *ACS Cent. Sci.* **4**, 440–450 (2018).
  72. Pang, J. *et al.* Flexible Zirconium MOFs as Bromine-Nanocontainers for Bromination Reactions under Ambient Conditions. *Angew. Chemie - Int. Ed.* **56**, 14622–14626 (2017).
  73. Yuan, S. *et al.* Flexible Zirconium Metal-Organic Frameworks as Bioinspired Switchable Catalysts. *Angew. Chemie - Int. Ed.* **55**, 10776–10780 (2016).
  74. Catalysts, S. Supporting Information.
  75. Furukawa, H. *et al.* Water Adsorption in Porous Metal–Organic Frameworks and Related Materials. *J. Am. Chem. Soc.* **136**, 4369–4381 (2014).
  76. Wang, H. *et al.* Topologically guided tuning of Zr-MOF pore structures for highly selective separation of C6 alkane isomers. *Nat. Commun.* **9**, 1–11 (2018).
  77. Sun, Y. & Zhou, H. C. Recent progress in the synthesis of metal-organic frameworks. *Sci. Technol. Adv. Mater.* **16**, (2015).
  78. Islamoglu, T. *et al.* Postsynthetic Tuning of Metal-Organic Frameworks for Targeted Applications. *Acc. Chem. Res.* **50**, 805–813 (2017).
  79. Wang, D., Weinstein, A. B., White, P. B. & Stahl, S. S. Ligand-Promoted Palladium-Catalyzed Aerobic Oxidation Reactions. *Chem. Rev.* **118**, 2636–2679 (2018).
  80. Dong, W. *et al.* Palladium nanoparticles embedded in metal-organic framework derived porous carbon: Synthesis and application for efficient Suzuki-Miyaura coupling reactions. *RSC Adv.* **6**, 37118–37123 (2016).
  81. Dhakshinamoorthy, A., Asiri, A. M. & Garcia, H. Metal-organic frameworks catalyzed C-C and C-heteroatom coupling reactions. *Chem. Soc. Rev.* **44**, 1922–1947 (2015).
  82. Vigo, U. De. Palladium Nanoparticles as Efficient Catalysts for Suzuki Cross-Coupling Reactions. (2012). doi:10.1021/jz2013984
  83. Isaeva, V. I. & Kustov, L. M. The application of metal-organic frameworks in catalysis (Review). (2010). doi:10.1134/S0965544110030011
  84. Dhakshinamoorthy, A., Asiri, M. & Garcia, H. Chem Soc Rev Metal – organic frameworks catalyzed C – C and C – heteroatom coupling reactions. 1922–1947 (2015). doi:10.1039/C4CS00254G
  85. Chen, L., Gao, Z. & Li, Y. Immobilization of Pd ( II ) on MOFs as a highly active heterogeneous catalyst for Suzuki – Miyaura and Ullmann-type coupling reactions. **245**, 122–128 (2015).
  86. Isaeva, V. I. & Kustov, L. M. The application of metal-organic frameworks in catalysis (Review). *Pet. Chem.* **50**, 167–180 (2010).
  87. Rogge, S. M. J. *et al.* Metal-organic and covalent organic frameworks as single-site catalysts. *Chem. Soc. Rev.* **46**, 3134–3184 (2017).
  88. Velthoven, N. Van *et al.* Single-Site Metal-Organic Framework Catalysts for the Oxidative Coupling of Arenes via C-H / C-H activation.
  89. Sun, Y. & Zhou, H. Recent progress in the synthesis of metal – organic frameworks. (2015). doi:10.1088/1468-6996/16/5/054202

90. Duan, H. *et al.* Single-site palladium(II) catalyst for oxidative heck reaction: Catalytic performance and kinetic investigations. *ACS Catal.* **5**, 3752–3759 (2015).
91. Lammert, M., Glißmann, C. & Stock, N. Supporting Information for Tuning the stability of bimetallic Ce ( IV )/ Zr ( IV ) - based MOFs with UiO-66 and MOF-808 structure. 1–38 (2017).
92. Zeininger, L., Portilla, L., Halik, M. & Hirsch, A. Quantitative Determination and Comparison of the Surface Binding of Phosphonic Acid , Carboxylic Acid , and Catechol Ligands on TiO 2 Nanoparticles. 13506–13512 (2016). doi:10.1002/chem.201601920
93. Brumbach, M. T., Boal, A. K. & Wheeler, D. R. Metalloporphyrin assemblies on pyridine-functionalized titanium dioxide. *Langmuir* **25**, 10685–10690 (2009).
94. Qu, Q. *et al.* Chemically binding carboxylic acids onto TiO<sub>2</sub> nanoparticles with adjustable coverage by solvothermal strategy. *Langmuir* **26**, 9539–9546 (2010).
95. Monolayers, S. *et al.* Controlling the Surface Reactivity of Titania via Electronic Tuning of. (2017). doi:10.1021/acscatal.7b02789
96. Lammert, M., Glißmann, C. & Stock, N. Tuning the stability of bimetallic Ce(IV)/Zr(IV)-based MOFs with UiO-66 and MOF-808 structures. **4**, 2425–2429 (2017).
97. Wang, P. Aggregation of TiO<sub>2</sub> Nanoparticles in Aqueous Media : Effects of pH , Ferric Ion and Humic Acid. 1–6 (2017). doi:10.19080/IJESNR.2017.01.555575
98. Kozlov, D. A., Lebedev, V. A., Polyakov, A. Y., Khazova, K. M. & Garshev, A. V. The microstructure effect on the Au / TiO<sub>2</sub> and Ag / TiO<sub>2</sub> nanocomposites photocatalytic activity. **9**, 266–278 (2018).
99. Metalation, C. C. Supporting Information.
100. Yuan, S. *et al.* Zuschriften Metal – Organic Frameworks Hot Paper Flexible Zirconium Metal-Organic Frameworks as Bioinspired Switchable Catalysts Zuschriften Angewandte. 10934–10938 (2016). doi:10.1002/ange.201604313
101. Øien, S. *et al.* Detailed structure analysis of atomic positions and defects in zirconium metal-organic frameworks. *Cryst. Growth Des.* **14**, 5370–5372 (2014).
102. Lawrence, M. C., Schneider, C. & Katz, M. J. Determining the structural stability of UiO-67 with respect to time: A solid-state NMR investigation. *Chem. Commun.* **52**, 4971–4974 (2016).

# Vulgariserende samenvatting

De traditionele technieken om koolstof-koolstof verbindingen te vormen, zijn geëvolueerd uit jarenlange optimalisatie op vlak van toxiciteit van de reagentia, efficiëntie, selectiviteit en substraat scope. Ondanks alle inspanningen, blijven deze technieken redelijk omslachtig omdat ze twee geprefunctionaliseerde koppelingspartners vereisen (een koolstof-halogeen verbinding en een koolstof-metaal verbinding). Na de reactie wordt een koolstof-koolstof binding gevormd, exact op de positie waar het metaal en het halogeen zich bevonden. Als gevolg worden grote hoeveelheden afval gecreëerd (nevenstromen van de prefunctionalizatie en zoutafval afkomstig van het metaal en halogeen na reactie), dit gaat natuurlijk gepaard met opzuiveringsstappen. Deze omslachtige methodes kunnen omzeild worden door gebruik te maken van de dehydrogenatieve “cross-coupling”. Dit is de directe koppeling van twee niet-geprefunctionaliseerde substraten (C-H verbindingen) onder zuurstof gas en geschikte katalysator. Deze reactie vormt een duurzaam alternatief waarin water het enige afvalproduct vormt. De koppeling verloopt echter minder selectief (meerdere C-H verbindingen in een molecule, die geactiveerd kunnen worden) maar ook minder actief (C-H verbindingen zijn inert).

*O*-xylene kan op drie manier met zichzelf koppelen ter vorming van drie verschillende isomeren. Slechts één van deze isomeren heeft industriële relevantie in een kortere productieroute van het polymeer Upilex. Deze thesis beschrijft de zoektocht naar een vaste drager om de dehydrogenatieve “cross coupling” van *o*-xylene selectief uit te voeren. Bovendien is het de bedoeling dat deze drager sterk interageert met de dure katalysator, zodat deze herbruikt kan worden om zo een meer economisch proces te bekomen. Hiervoor werd een belangrijke ligand (type pyridine), nodig voor selectiviteit naar het gewenste isomeer, op een vaste drager gezet (vb. MOF-808, TiO<sub>2</sub> nanopartikels en poly(4-vinylpyridine)). De reactie verliep echter niet selectief wanneer de ligand geïmobiliseerd was omdat het mechanisme dit niet toestond vanwege “bimetallisch karakter”. De reactie gebeurt dan tussen twee naburige katalysator moleculen die beiden een ligand vereisen (dit is onmogelijk wanneer de ligand geïmobiliseerd is). Wanneer er kleine hoeveelheden ‘mobiele’ ligand werden toegevoegd, werden er hogere isomeer selectiviteiten bekomen, voor poly(4-vinylpyridine) althans, maar niet bij de andere geïmobiliseerde liganden. Poly(4-vinylpyridine) is een drager waarbij de katalysator enkel op de geïmobiliseerde ligand kan zitten of in oplossing, terwijl andere dragers zoals MOF-808 en TiO<sub>2</sub> nanopartikels naast de geïmobiliseerde liganden respectievelijk open coordinatie sites en oppervlakte functionele groepen hebben, waarmee de katalysator moleculen en andere reagentia (zoals de ‘mobiele’ liganden) kunnen interageren. Hierdoor bleef een deel katalysator moleculen ligandloos, wat leidde tot lagere selectiviteit. Zo werd er niet echt een recycleerbaar vast dragermateriaal bekomen, maar eerder inzichten over het mechanisme van de reactie en hoe hierop geanticipeerd kan worden.